FOSSIL

DOE/MC/26373-3530
(DE94000055)

DEVELOPMENT OF CERAMIC MEMBRANE REACTORS FOR HIGH TEMPERATURE GAS CLEANUP

Final Report

By
Daryl L. Roberts
I.C. Abraham
Y. Blum
D.E. Gottschlich
A. Hirschon
J. Douglas Way
John Collins

June 1993

Work Performed Under Contract No. AC21-89MC26373

For
U.S. Department of Energy
Morgantown Energy Technology Center
Morgantown, West Virginia

By
SRI International
Menlo Park, California

DOE/MC/26373-3530
(DE94000055)
Distribution Categories UC-114 and UC-106

Development of Ceramic Membrane Reactors For High Temperature Gas Cleanup

Final Report

Daryl L. Roberts
I.C. Abraham
Y. Blum
D.E. Gottschlich
A. Hirschon
J. Douglas Way
John Collins

Work Performed Under Contract No.: DE-AC21-89MC26373

For
U.S. Department of Energy
Office of Fossil Energy
Morgantown Energy Technology Center
P.O. Box 880
Morgantown, West Virginia 26507-0880

By
SRI International
333 Ravenswood Avenue
Menlo Park, California 94025-3493

June 1993

SUMMARY

The U.S. Department of Energy (DOE) is seeking to develop high temperature, high pressure ceramic membrane technology to perform a variety of gas separation processes to improve the efficiency and economics of advanced power generation systems such as direct coal-fueled turbines (DCFT) and the integrated gasification combined cycle (IGCC) process. The temperatures encountered in these power generation systems are far above the temperature range for organic membrane materials (typically 150-200°C for polymers such as silicone rubber, polysulfone, and cellulose esters). Inorganic materials such as ceramics are therefore the most likely membrane materials for use at high temperatures.

The focus of this project was control of H_2S and NH_3 in IGCC systems. The IGCC process consists basically of a gasifier to produce synthetic gas, followed by a gas turbine generator. The temperature and pressure ranges encountered in the IGCC process are 1,000 to 2,000°F and 200 to 1,000 psia. There are several potential applications for a high temperature membrane reactor process in the IGCC process. Downstream of the hot particle removal device, for example, both H_2S and NH_3 could be removed and catalytically decomposed, leaving the fuel value of the gasifier stream intact. Alternatively, H_2S and NH_3 could be decomposed directly in the gasifier. In either case, a membrane reactor has the potential to efficiently effect both H_2S and NH_3 decomposition. The primary advantages of using a membrane reactor over a conventional reactor are that the fraction of the contaminant decomposed is higher and the reaction rate faster. Overall, the technology of membrane reactors is likely to impact several DOE program areas.

The objective of this project was to develop high temperature, high pressure catalytic ceramic membrane reactors and to demonstrate the feasibility of using these membrane reactors to control gaseous contaminants (hydrogen sulfide and ammonia) in IGCC systems. Our strategy was to first develop catalysts and membranes suitable for the IGCC application and then combine these two components as a complete membrane reactor system. We also developed a computer model of the membrane reactor and used it, along with experimental data, to perform an economic analysis of the IGCC application.

A survey of the literature identified two promising catalysts for use in a membrane reactor: MoS_2 for H_2S decomposition, and Ni for NH_3 decomposition (both on an alumina substrate). We prepared these catalysts and experimentally determined their catalytic activity for H_2S and NH_3 decomposition. Both catalysts significantly increased the decomposition rates. To make a suitable membrane, we used four substrates (alumina microfilter monolith, alumina microfilter disks,

alumina ultrafilter tubes, and Vycor glass) and five coating materials (poly-N-methyl silazane, polycyclohidridomethyl silazane, alumina-based glaze, aluminum phosphorus oxides, and palladium). Only the palladium films on an alumina ultrafilter were successful. The other membranes were plagued with cracks and poor reproducibility. The palladium membrane showed a high selectivity for H_2 over N_2, approaching 200 under some conditions.

A membrane reactor we successfully demonstrated for decomposition of NH_3 used the alumina supported Ni catalyst with the palladium membrane under conditions similar to that in an IGCC process. The membrane reactor resulted in significantly higher NH_3 decomposition than did a conventional reactor (by at least a factor of 2) and achieved almost complete NH_3 removal (95%) at 600°C.

A computer model was developed starting from the fundamental equations describing mass transfer and chemical reaction. The model was solved using the Gears numerical method on a personal computer. The model was used to perform an economic analysis of a membrane reactor system for H_2S and NH_3 removal from an IGCC process. The results indicated that achieving the desired fraction of H_2S is very difficult even with a membrane reactor, because of the low value of the H_2S decomposition equilibrium constant and the high ratio of H_2 to H_2S in the feed stream. For NH_3, our results were promising—the maximum conversion that could be achieved was 89%. To achieve 90% NH_3 decomposition, the NH_3 should be preconcentrated in the feed before the feed enters the membrane reactor. If the feed NH_3 concentration can be increased to 5%, the ammonia decomposition costs will increase the total cost of producing electricity by only 1%. These calculations were performed using early experimental results. Later experiments showed improved membrane properties; if these data were used in the economic analysis, higher conversions and lower costs would have resulted.

CONTENTS

SUMMARY ii

NOMENCLATURE 1

INTRODUCTION 3

REVIEW OF PREVIOUS WORK 4

Membranes 4

Catalytic Decomposition of Hydrogen Sulfide 7

Catalytic Decomposition of Ammonia 11

Membrane Reactors 13

CATALYST DEVELOPMENT 15

Catalyst Preparation 15

Catalyst Performance 16

H_2S Decomposition 16

NH_3 Decomposition 22

MEMBRANE DEVELOPMENT 32

Palladium Films on Alumina Ultrafilters 32

Preparation of Palladium Films by Electroless Plating 34

Bath/Solution Preparation 34

Sensitizing Bath Preparation 35

Activation Bath Preparation 35

Plating Bath Preparation 36

Membrane Pretreatment 36

Membrane Activation 38

Membrane Plating 38

Palladium Membrane Results 39

Polysilazanes on Alumina Substrates 42

Norton Alumina Monolith 48

DuPont PRD 86 48

Refractron Microfilter 50

Vycor Glass 52

Leachable Alumina Glaze on Alumina Microfilters 52

Miscellaneous Membrane Formulations 56

MEMBRANE REACTOR EXPERIMENTS 58

MEMBRANE REACTOR MODELING 61

TECHNICAL AND ECONOMIC EVALUATION OF MEMBRANE REACTORS IN AN IGCC ENVIRONMENT 65
Membrane Reactor System Parameters 72
H_2S Decomposition 73
NH_3 Decomposition 75
CONCLUSIONS 88
REFERENCES 89
APPENDIX A: THERMODYNAMICS OF THE DECOMPOSITION OF HYDROGEN SULFIDE A-1
APPENDIX B: REACTION RATE FOR DECOMPOSITION OF HYDROGEN SULFIDE B-1

FIGURES

1	Postulated mechanism for catalysis of hydrogen sulfide decomposition by molybdenum disulfide	9
2	Test system for catalyst activity measurement	17
3	Reactor residence time at feed pressure of 200 psia, various flow rates	18
4	Decomposition of H_2S on MoS_2 catalyst	19
5	Analysis of catalytic activity of MoS_2	20
6	Extent of NH_3 decomposition for alumina tube reactor with alumina particles and with catalyst particles	23
7	Catalytic reaction system for kinetic experiments	24
8	Effect of flow rate on NH_3 decomposition rate	26
9	Ammonia decomposition rate data (400°C)	27
10	Ammonia decomposition rate data (450°C)	28
11	Ammonia decomposition rate data (500°C)	29
12	Predicted versus observed reaction rates for modified Temkin-Pyzhev equation	31
13	Shell and tube test apparatus for permeation tests	40
14	Comparison of H_2 permeation rates at 823 K	41
15	H_2 permeation data for membrane 2	44
16	N_2 permeation data for membrane 3	45
17	H_2 selectivity of membrane 3 as a function of transmembrane pressure difference	46
18	Polysilazanes used for coating alumina substrates	47
19	Cross section of Norton's asymmetric filter near the surface of an internal tube after deposition of polysilazane-derived skin	49
20	Cross section of native Refractron disk	51
21	Leaching of potassium ion from Aremco 617 glaze	53

22	Inorganic glaze on Refractron disk	54
23	Flow streams in membrane reactor system	59
24	Membrane reactor experiment results	60
25	Block flow diagram of IGCC base case	66
26	Simplified flow diagram of conventional IGCC technology	67
27	Control of H_2S and NH_3 with hydrogen-selective membrane reactors	68
28	Effect of reactor temperature on decomposition of H_2S	74
29	Removal of H_2S and NH_3 before decomposition in a membrane reactor	76
30	Removal of H_2 before decomposition of H_2S and NH_3 in membrane reactors	77
31	Effect of H_2S preconcentration on decomposition of H_2S	78
32	Effect of feed H_2 preconcentration on decomposition of H_2S	79
33	Equilibrium coefficients for NH_3 and H_2S decomposition	80
34	Ammonia decomposition with NH_3 preconcentration	81
35	Ammonia decomposition with H_2 removal	83
36	Effect of ammonia preconcentration on membrane reactor cost	84
37	Ammonia removal cost with H_2 removal	85
A-1	Equilibrium coefficient for decomposition of H_2S	A-4

TABLES

1	Computer Search Strategy	5
2	Commercially Available Porous Inorganic Membranes	5
3	Catalytic Activity of Molybdenum Disulfide Catalyst	8
4	Crystal Phases Before and After Reaction with H_2S	10
5	Decomposition of NH_3 on Various Catalysts at 550°C	12
6	Decomposition of NH_3 on Various Catalysts at 800°C	13
7	Data Used to Determine H_2S Reaction Rate Coefficient	21
8	Comparison of Permeation Rates of Hydrogen Through Commercial and Laboratory Membranes	33
9	Membranes Used in Permeation Experiments	39
10	Membranes Made with PCMS on Refractron Alumina Microfilters and Vycor Glass	43
11	Membranes Made with Aremco 617 on Refractron Alumina Microfilters	55
12	Properties of Various Batches of Aremco 617	56
13	Membranes Made with PEG in Aremco 617 on Refractron Microfilters	57
14	Permeation Behavior of $AlPO_4$-Coated Media	57
15	Experimental Conditions for Membrane Reactor Experiments	58
16	Inlet Stream Conditions for Zinc Ferrite System in IGCC Base Case	69
17	Breakdown of Process Plant Costs by Plant Section	70
18	First Year O&M Cost Summary	71
19	Key Economic Parameters Used in the Economic Analysis	86
20	Economic Results for Membrane Reactor Decomposition	87
A-1	Thermodynamic Parameters for Decomposition of H_2S	A-3
B-1	Data Used to Determine H_2S Reaction Rate Coefficient	B-2

NOMENCLATURE

E_a	=	Activation energy for NH_3 reaction rate equation (J/mol)
E_b	=	Pressure factor for NH_3 reaction rate constant (m^3/mol)
f_i	=	Fugacity of species i (atm)
F_i	=	Molar flow rate of species i on feed side of membrane (mol/s)
k	=	NH_3 reaction rate coefficient $\left(\frac{\text{mol}}{\text{m}^3\text{-s-atm}^{-\beta}}\right)$
k_o	=	Pre-exponential factor in NH_3 reaction rate coefficient $\left(\frac{\text{mol}}{\text{m}^3\text{-s-atm}^{-\beta}}\right)$
k_1	=	H_2S reaction rate coefficient (s^{-1})
K_{eq}	=	Equilibrium coefficient
L	=	Axial distance variable
L_O	=	Length of reactor
N_i	=	Permeation flux of species i (mol/cm^2/s)
P	=	Total reactor pressure for use in modified Temkin-Pyzhev equation (atm)
$\bar{P}_i$	=	Permeance coefficient for species i (mol/cm^2 s cm Hg)
$\bar{P}_{H_2}$	=	Permeance coefficient for hydrogen (mol/cm^2 s (cm Hg)$^{1/2}$)
P_T	=	Total pressure on feed side of membrane (atm)
Q_i	=	Molar flow rate of species i on permeate side of membrane
r	=	Reaction rate (mol/m^3)
R	=	Gas constant
R_i	=	Inside radius of membrane reactor tube (cm)
T	=	Temperature (K)
X_i	=	Mole fraction of species i on feed side of membrane
Y_i	=	Mole fraction of species i on permeate side of membrane

β	=	Kinetic parameter for NH_3 reaction rate equation
γ	=	Ratio of total pressure on permeate side of membrane to that on feed side
ΔP	=	Transmembrane pressure difference (atm)
ε	=	Catalyst bed porosity

INTRODUCTION

The U.S. Department of Energy (DOE) is seeking to develop high temperature, high pressure ceramic membrane technology to perform a variety of gas separation processes to improve the efficiency and economics of advanced power generation systems such as direct coal-fueled turbines (DCFT) and the integrated gasification combined cycle (IGCC) process. The temperatures encountered in these power generation systems are far above the temperature range for organic membrane materials (typically 150-200°C for polymers such as silicone rubber, polysulfone, and cellulose esters). Inorganic materials such as ceramics are therefore the most likely membrane materials for use at high temperatures.

The focus of this project was control of H_2S and NH_3 in IGCC systems. The IGCC process consists basically of a gasifier to produce synthetic gas, followed by a gas turbine generator. The temperature and pressure ranges encountered in the IGCC process are 1,000° to 2,000°F and 200 to 1,000 psia. There are several potential applications for a high temperature membrane reactor process in the IGCC process. Downstream of the hot particle removal device, for example, both H_2S and NH_3 could be removed and catalytically decomposed, leaving the fuel value of the gasifier stream intact. Alternatively, H_2S and NH_3 could be decomposed directly in the gasifier. In either case, a membrane reactor has the potential to efficiently effect both H_2S and NH_3 decomposition. The primary advantages of using a membrane reactor over a conventional reactor are that the fraction of the contaminant decomposed is higher and the reaction rate faster. Overall, the technology of membrane reactors is likely to impact several DOE program areas.

The objective of this project was to develop high temperature, high pressure catalytic ceramic membrane reactors and to demonstrate the feasibility of using these membrane reactors to control gaseous contaminants (hydrogen sulfide and ammonia) in IGCC systems. Our strategy was to first develop catalysts and membranes suitable for the IGCC application and then combine these two components as a complete membrane reactor system. We also developed a computer model of the membrane reactor and used it, along with experimental data, to perform an economic analysis of the IGCC application. Our results have demonstrated the concept of using a membrane reactor to remove trace contaminants from an IGCC process. Experiments showed that NH_3 decomposition efficiencies of 95% can be achieved. Our economic evaluation predicts ammonia decomposition costs of less than 1% of the total cost of electricity; improved membranes would give even higher conversions and lower costs.

REVIEW OF PREVIOUS WORK

We used computerized and ad hoc methods for our literature search. The computerized search used the Chemical Abstracts data base back to 1967, our strategy is presented in Table 1. We searched primarily in the areas of H_2S and NH_3 decomposition, since we believed our files were sufficient for our review of membrane technology.

MEMBRANES

Inorganic membrane materials are the only suitable ones for IGCC/membrane reactor use. The most comprehensive single source of information on commercial inorganic membranes is a recent review by Egan (1989). This review covers inorganic membranes made from metals, metal oxides, glasses, and carbon; explains briefly the relevant transport mechanisms and manufacturing techniques; and includes 199 references. A wide range of pore sizes is available in commercial membranes (Table 2). Mechanisms of transport in inorganic materials include viscous flow, Knudsen diffusion, surface diffusion, capillary condensation, and molecular sieving. These mechanisms, except molecular sieving, are described by Hwang and Kammermeyer (1984). Descriptions of molecular sieving have been given by Koresh and Sofer (1987) and by Way and Roberts (1989).

Research on inorganic membranes today is focusing on finer pore sizes, pore stability, and manufacturing reproducibility. For example, Anderson et al. (1988) are using soluble organometallic precursors and decomposing these in the pores of inorganic ultrafilters. Results of recent work show pore sizes are now approaching the 10 Å size range. Keizer et al. (1988) have studied the dip coating of an alumina boehmite sol onto a microporous (1,600 Å) alumina support. This technique resulted in a thin layer (4 μm) with 27 Å average pore size. Suzuki (1987) has made inorganic membranes with pores smaller than 20 Å by synthesizing zeolites in the pores of metallic, glass, and metal oxide microporous substrates.

There is little work reported with membranes at conditions of interest to DOE. Bhave et al. (1989) reported that the pores of the commercial Alcoa product (alumina ultrafilter) open up upon heating. The pores are originally 40 Å and open to 57 Å if heated to 1,000°F, to 63 Å if heated to 1,200°F, and to 76 Å if heated to 1,500°F. It is not clear if these pores would continue growing in long-term testing. Koresh and Sofer (1987) reported CH_4/H_2 separation at 930°F in carbon

Table 1
COMPUTER SEARCH STRATEGY
(Chemical Abstracts, 1967-present)

Item No.	Key Words	Number of Citations
1	Hydrogen Sulfide Decomposition	301
2	Ammonia Decomposition	1,404
3	Catalytic Decomposition	17,438
4	Membrane, Permselect, Reactor	9,841
5	Catalytic Dehydrogenation	13,999
6	(1 or 2) and (3 or 4 or 5)	463
7	(1 or 2) and 3	461
8	(1 or 2) and 4	3

Table 2
COMMERCIALLY AVAILABLE POROUS INORGANIC MEMBRANES

Manufacturer	Membrane Material	Support Material	Membrane Pore Size	Membrane Configuration
Alcoa	Al_2O_3 Al_2O_3	Al_2O_3 Al_2O_3	40-1000 Å 0.2-5 μm	Monolith/tube
Anotec/Alcan	Al_2O_3 Al_2O_3	Al_2O_3 Al_2O_3	250 Å 0.2 μm	Disk
Asahi Glass	Glass Glass	(90% SiO_2) (60% SiO_2)	40-500 Å < 5 μm	Tube/disk
Bolt Technical Ceramics	Al_2O_3, SiC		1-40 μm	Tube
CARRE/DuPont	ZrO_2	SS, Carbon	40 Å-0.1 μm	Tube
Ceram Filters	SiC		0.15-8 μm	Tube, monolith

Table 2
COMMERCIALLY AVAILABLE POROUS INORGANIC MEMBRANES (Concluded)

Manufacturer	Membrane Material	Support Material	Membrane Pore Size	Membrane Configuration
CeraMem	Alumina Zirconia	Cordierite Alumina	0.1-0.2 μm 200-300 Å	Monolith
Coors	Ceramic		0.5-108 μm	—
Corning	Glass Cordierite, mullite		40 Å 2.6-4.9 μm	Tube Monolith
DuPont	Alumina, mullite silica, cordierite		0.06-1.0 μm	Tube
Fuji Filters	Glass		40 Å - 1.2 μm	Tube
GFT/Carbone Lorraine	Carbon		40 Å - 1.0 μm	Tube
Mott	SS, Ni, Au, Ag, Pt, etc.		0.5-100 μm	Tube, disk, rod
NGK	Al_2O_3, SiC	Al_2O_3, SiC	0.2-13 μm	Tube, monolith
Norton/Millipore	Al_2O_3	Al_2O_3	0.2-1.0 μm	Monolith/tube
Osmonics	Ag Ceramic		0.2-5 μm 0.3-25 μm	Disk Disk, Tube
PTI Technologies	SS		0.5-2.0 μm	—
Pall	SS, Ni, etc.		0.5 μm	Tube
Poretics	Silver Ceramic (Al, Si)		0.2-5 μm 0.3-25 μm	Disk Disk
SFEC	ZrO_2	Carbon	40 Å - 0.1 μm	Tube
Schott Glass	Glass		100 Å - 0.1 μm	Tube
TDK	ZrO_2	Al_2O_3	100 Å	Tube
Toyobo	Glass		200 Å	Tube
Union Carbide	ZrO_2	Carbon	30 Å	Tube

Source: Egan (1989).

molecular sieve membranes. There appear to be no other data available at temperatures above 300°F. Keizer et al. (1988) state that their alumina membrane can operate at 1,470°F, but they present no data for temperatures above 300°F. We postulate that work at higher temperatures is proceeding, but slowly, at several research groups worldwide (Twente University, Alcoa, Worcester Polytechnic Institute, University of Wisconsin, NGK, GFT).

The vast majority of the membranes either commercially available or in the development stage have pores too big to be useful for gas separations. In passive membranes with pores bigger than 10 Å, Knudsen diffusion is the only selective mechanism for gas transport at temperatures higher than 1,000°F. The selectivity predicted by Knudsen diffusion (ratio of square roots of molecular weights) is well below the selectivity necessary for commercial application (as exhibited by the selectivities of polymeric materials now in commercial practice). However, this mechanism may be the only one available in inorganic membranes for some time, pending the further development of molecular sieving membranes (Way and Roberts, 1989; Koresh and Sofer, 1987) or chemically active inorganic membranes such as molten salts (Moore et al., 1974; Pez and Carlin, 1986). We can anticipate that pore structure stability will be a major issue for such membranes at conditions of interest to DOE.

CATALYTIC DECOMPOSITION OF HYDROGEN SULFIDE

Many studies have been made of hydrogen sulfide (H_2S) decomposition, primarily because of its widespread interest to the petrochemical and refining industries. Catalysts that have been studied include vanadium, copper, and zinc sulfides (Chivers and Lau, 1987a); chromium, iron, and nickel sulfides (Chivers et al., 1980; Chivers and Lau, 1987b); tungsten disulfide (Fukuda et al., 1978); and molybdenum disulfide (Fukuda et al., 1978; Sugioka and Aomura, 1984; Katsumoto et al., 1973; Chivers and Lau, 1980, 1987a,b).

Molybdenum disulfide catalyst is considered the best performer by a number of investigators. Fukuda et al., (1978) studied low pressures (below 100 mm Hg) and high temperatures (930-1,470°F) and found that the rate of H_2S decomposition with MoS_2 catalyst was 8 to 50 times the uncatalyzed rate (Table 3) and approximately twice the rate obtained with the WS_2 catalyst. These results support those of Raymont (1975) in that the rate of thermal decomposition approximately equals that of the catalyzed decomposition as the temperature approaches 1,800°F.

Fukuda and co-workers maintained a closed loop of reactant H_2S and product hydrogen but condensed the product sulfur. With this technique, the amount of sulfur produced could be compared to the amount of hydrogen produced. These amounts were in stoichiometric agreement, verifying that the catalyst was not consuming sulfur during the reaction. Hydrogen built up in the

Table 3
CATALYTIC ACTIVITY OF MOLYBDENUM DISULFIDE CATALYST

Temperature (°F)	Initial Rate with MoS_2* (mol%/min)	Initial Rate without Catalyst (mol%/min)
930	0.08	—
1,020	0.35	0.007
1,290	4.37	0.13
1,380	7.20	0.30
1,470	9.15	1.10

*Unsupported MoS_2.
Source: Fukuda et al. (1978).

gas phase with time (reactions up to 20 hours long), generally to about 10 mol% after 5 hours. The rate of reaction was slowed with the buildup of hydrogen. Dispersion of MoS_2 onto an Al_2O_3 substrate and calcination at 2,080°F resulted in a catalyst that was approximately 30% more active than the unsupported MoS_2 catalyst.

Sugioka and Aomura (1984) also investigated H_2S decomposition with MoS_2 catalyst in a low pressure (45 mm Hg) system in the temperature range 930-1,470°F. MoS_2 catalyst prepared by evacuation at 500°C caused a decomposition rate of H_2S that was more than five times that of the uncatalyzed reaction. Furthermore, if the MoS_2 catalyst was reduced in the presence of H_2 prior to use, the activity increased by a factor of 2 above that of the evacuated catalyst. This result indicated that the fully sulfided state is not essential for molybdenum sulfides to act as catalysts. These authors pose a mechanism of H_2S decomposition that involves addition of H_2S to a vacant site on MoS_2 and then subsequent cleavage of the S-H bond, as illustrated in Figure 1. The rate limiting step is thought to be the desorption of the S atom from the MoS_2.

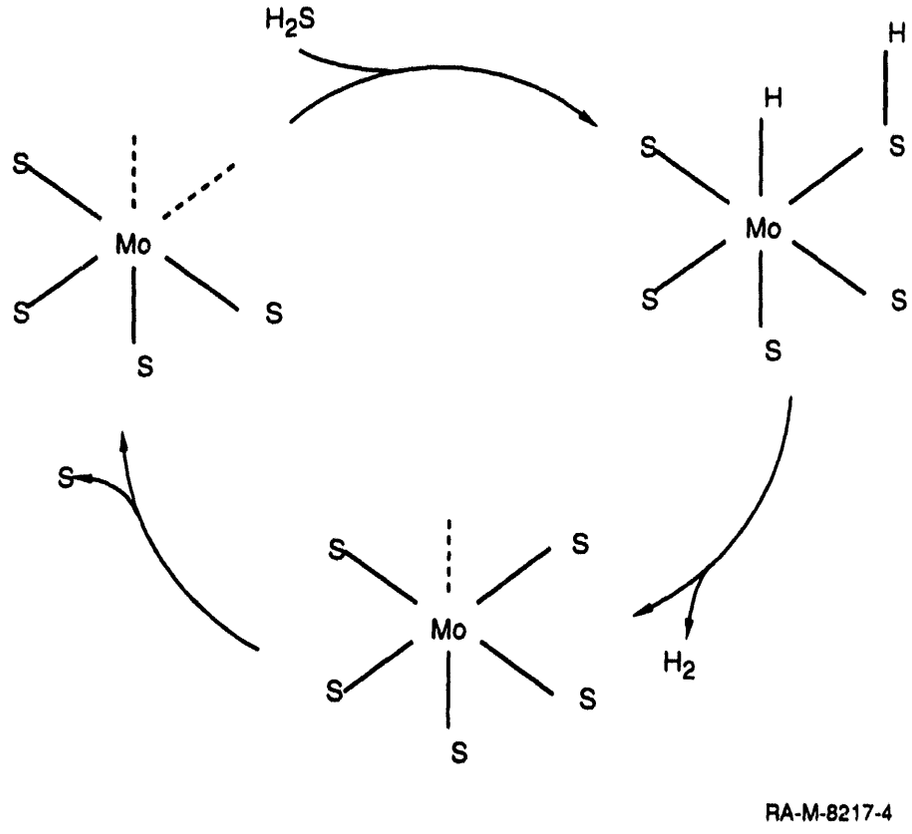

Figure 1. Postulated mechanism for catalysis of hydrogen sulfide decomposition by molybdenum disulfide.

SOURCE: Sugioka and Aomura (1984).

Chivers et al. (1980) reported studies of Cr_2S_3, MoS_2, WS_2, FeS_2, CoS_2, NiS_2, FeS, CoS, NiS, Cu_2S, Cu_9S_5, and CuS catalysts. Of these, only the Cr_2S_3, MoS_2, WS_2, and Cu_9S_5 catalysts remained unchanged after reaction (Table 4). The Cr_2S_3 and WS_2 catalysts were superior below 1,100°F, and the MoS_2 catalyst was superior above 1,100°F. The rate of conversion at 1,470°F with the MoS_2 catalyst was about 25% higher than that of the uncatalyzed (quartz blank cell) reaction.

Table 4
CRYSTAL PHASES BEFORE AND AFTER REACTION WITH H_2S

Original	After Reaction
MoS_2	MoS_2
WS_2	WS_2
Cr_2S_3	Cr_2S_3
FeS_2	Fe_7S_8
CoS_2	$CoS_{1.13\text{-}1.20}$
NiS_2	$NiS_{1.20}$
FeS	Fe_7S_8
CoS	$CoS_{1.13\text{-}1.20}$
NiS	$NiS_{1.20}$
Cu_2S	Cu_9S_5
Cu_9S_5	Cu_9S_5
CuS	Cu_9S_5

The literature on MoS_2 catalyst is unequivocal that MoS_2 is not consumed by reaction with H_2S. However, some investigators report that the ratio of catalyzed to uncatalyzed reactions approaches 1 in the neighborhood of 1,800°F. If such were the case, membrane reactors with uncatalyzed thermal decomposition would be as effective as catalyzed ones under some conditions of interest to DOE, and this situation would imply that there is a need for superior catalysts.

The literature offers no data on H_2S decomposition when the partial pressure of H_2 is 40-100 psia, as under IGCC conditions. There is, however, evidence that the presence of H_2 slows the net forward rate of reaction (e.g., in Figures 2, 3, and 4, Fukuda et al., 1978), but this observation is simply in accord with "mass action" concepts. The general problem of the high partial pressure of hydrogen will plague all membrane reactor concepts wherein a product of the reaction already exists in the feed gas.

CATALYTIC DECOMPOSITION OF AMMONIA

Krishnan et al. (1987) have published a comprehensive review of ammonia decomposition catalysis with approximately 40 references. The decomposition proceeds by five steps, in which adsorbed NH_x species form surface adstates of nitrogen atoms and hydrogen atoms, followed by desorption of N_2 and H_2:

$$NH_3\ (g) \rightarrow NH_2\ (a) + H\ (a) \quad (1)$$

$$NH_2\ (a) \rightarrow NH\ (a) + H\ (a) \quad (2)$$

$$NH\ (a) \rightarrow N\ (a) + H\ (a) \quad (3)$$

$$2H\ (a) \rightarrow H_2\ (g) \quad (4)$$

$$2N\ (a) \rightarrow N_2\ (g) \quad (5)$$

Metals that have been studied for this reaction include Co, Cu, Fe, Ir, Ni, Pd, Pt, Re, Rh, Ru, and W (Rostrup-Nielson, 1973; Taylor et al., 1974; Klimisch and Taylor, 1975; Friedlander et al., 1977a,b; Gates et al., 1979; Ertl and Huber, 1980; McCabe, 1980; Tsai et al., 1985). Metals with a moderate heat of formation, such as Ru, Co, Ir, and Ni are superior (Gates et al., 1979). This result derives from the mechanism of the decomposition, wherein the strength of the bond between the catalyst surface and the nitrogen adstate is very important (Krishnan et al., 1988).

The method of preparation and combinations of metals have an important influence on catalytic activity (Taylor et al., 1974; Klimisch and Taylor, 1975; Friedlander et al., 1977a,b). For example, reduction of Ni or Ru metals prior to reaction increases the catalytic activity with respect to oxides of the same metals. The presence of noble metals such as Pd or Ru allows Ni to be reduced more easily.

Steam, sulfur, and hydrogen can have various inhibiting or deleterious effects. Friedlander et al. (1977a,b) studied steam:ammonia ratios up to 12:1, at which point the inhibiting effect leveled off. Steam appears to have an effect on the reduction of nickel and thereby affects the catalytic sites. Hydrogen inhibits the forward reaction, but this effect declines substantially above 930°F (Tsai et al., 1985). Krishnan et al. (1988) examined the effect of H_2S and steam on various supported nickel, Ni/Ir, and Ni/Mn catalysts supported on alumina or $MgAl_2O_4$. At low temperatures (930°F), the catalysts were not very sulfur tolerant (Table 5). At 1470°F, the catalysts were sulfur tolerant (Table 6), but most had physical deterioration problems. The best catalysts were ones supported on $MgAl_2O_4$.

Table 5
DECOMPOSITION OF NH_3 ON VARIOUS CATALYSTS AT 550°C[a]

Catalyst	Steady State Conversion of NH_3 (%)	
	Low Steam-No H_2S	Low Steam-Low H_2S
Supported Ni (HTSR-1)[b]	33	<1
Supported Ni-1% Ir/(HTSR-2)[b]	80	<1
$Ni/MgAl_2O_4$ (R-67)[c]	<1	<1
Ni/Al_2O_3 (G-65)[d]	41	<1
$Ni\text{-}Ir/Al_2O_3$ (G-65*)[e]	71	55
$Ni\text{-}Mn/Al_2O_3$	<1	<1
$Co\text{-}Mo/Al_2O_3$	<1	<1
$ZnFe_2O_4$ with 10% NiO[f]	10	<1
$ZnFe_2O_4$ with 11% CuO[g]	<1	<1

[a]Low steam = 7.2%; low H_2S = 100 ppm; space velocity = 10,000 h^{-1} unless otherwise noted.

[b]HTSR is a high temperature steam reforming catalyst made by Haldor-Topsoe, A/S, Copenhagen, Denmark.

[c]R-67 is also made by Haldor-Topsoe, A/S.

[d]G-65 is a nickel-based methanation catalyst made by United Catalysts, Inc., Louisville, Kentucky.

[e]G-65* is an iridium-promoted version of G-65.

[f]Space velocity = 5,000 h^{-1}.

[g]Space velocity = 2,000 h^{-1}.

Source: Krishnan et al., 1988.

Table 6
DECOMPOSITION OF NH_3 ON VARIOUS CATALYSTS AT 800°C[a]

Catalyst[b]	Steady State Conversion of NH_3 (%)		
	Low Steam-Low H_2S	High Stream-Low H_2S	High Stream-High H_2S
Supported Ni (HTSR-1)	70	92	92
Supported Ni-1% ir (HTSR-2)	—	96	—
$Ni/MgAl_2O_4$ (R-67)	80	70	40
Ni/Al_2O_3 (G-65)	40	—	—
$Ni\text{-}Ir/Al_2O_3$ (G-65*)	—	90	—
$Ni\text{-}Mn/Al_2O_3$	50	38	25
MoS_2	70[c]	—	—

[a]Space velocity = 10,000 h^{-1}; low steam = 7.2%; high steam = 27.0%; low H_2S = 100 ppm; high H_2S = 3,000 ppm.

[b]Alumina supports contained about 7% CaO as the stabilizing agent.

[c]H_2S concentration = 3,000 ppm.

Source: Krishnan et al., 1988.

MEMBRANE REACTORS

Two perspectives exist in the literature of membrane reactors, one that views the reaction as a tool to enhance separation and one that views it as a tool to enhance the chemical conversion. A review by Armor (1989) emphasizes the second view. This review outlines work on hydrogenation, dehydrogenation, dehydrocyclodimerization, oxidation, and oxidative dehydrodimerization reactions and the use of membranes as catalyst supports. Substantial work has apparently been performed by Gryaznov and co-workers at the A.V. Topchiev Institute in the Soviet Union (Gryaznov, 1986; Gryaznov and Slinko, 1982; Mischenko et al., 1979). In one particularly interesting example, Gryaznov and Karavanov (1979) used a palladium-nickel tube to produce vitamin K_4 in a one-step hydrogenation of quinone and acetic anhydride.

Dehydrogenation of cyclohexane to form benzene has been a popular reaction to study in a membrane reactor (Shinji et al., 1982; Itoh et al., 1985; Mohan and Govind, 1986; Itoh et al. 1987; Sun and Khang, 1988). Because cyclohexane and benzene are fairly large molecules, Vycor glass tubes with a 40 Å pore size provide by Knudsen diffusion a sufficiently selective removal of the hydrogen formed. A platinum catalyst dispersed on alumina has typically been used for this reaction; temperatures have been in the range of 400°F, and the pressure has been atmospheric.

Literature focus on the use of membrane reactors to enhance separation has been on hydrogen sulfide removal (Kameyama et al., 1979, 1981a,b; Abe, 1987). Kameyama and co-workers employed Vycor glass tubular membranes with no catalyst in the temperature range 930°F to 1,470°F and pressures up to 60 psia. Kameyama et al. (1981b) also used an alumina membrane with 1,000 Å pores and a MoS_2 catalyst. At 1,470°F with a Vycor glass membrane, there was no difference in the extent of conversion with and without the MoS_2 catalyst. These investigators also ran a Vycor membrane for 216 hours at 1,100-1,470°F with no loss of performance. Abe (1987) used molybdenum sulfide beads as a catalyst in alumina membranes to decompose H_2S. By placing the catalyst in different areas in the membrane (inside the membrane tube, on the inside wall of the membrane tube), they were able to obtain different conversions. The temperature and pressure were near 1,470°F and 55 psia, respectively. Fukuda et al. (1978) simulated one feature of a membrane reactor in their study of H_2S decomposition with MoS_2 and WS_2 catalysts by continuously removing the sulfur and intermittently removing the product hydrogen.

The theory of tubular membrane reactors has been adequately expressed by Itoh et al. (1985) and by Mohan and Govind (1986). If plug flow is assumed, as these investigators did, the relevant differential equations are one-dimensional. When the catalyst is in the walls of the membrane rather than inside the membrane tube, the reaction rate terms must be included in the equations that describe the wall transport. This approach results in a second-order differential equation (Sun and Khang, 1988).

CATALYST DEVELOPMENT

On the basis of the literature survey presented previously, we selected two catalysts to prepare and evaluate for H_2S and NH_3 decomposition. For H_2S decomposition, we chose an alumina supported MoS_2 catalyst. MoS_2 was chosen because it significantly enhances the H_2S decomposition rate and is not consumed by reaction with H_2S. For NH_3 decomposition, we chose an alumina supported Ni catalyst because of its high catalytic activity and low cost relative to other catalysts.

CATALYST PREPARATION

We prepared both H_2S decomposition and NH_3 decomposition catalysts by imbibing alumina particles with an aqueous solution. The alumina particles were obtained from United Technologies, Inc., Louisville, KY (Product No. CS308). Particle diameters were between 246 μm and 833 μm (20/60 mesh). To make the MoS_2 catalyst for H_2S decomposition, we prepared an aqueous solution consisting of 8 g of ammonium molybdate ($[NH_4]_6\ Mo_7O_{24}\cdot 4H_2O$) dissolved in 40 mL of water. We added all of this solution to 50 g of alumina particles. This volume of solution was calculated to approximately equal the pore volume of the alumina particles. The wetted particles were dried overnight at room temperature and for 24 hours at 120°C, and then calcined at 400°C for 2 hours. The particles were sulfided by flowing a gas mixture of H_2S in H_2 (10% H_2S; 1 atm) over the particles while raising the temperature from room temperature to 400°C (at 150°C per hour). The temperature was held at 400°C for 2 hours, and then the oven was turned off. Nitrogen gas was introduced to purge the system, and the resulting 50 g of catalyst was stored under nitrogen.

The catalyst for ammonia decomposition was prepared similarly by imbibing an aqueous solution consisting of 21.5 g of nickel nitrate ($Ni(NO_3)_2\cdot 6H_2O$) in 40 mL of water into a fresh batch of alumina particles. The Ni solution was slowly added to 50 g of alumina particles. The particles were dried overnight at room temperature and at 120°C for 24 hours, and then calcined at 400°C for 2 hours. The particles were then placed in a tube and exposed to hydrogen at 1 atm pressure. The gas temperature was raised at 150°C per hour to 400°C and held at 400°C for 2 hours. The oven was turned off, the system was purged with nitrogen, and the resulting 50 g of catalyst were stored under nitrogen.

CATALYST PERFORMANCE

H_2S Decomposition

The apparatus we used to measure the activity of the H_2S catalyst is shown in Figure 2. A gas mixture (for example, 0.5% H_2S, balance He) was passed through a tubular reactor where the H_2S decomposed. The product gas was analyzed by gas chromatography. By varying the flow rate and measuring the extent of H_2S decomposition, we obtained reaction rate coefficients. These rate coefficients were used in our computer model to simulate the membrane reactor performance. To provide temperature control over the reaction conditions, the reactor was held in a furnace capable of 800°C operation (Applied Test Systems Series 3210). Gas exiting the furnace was cooled to capture sulfur (if any) and to allow injection into the chromatograph. Reactor pressure was maintained as high as 500 psig with a back pressure regulator. The stainless steel reactor tube was 7.0 mm I.D. (9.5 mm O.D.) and 30.5 cm long. The residence time in this reactor varied depending upon the feed flow rate, temperature, and porosity of the catalyst; typically we had residence times of 2 to 10 seconds in our experiments.

Three grams of the MoS_2 catalyst were placed in the reactor tube, and a feed gas mixture (0.5% H_2S in He) was passed over the catalyst particles. We varied the temperature of the reactor between 400°C and 700°C. The reactor pressure was maintained at 200 psia. The feed gas flow rate was held constant at either 250 standard cubic centimeters per minute (sccm) or 470 sccm; the residence time was about 4 seconds at the lower flow rate and about 2 seconds at the higher flow rate (Figure 3). At higher temperatures more than 60% of the H_2S was decomposed, whereas below 400°C no decomposition could be measured (Figure 4). The fact that the fractional conversion was practically the same with either flow rate (and therefore with either residence time) suggests that the reaction time is less than 2 seconds.

To ensure that the reduction in H_2S concentration as the gas passes through the reactor is due to catalytic decomposition and not to an irreversible reaction with the catalyst (e.g., $H_2S + MoS_2 \rightarrow H_2 + MoS_3$, resulting in consumption of the catalyst), we ran our H_2S decomposition tests for a total of 14 hours. During this time, the number of moles of H_2S decomposed was approximately 20 times more than the number of moles of MoS_2 present at the outset of the test. For example, during one run at 650°C, the moles of H_2S decomposed exceeded the moles of MoS_2 present by a factor of 10 (Figure 5). The fractional conversion was constant (within experimental error) for this 400-minute run. We also measured the catalytic activity of the catalyst support particles (alumina) without the MoS_2 catalyst. At temperatures up to 800°C and a residence time of

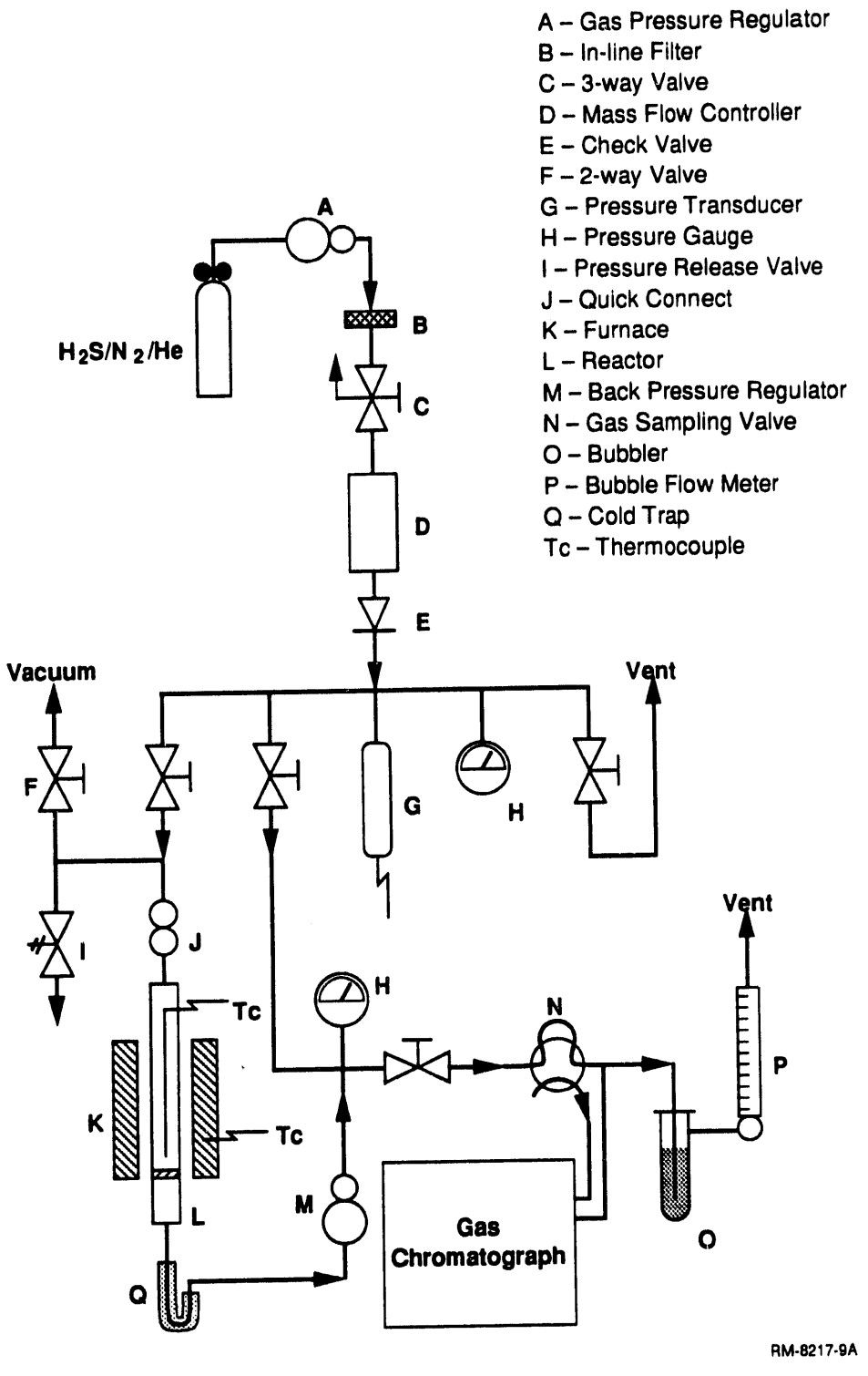

Figure 2. Test system for catalyst activity measurement.

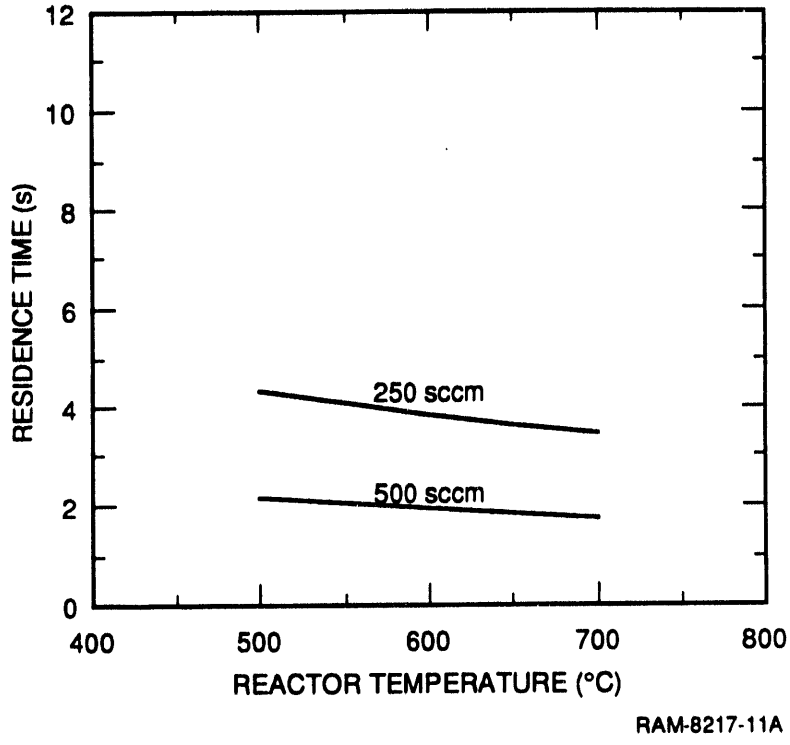

Figure 3. Reactor residence time at feed pressure of 200 psia, various flow rates.

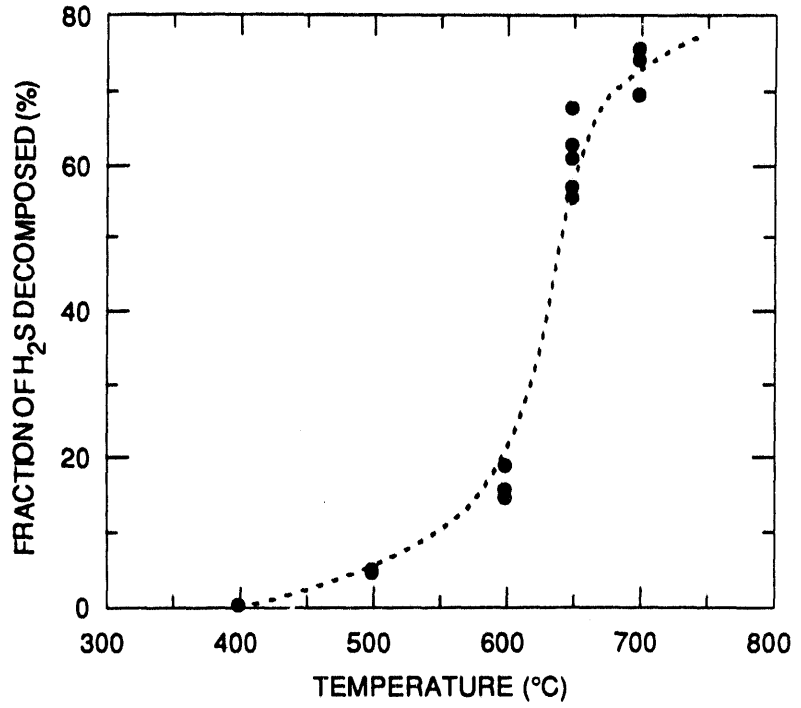

(a) Feed gas flow rate was 250 sccm (residence time near 4 seconds)

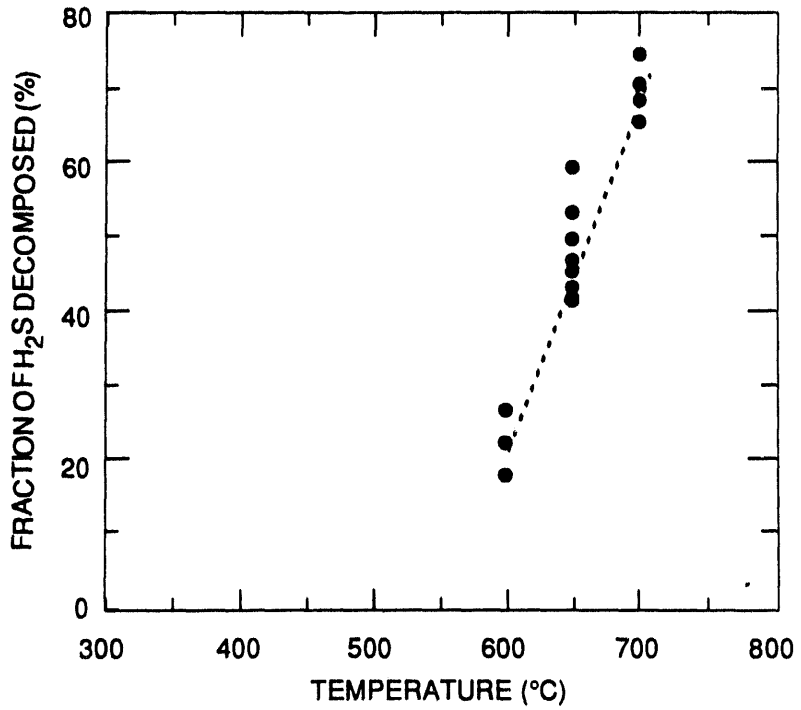

(b) Feed gas flow rate was 470 sccm (residence time near 2 seconds)

RAM-8217-10

Figure 4. Decomposition of H_2S on MoS_2 catalyst.

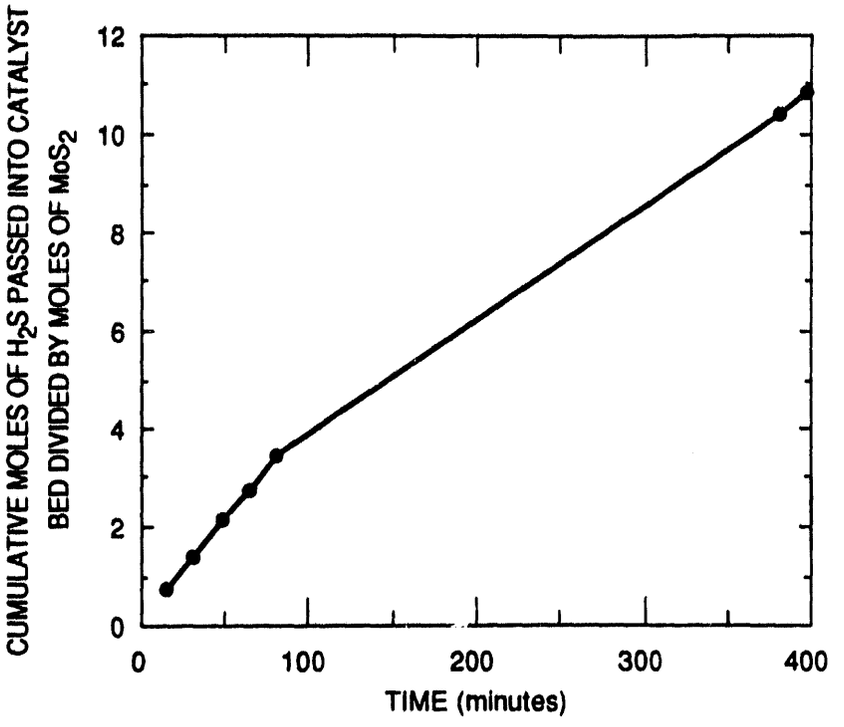

(a) Ratio of H_2S decomposed to MoS_2 in reactor

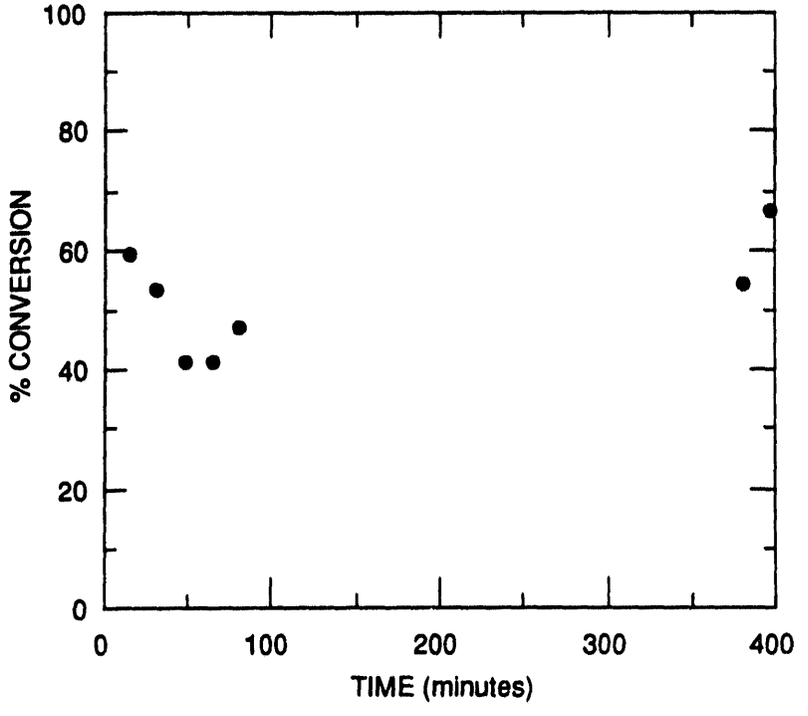

(b) Fractional decomposition of H_2S

RAM-8217-12B

Figure 5. Analysis of catalytic activity of MoS_2.

This one run at 650°C followed 71/2 hours of catalyst use at various temperatures. (flow rate changed at 90 minutes; see Figure 5a)

about 4 seconds (total pressure 200 psia), there was no detectable decomposition of H_2S, indicating that the native alumina particles had no catalytic activity and, further, that the rate of thermal decomposition was negligible. These results show that decomposition of H_2S in our reactor is caused entirely by the activity of the MoS_2 catalyst.

We estimated the reaction rate coefficient for H_2S decomposition using data from Figure 4a. In using these data, we assumed that the reaction was first-order and that there was no significant reverse reaction during the experiments. The data used to determine the reaction rate coefficient are included in Table 7. The reaction rate coefficient is given as a function of temperature by

$$k_1 = 305\ s^{-1} * \exp(-7790\ K/T) \tag{6}$$

The reaction rate is given by

$$r = \varepsilon\, k_1 \left(\frac{P_T}{RT}\right)\left[X_{H_2S} - \left(\frac{P_T}{RT}\right)^{1/2} \frac{X_{H_2} X_{S_2}^{1/2}}{K_{eq} \cdot (1\ atm^{-1/2})}\right] \tag{7}$$

where

r	=	Reaction rate (mol/m^3)
ε	=	Catalyst bed porosity
k_1	=	H_2S reaction rate coefficient (s^{-1})
P_T	=	Total pressure (atm)
R	=	Gas constant
T	=	Temperature (K)
X	=	Mole fraction
K_{eq}	=	Equilibrium coefficient

Table 7
DATA USED TO DETERMINE H_2S REACTION RATE COEFFICIENT

Temperature (°C)	Reaction Time (s)	Fraction of H_2S Decomposed (%)	Reaction Rate Coefficient (s^{-1})
500	4	5.1	1.28×10^{-2}
600	4	16.2	4.06×10^{-2}

NH_3 Decomposition

Preliminary measurements of the ammonia decomposition catalyst activity were made with 1.0 g of catalyst in the reactor system described above for H_2S decomposition. An alumina reactor tube (3.2 mm I.D., 6.4 mm O.D., 22.9 cm long) was used because we expected the walls of the membrane reactor would be alumina, and stainless steel has catalytic activity for NH_3 decomposition. To show that the observed NH_3 decomposition was due to activity of the catalyst and not to activity of the catalyst support or to thermal decomposition, we performed experiments with the tube packed with Ni catalyst and packed with the catalyst support (alumina) only.

A feed gas mixture of 0.3% NH_3 and 0.3% Ar[1] (balance helium) was passed through the reactor at a flow rate of 250 sccm and 200 psig. The residence time in the catalyst bed varied from 1.2 to 1.8 seconds over the temperature range 400°C to 700°C. With the Ni catalyst in the reactor, we observed no NH_3 decomposition below 400°C; above this temperature, the fractional conversion rose sharply to about 40% at 500°C and then increased gradually as the temperature was increased to 650°C (Figure 6). The figure shows that the catalyst greatly increases the NH_3 decomposition rate.

Our subcontractor, Oregon State University (OSU), conducted a more detailed analysis of the thermal decomposition of NH_3 between 500°C and 750°C and at various pressures. We found no detectable decomposition below 650°C, but at 750°C we found 4% and 9% decomposition for pressures of 250 psig and 500 psig, respectively. The feed gas was a mixture of 2750 parts per million (by volume) NH_3 in He at a flow rate of 300 sccm.

Studies on the decomposition of NH_3 using the nickel-based catalyst provided by SRI were also conducted by OSU over a wide range of temperatures and pressures. Figure 7 is a schematic of the OSU reactor, which consisted of a catalyst bed inside a quartz U-tube. The inside diameter of the tube in the catalyst bed section was 3 mm in some experiments and 6 mm in other experiments. The reactor was operated in the differential mode by keeping the NH_3 conversion below about 5%. Since the conversion is low, it is valid to assume a constant decomposition rate in the reactor.

[1] Argon serves as an internal standard. With equimolar concentrations of NH_3 and Ar in the feed gas, full conversion of the NH_3 produces a hydrogen/argon ratio of 1.5.

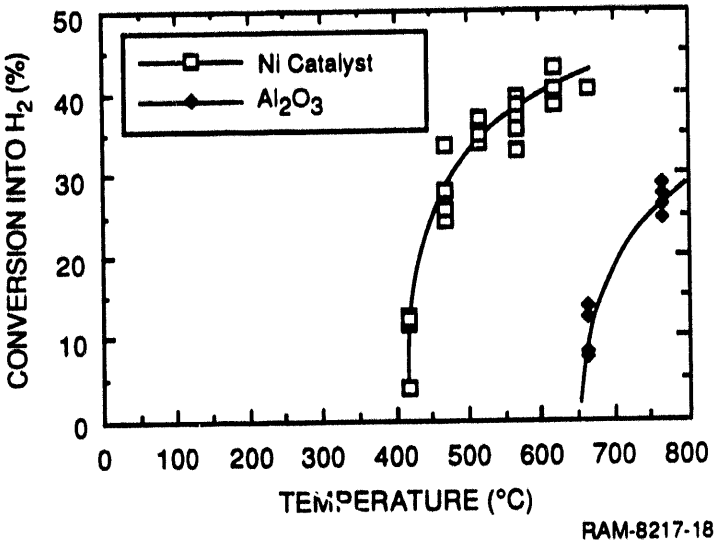

Figure 6. Extent of NH_3 conversion to hydrogen for alumina tube reactor with alumina particles and with catalyst particles.

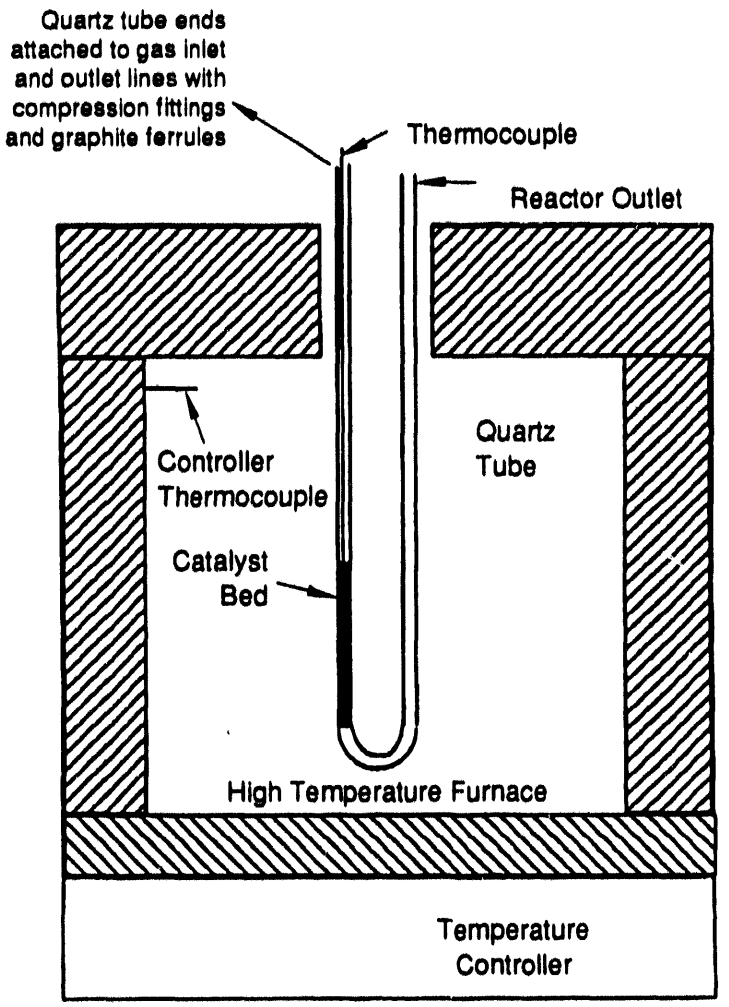

Note: Drawing is not to scale.

RM-8217-35

Figure 7. Catalytic reaction system for kinetic experiments.

Because the objective of the kinetic experiments was to measure the rate of decomposition on the catalyst surface, it is important to minimize the effect of interphase and intraparticle mass transfer on the measured reaction rates. Intraparticle mass transfer resistance was minimized by using small catalyst particles (595-850 μm). Unfortunately, the small catalyst particles and low flow rates typically used in laboratory scale reactors often result in significant interphase mass transfer resistance, especially when reactants are present at dilute concentrations (Satterfield, 1980). Interphase mass transfer resistance is readily detected in a differential reactor by varying the gas flow rate at constant inlet gas conditions. It is indicated by an increase in the observed reaction rate with increasing flow rate.

Figure 8 shows the results of an experiment designed to detect the presence of interphase mass transfer resistance. This experiment was conducted at a temperature of 673 K and pressure of 35 atm in the 6-mm-I.D. quartz tube. The NH_3 and H_2 mole fractions in the inlet gas were 0.0053 and 0.018, respectively. Since the observed reaction rate increases with increasing flow rate (Re_p), interphase mass transfer resistance is present at the lower flow rates but not in the region where the observed reaction rate is independent of flow rate. Similar experiments were conducted each time inlet gas conditions were changed, to ensure that data were collected in the region where the reaction rate was independent of flow rate. As temperature and the resulting reaction rate increased, it was necessary to increase the H_2 mole fraction to obtain data free from interphase mass transfer effects. The 3-mm-I.D. quartz tube was used at the higher temperatures to increase the gas velocity in the catalyst bed, the result being a decrease in the interphase mass transfer resistance. All data used to determine the kinetic parameters were from the region where the observed reaction was independent of flow rate. Data were not collected at temperatures higher than 823 K because the reaction rate was so high that collection of data free from interphase mass transfer resistance was extremely difficult. Selected results from these kinetic studies are illustrated in Figures 9 through 11.

The kinetic data were fit to a rate equation based on a modified Temkin-Pyzhev mechanism (Satterfield, 1980; Nielson, 1971). The rate equation written in terms of the rate of NH_3 generation is as follows:

$$1.5\ H_2 + 0.5\ N_2 \leftrightarrow NH_3 \tag{8}$$

$$r_A = k\left[\frac{f_N}{K_{eq}^2}\left(\frac{f_H^3}{f_A^2}\right)^{1-\beta} - \left(\frac{f_A^2}{f_H^3}\right)^{\beta}\right] \tag{9}$$

where

$$k = k_o \exp[E_a + E_b P]/RT \tag{10}$$

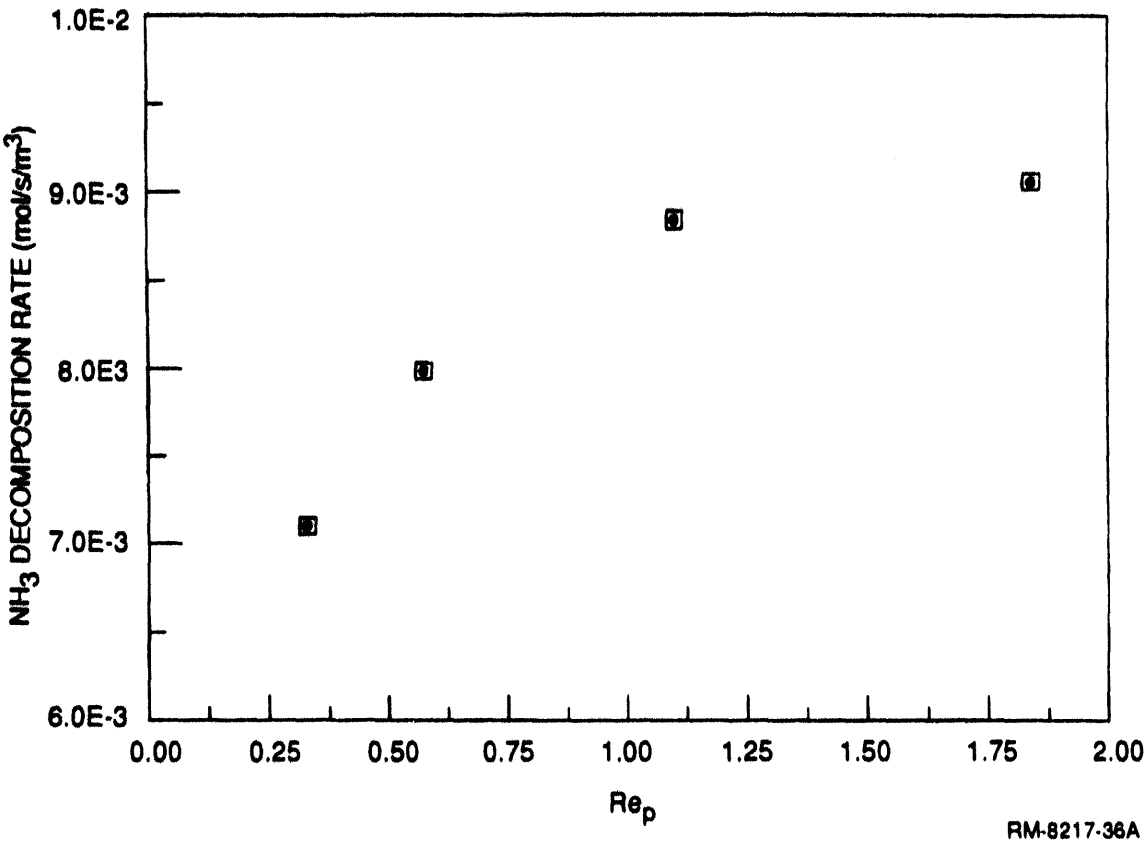

Figure 8. Effect of flow rate on NH_3 decomposition rate.

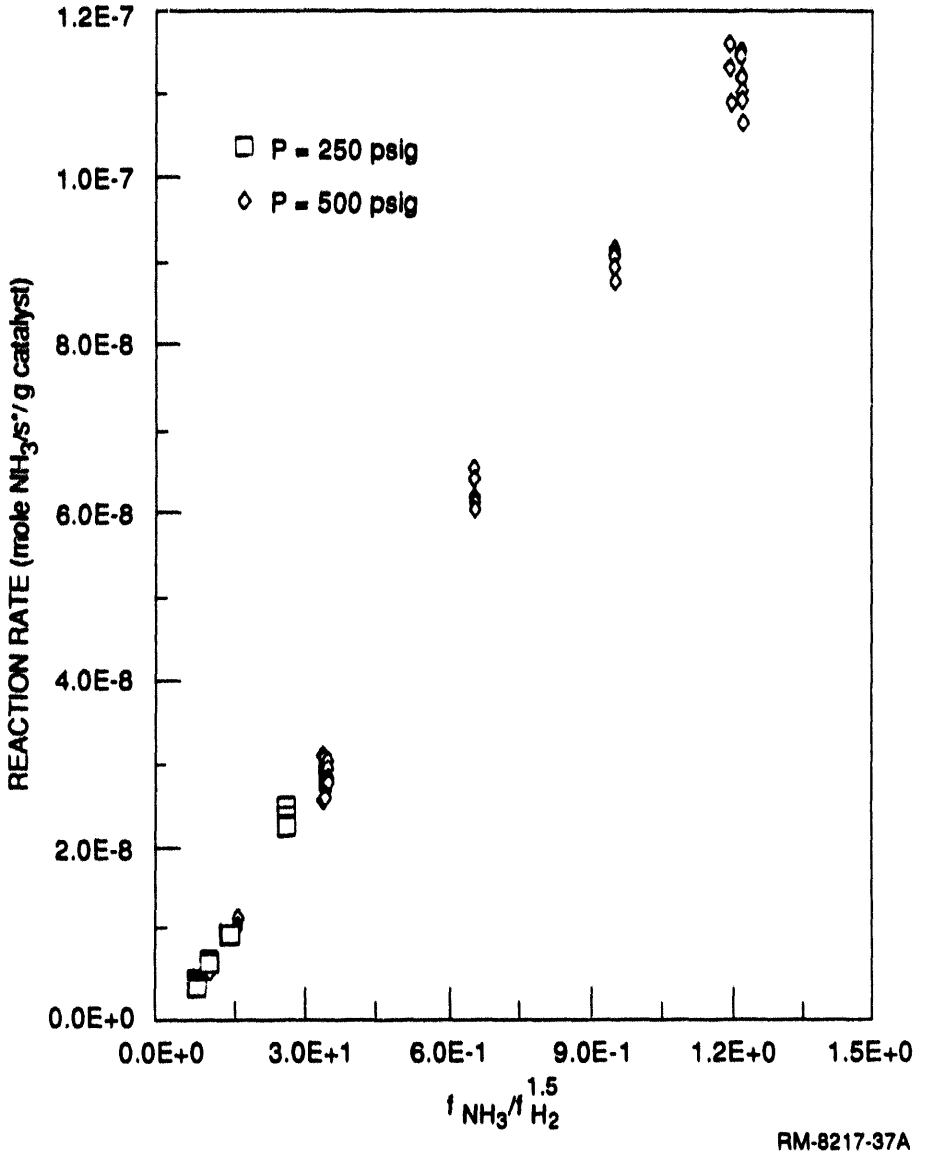

Figure 9. Ammonia decomposition rate data (400° C).

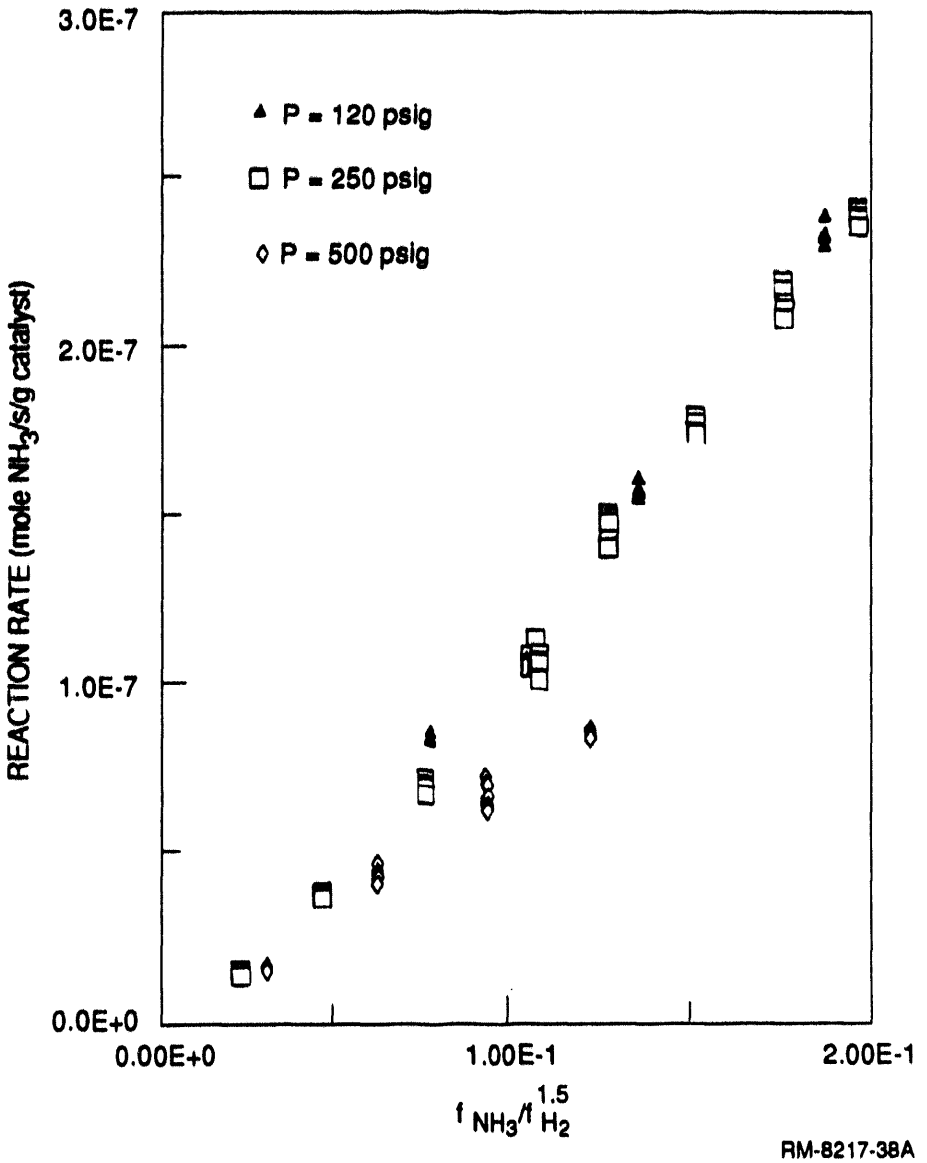

Figure 10. Ammonia decomposition rate data (450° C).

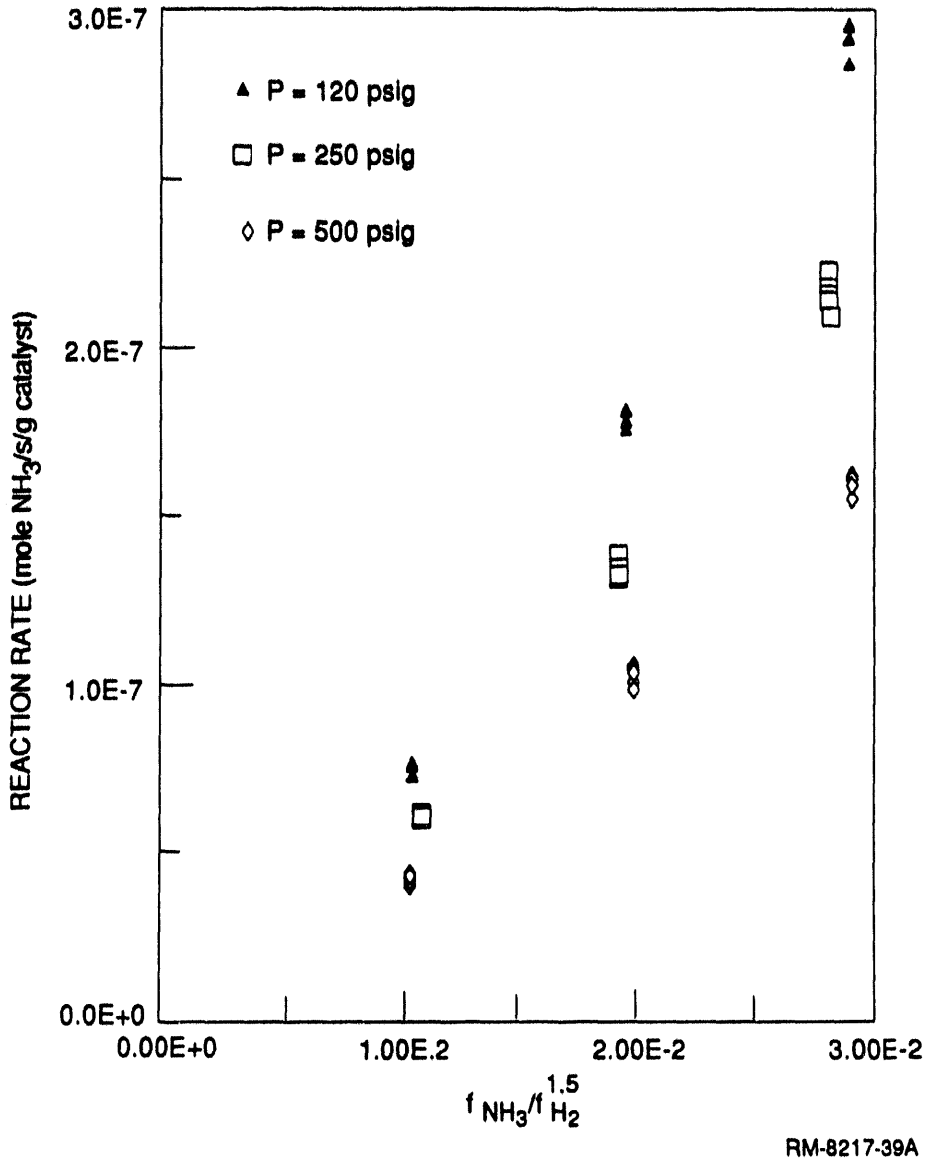

Figure 11. Ammonia decomposition rate data (500° C).

and

$$K_{eq} = \frac{f_N^{0.5} f_H^{1.5}}{f_A} \tag{11}$$

The first term within the brackets of the rate equation is the rate of ammonia synthesis, while the second term is the rate of ammonia decomposition. Fugacities are used to account for deviation from ideal gas behavior at high pressure operation.

There are four kinetic parameters that must be determined: the pre-exponential factor (k_o), the activation energy parameters (E_a, E_b), and β. The kinetic parameters were obtained by multiple linear regression analysis of the rate data. A value of 0.654 was obtained for β. The resulting relationship for the rate constant is

$$k \left(\frac{\text{mol}}{\text{m}^3 \text{ - s - atm}^{-\beta}} \right) = 4.902 \times 10^{15} \exp\{-[2.157 + 1.16 \times 10^{-3} P]/RT\} \tag{12}$$

Figure 12 presents a plot comparing the observed reaction rate and the reaction rate predicted from the modified Temkin-Pyzhev equation with the measured kinetic parameters. The agreement is very good—correlation coefficient (r) = 0.994.

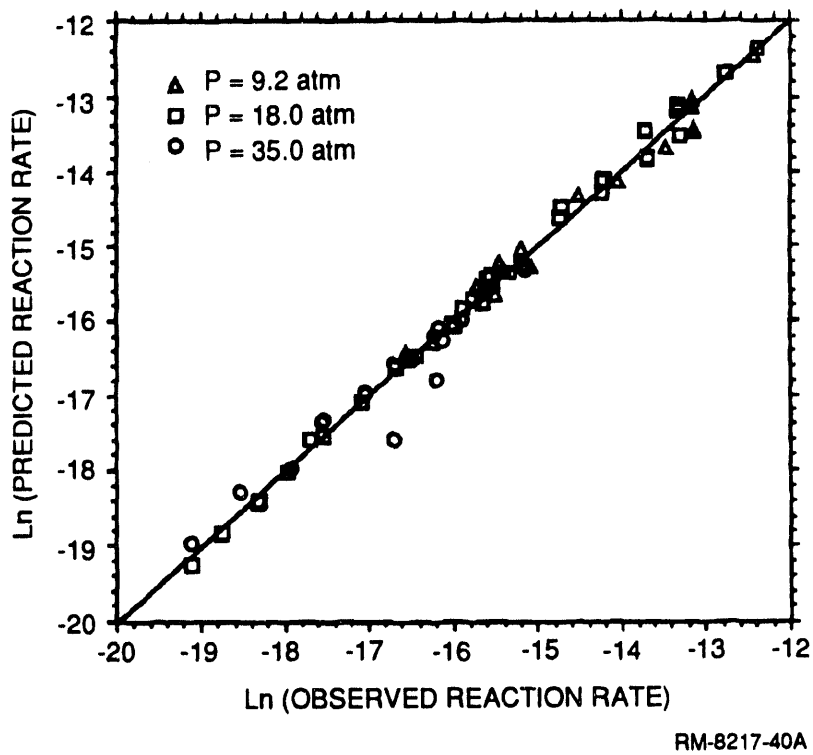

Figure 12. Comparison of observed reaction rates and those predicted from the modified Temkin-Pyzhev equation.

MEMBRANE DEVELOPMENT

A critical part of the membrane reactor is the membrane itself. The hostile thermochemical environment (1000°F to 2000°F, 200 psia to 1000 psia, 20% or higher water vapor content, thousands of parts per million H_2S) puts severe limitations on the selection of suitable materials. For example, all organic materials are immediately eliminated from consideration.

Some nonmetallic inorganic membranes exhibit an ability to separate gases on the basis of the Knudsen mechanism. The Knudsen mechanism, however, imparts a very low selectivity (e.g., 3.74 for H_2 over N_2) and is commercially irrelevant (despite the operation by the U.S. Government and others of uranium enrichment by way of Knudsen separation of $^{235}UF_6$ from $^{238}UF_6$).

Some inorganic barriers have recently been shown to exhibit remarkable permselectivity at room temperature (Roberts et al., 1992; Koresh and Sofer, 1987). At temperatures above 700°F, however, there is a decrease in performance and a loss in stability. These membranes are thought to contain pores in the size range 3 Å to 5 Å and are thought to function as a "molecular sieve," allowing smaller gas molecules to permeate and retaining others. At 300°F, hydrogen/nitrogen selectivities greater than 1000 have been observed. Films of a variety of metals permeate hydrogen and essentially nothing else (Barrer, 1951). It is these "molecular sieve" films or hydrogen permeable dense films that are essential for a membrane reactor to function in the decomposition of H_2S and/or NH_3.

To try to make a suitable membrane, we used four different substrates (alumina microfilter monolith, alumina microfilter disks, alumina ultrafilter tubes, and Vycor glass) and five different coating materials (poly N-methyl silazane, polycyclohydridomethyl silazane, an alumina-based glaze, aluminum phosphorus oxides, and palladium). Only the palladium films on an alumina ultrafilter were successful. The other approaches were plagued with cracks and poor reproducibility. We explain below the methods used for making each type of membrane and the results.

PALLADIUM FILMS ON ALUMINA ULTRAFILTERS

Uemiya et al. (1988) demonstrated the high flux of hydrogen through a palladium-on-Vycor composite membrane [effective H_2 permeance of 3×10^{-3} $cm^3(STP)/cm^2$ s cm Hg, 500°C, 3 atm partial pressure of H_2 on feed side, 1 atm partial pressure H_2 on permeate side]. This permeation rate is only a factor of 3.3 lower than that of hydrogen through a nanoporous, asymmetric alumina membrane (Okubo et al., 1991) and exceeds that of commercially

available polymer membranes and of experimental TiO_2/Vycor membranes (Table 8). It would be possible to have a highly advantageous membrane, then, if we could put a palladium film on a substrate that would be industrially robust under the planned operating conditions.

Other metals (Ti, Ni, V, and Mo) have reasonable hydrogen permeation properties above 1000°F, but we chose palladium because with palladium we can prove the principle of a metal-on-ceramic membrane and because palladium was either more chemically compatible with the feed gas or more permeable to hydrogen than other metals. We believe the problem of hydrogen embrittlement of Pd can be avoided in operation by not adding hydrogen to the system at temperatures below 500°F and by degassing the membrane before cooling. In this way, the formation of the "β-phase" in the H-Pd phase diagram can be avoided (Wise, 1968). Sulfur contamination, however, would likely keep pure Pd films from being used in commercial practice. Platinum membranes are more resistant to sulfur but have a low H_2 permeability; commercial membranes are likely to be made from a platinum/palladium alloy to achieve sulfur resistance and high H_2 permeability.

Table 8
COMPARISON OF PERMEATION RATES OF HYDROGEN THROUGH COMMERCIAL AND LABORATORY MEMBRANES

Membrane	H_2 Permeance $\left(\frac{cm^3(STP)}{cm^2 \cdot s \cdot cm\ Hg}\right)$	$\alpha(H_2/N_2)$	Temperature (°C)	Reference/ Investigator
Cellulose ester, spiral wound module	2×10^{-4}	67	25	W. R. Grace product literature
Asymmetric Al_2O_3 ceramic membrane, 50-Å pores, 5-μm top layer	9.6×10^{-3}	3.7	---	Okubo et al., 1991
Pd/Vycor composite, 13-μm Pd layer	2.88×10^{-3}	Infinite	500	Uemiya et al., 1988
TiO_2/Vycor composite, 30-minute reaction time	2.2×10^{-5}	200	450	G. R. Gavalas, California Institute of Technology

Preparation of Palladium Films by Electroless Plating

Metallic palladium can be precipitated onto a substrate by reacting a palladium amine complex with a reducing agent (Rhoda, 1959):

$$Pd(NH_3)_6^{+} + NH_2NH_2 \rightarrow Pd^{o} + XX \qquad (13)$$

There is a considerable amount of folklore associated with putting a high quality Pd film on the surface of a ceramic substrate. Surface activation is a key element of achieving adherence of the precipitated Pd. The goal of activation is to atomically disperse a monolayer of Pd onto the surface so that precipitated Pd finds a compatible surface on which to deposit. Activation consists of immersing the surface in a sensitizing bath that contains stannous (Sn^{+2}) and stannic (Sn^{+4}) chloride and then immersing it in an acidic $PdCl_2$ bath. The sensitizing bath is prepared by aging a $SnCl_4$ solution for several days and then adding this solution to an $SnCl_2$ solution.

Preparation of the metal-ceramic membranes developed in this study involves four steps:

- Bath/solution preparation
- Membrane pretreatment
- Membrane activation
- Plating.

Each of these steps is described below.

Bath/Solution Preparation

Three baths are used in the membrane preparation process:

- Sensitizing bath
- Activation bath
- Plating bath.

One or more solutions are required to make each bath. Recipes for preparing the solutions and baths are presented below.

Sensitizing Bath Preparation. Two solutions are used to make the sensitizing bath used during membrane activation. One solution is a 0.1 M solution of $SnCl_4 \cdot 5H_2O$ in H_2O and the other is a 2.6 M solution of $SnCl_2 \cdot 2H_2O$ in concentrated (37 wt%) HCl.

The recipe for preparing the 0.1 M solution of $SnCl_4 \cdot 5H_2O$ is as follows:

- Dissolve 20.9 g of $SnCl_4 \cdot 5H_2O$ in 1000 mL of De-ionized H_2O
- Allow the solution to age for one week.

After about one week of aging, a colloidal solution is formed. This solution can be stored indefinitely before it is used to make the sensitizing bath.

The 2.6 M solution of $SnCl_2 \cdot 2H_2O$ is prepared by dissolving 587 g of $SnCl_2 \cdot 2H_2O$ in 780 mL of concentrated HCl. The volume of the resulting solution is about 1000 mL and the HCl concentration is around 9.4 M. This solution can be stored indefinitely.

The volume of the sensitizing bath used in the activation process is 110 mL. This bath is prepared about 1 to 2 hours prior to the activation process. The recipe is as follows:

- Add 96.25 mL of DIH_2O to bath container
- Add 8.25 mL of aged $SnCl_4 \cdot 5H_2O$ solution to the DIH_2O
- Add 5.5 mL of the $SnCl_2 \cdot 2H_2O$ solution.

The bath container is just a glass jar or beaker. After the bath is prepared, it is periodically shaken prior to use to keep the colloidal suspension evenly distributed. The shelf life of the sensitizing bath is not known. We use fresh sensitizing bath each day.

Activation Bath Preparation. The activation bath is a dilute acidic solution of $PdCl_2$. The recipe for the solution used to make this bath is as follows:

- Add 5 mL of concentrated HCl to 995 mL of DIH_2O
- Add 0.267 g of $PdCl_2$
- Allow solution to sit for several hours to dissolve $PdCl_2$.

The resulting solution can be stored indefinitely. This solution can be used as is for the activation bath, or it can be diluted with DIH_2O. We generally dilute the solution with equal parts of DIH_2O and use this as the activation solution. A fresh activation bath is used each day.

Plating Bath Preparation. Palladium is used in the form of tetraammine chloride, $Pd(NH_2)_4Cl_2$, in the plating bath. The tetraammine complex is prepared by adding 28 wt% NH_3 to an acidic $PdCl_2$ stock solution. The $PdCl_2$ stock solution is prepared as follows:

- Add 20 mL of concentrated HCl to 980 mL of DIH_2O
- Add 10 g of $PdCl_2$ to the acidic solution
- Allow solution to sit for several hours to dissolve $PdCl_2$.

The resulting solution can be stored indefinitely prior to use.

The tetraammine complex solution is prepared in the following manner:

- Add 120 mL DIH_2O to 1000 mL of $PdCl_2$ stock solution
- Slowly add 715 mL of 28 wt% NH_3
- Allow solution to sit for 2 to 3 days.

Following addition of the NH_3, a pink precipitate is formed in the solution. The precipitate completely redissolves in 2 to 3 days. The resulting complex solution can be stored indefinitely.

We use plating baths that are 25 mL in volume. The plating baths are prepared as follows:

- Add 1.75 g of Na_2EDTA to 25 mL of complex solution
- Allow solution to sit at least 45 minutes before plating
- Add 0.25 mL of 1.0 M hydrazine just before plating.

The hydrazine is added right before the membrane is put in the plating solution.

Membrane Pretreatment

The ceramic membranes used in this study are the T170 ceramic filters from U.S. Filter Corporation. Filters are available in lengths of 25 to 75 cm. Prior to plating, the filters are cut to the desired length of 5 to 6 cm with a diamond saw, sanded, and cleaned. After cleaning, each end is sealed with Aremco 617.

Application of the Aremco 617 end seals increases the O.D. of the ceramic filter. If the O.D. is not decreased before sealing, the filters are too big to fit in the Swagelok unions used in the membrane testing apparatus. The O.D. is decreased by sanding the outside of the ceramic tube. The 10-mm-O.D. ceramic tube is secured in a 10-mm to 1/4 in. Swagelok reducing union with nylon ferrules. A 1/4 in. O.D. stainless steel tube is attached to the other end. The stainless steel

tube is then put in a drill chuck. The drill is set to a low speed and the outside of the tube is gently sanded until the O.D. of each end is about 9.8 mm.

After sanding, the ceramic tubes are cleaned. Cleaning involves the following steps:

- Ultrasonic rinse in DIH_2O for 5 minutes
- Ultrasonic rinse in alkaline solution for 5 minutes
- Rinse with cold DIH_2O for 1 minute
- Soak in 25 wt% acetic acid for 5 minutes
- Ultrasonic rinse in cold DIH_2O for 3 minutes
- Ultrasonic rinse in 60°C DIH_2O for 1 minute
- Rinse in 60°C DIH_2O for 1 minute
- Ultrasonic rinse in isopropyl alcohol for 5 minutes.

The alkaline cleaning solution is prepared as follows:

- Dissolve 0.25 g Alconox in 250 mL of 50°C DIH_2O
- Add 10 mL of 28 wt% NH_3
- Add 250 mL of cold DIH_2O.

After cleaning, the ceramic tubes are ready for application of the Aremco 617 sealant to the ends. The end seals are needed to prevent bypassing of gas through the porous support at the membrane inlet. The sealant is applied about 0.5 to 1.0 cm from the ends on the inside of the tube, around the outer rims, and about 1.5 to 2.0 cm from the ends on the outside of the tube. The sealant application lengths on the metal-ceramic membrane tested from 7 September 1992 to 9 September 1992 were 0.5 cm on the inside and 2.0 cm on the outside of the tube.

Sealant is applied with a fine paint brush. The curing schedule is as follows:

- Cure at room temperature for 1 hour
- Heat to 780°C at 6°C/minute ramp rate
- Hold oven at 780°C for 15 minutes
- Allow oven to cool naturally back to around 100°C.

The sealing procedure is repeated so that two coats of Aremco 617 are applied to each membrane.

Membrane Activation

Prior to plating, the inside surface of the membrane must be uniformly seeded with Pd crystals. The seeding process is performed in a sensitizing bath and an activation bath. To prevent activation of the outside surface of the membrane, Teflon tape is wrapped several times around the tube. The membrane is then activated in the following manner:

- Soak in sensitizing bath for 5 minutes
- Rinse with DIH_2O
- Soak in activation bath for 5 minutes
- Rinse with DIH_2O
- Repeat until membrane is uniformly activated.

Both the sensitizing and activation baths are at room temperature. The process is generally repeated 3 to 5 times, until the surface is uniformly activated. The activated surface is light brown in appearance. Following activation, the Teflon tape is removed and the membrane is rinsed in DI H_2O.

Membrane Plating

Teflon tape is wrapped several times around the outside of the tube to protect the sealant from the plating bath. The membrane is then placed in the plating bath just after the addition of hydrazine. The plating bath container is a 30 mL glass vial with a screw-on cap. After addition of the membrane, the cap is loosely screwed back on the container and then the container is put in a 75-80°C water bath. The vial is gently shaken about once every 15 minutes. The membrane is removed from the bath after 1 hour, rinsed off, and fresh Teflon tape applied. It is then placed in a fresh plating bath for another hour of plating. The process is repeated until the desired Pd film thickness is obtained. Approximately 2.5 μm of Pd is deposited per hour when 6-cm samples are plated using this procedure. The membrane tested on 7 September 1992 to 9 September 1992 was plated for 7.5 hours to obtain a 20 μm Pd film.

After plating, the membrane is rinsed and then dried at 110°C. An estimate of the Pd film thickness is obtained from the difference in the initial and final membrane weights, or by microscopic examination.

Palladium Membrane Results

A shell and tube test apparatus was used in the permeation experiments (Figure 13). The active length and area of the membrane were approximately 5 cm and 11 cm^2, respectively. The I.D. of the composite membrane was 0.7 cm and the O.D. was 1 cm. The membrane was sealed with Swagelok unions and ferrules made from Grafoil tape. A 10-mm to 1/4 in. reducing union was used to connect the membrane to 1/4 in. O.D. ceramic tubing. Graphite ferrules were used for the ceramic tubing. The resulting assembly then became the tube side in the shell and tube membrane permeation apparatus.

Permeation experiments were performed on three individual membranes (Table 9). The H_2 permeation rates for the three membranes at 823 K are shown in Figure 14. Membrane 1 had the highest permeability but failed after five experiments. The results indicate that the H_2 permeation rate for Membranes 1 and 2 are dependent upon pressure to the 0.5-0.6 power, very close to that expected from Sievert's law (Hwang and Kammermeyer, 1984). (Sievert's law suggests a rate dependance upon pressure to the 0.5 power.) The permeation rate of Membrane 3 was dependent upon pressure to the 0.7 power because of rate limitations caused by a layer of impurities that was deposited on the membrane during the experiments.

Table 9

MEMBRANES USED IN PERMEATION EXPERIMENTS

Membrane	Pd Thickness (μm)	Ceramic Support Pore Size	Permeability at 823 K $\left(\frac{mol\text{-}m}{s\text{-}m^2\text{-}kPa^{0.55}}\right)$
1	20	100 Å	4.7×10^{-7}
2	17	0.2 μm	4.0×10^{-7}
3	19	0.2 μm	2.7×10^{-7}

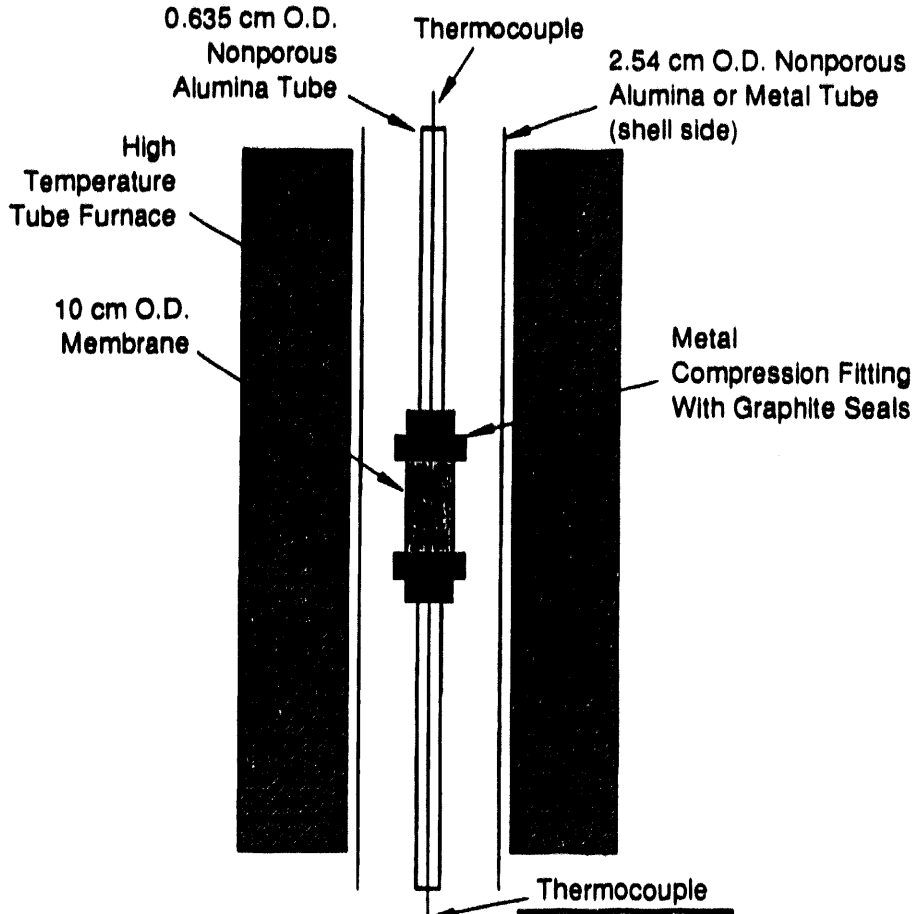

Figure 13. Shell and tube test apparatus for permeation tests.

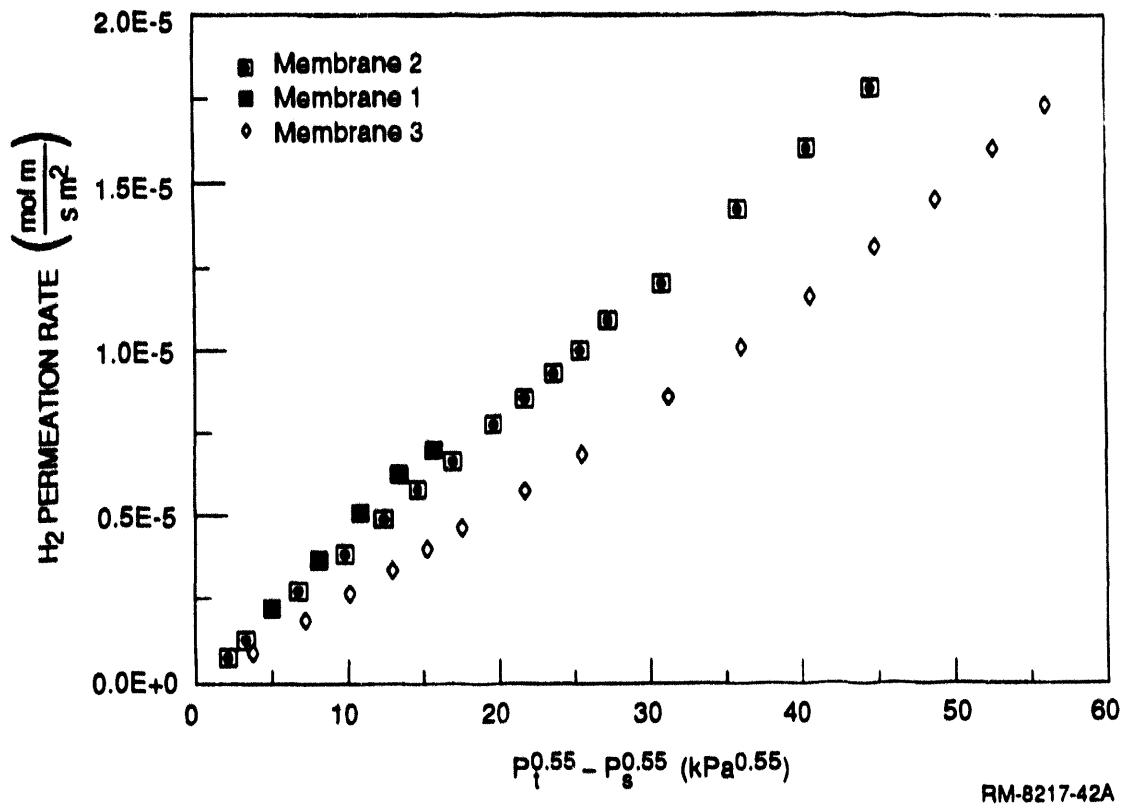

Figure 14. Comparison of H_2 permeation rates at 823 K.

Figure 15 shows H_2 permeation data for Membrane 2 as a function of temperature between 723 K and 873 K. The nitrogen permeation rate and selectivity[2] for Membrane 3 are shown in Figures 16 and 17. The selectivity for H_2 over N_2 varies with transmembrane pressure difference (ΔP) and temperature. At 723 K and a low ΔP the selectivity is close to 200, while at high ΔP the selectivity drops to less than 50. While these selectivity results suggest that a low ΔP will give the best performance, a low ΔP will result in a low overall permeation rate and, consequently, require a high membrane area and cost.

POLYSILAZANES ON ALUMINA SUBSTRATES

Polysilazanes are polymers that form ceramics when pyrolyzed (Blum et al., 1986, 1989). The resulting ceramics have no measurable porosity but have a density less than that of the fully densified ceramic. Therefore, the ceramic layer created via pyrolysis can have angstrom sized holes capable of selective permeation by molecular sieving. We studied two specific polysilazanes (see Figure 18): poly-N-methyl silazane (PNMS) and polycyclohydridomethyl silazane (PCMS).

We attempted to make polysilazane films on three separate ceramic substrates: (1) an asymmetric alumina monolith made by Norton Company (product name Ceraflo; Worcester, MA), (2) a developmental cordierite hollow tube made by DuPont (product code PRD-86, Wilmington, DE), and (3) an asymmetric microfilter disk made by Refractron Technologies, Inc. (Refractite III; Newark, NY). In addition, we used Corning's Vycor Glass (Product 7930; Corning, NY; 8 mm O.D.) as a substrate briefly in later stages of the research.

Table 10 is a brief summary of the permeation data obtained during the polysilazane membrane development work. All of the hydrogen/nitrogen permeance ratios we achieved were less than that expected from Knudsen diffusion. Further, good permeation data could only be obtained with one polysilazane (PCMS) on only the Refractron disk and Vycor glass substrates. We review below the experimental techniques and difficulties experienced with each type of inorganic substrate.

[2] Selectivity is defined as the H_2 permeation rate divided by the nitrogen permeation rate for a given transmembrane pressure difference.

Table 10

MEMBRANES MADE WITH PCMS ON REFRACTRON ALUMINA MICROFILTERS AND VYCOR GLASS

Sample Identifier	Cure Conditions	H_2 Permeance (cm^3(STP)/cm^2 s cm Hg)	H_2/N_2 Permeance Ratio
REF-2	1 coat/N_2 cure	7.55×10^{-2}	2.29
REF-3	2 coats/NH_3 cure	$(2.92 \pm 0.25) \times 10^{-2}$	3.22
REF-5	3 coats/NH_3 cure	7.03×10^{-4}	2.97
REF-10	4 coats/NH_3 cure	2.15×10^{-5}	2.99
Vycor-2	1 coat/NH_3 cure	1.14×10^{-4}	3.30

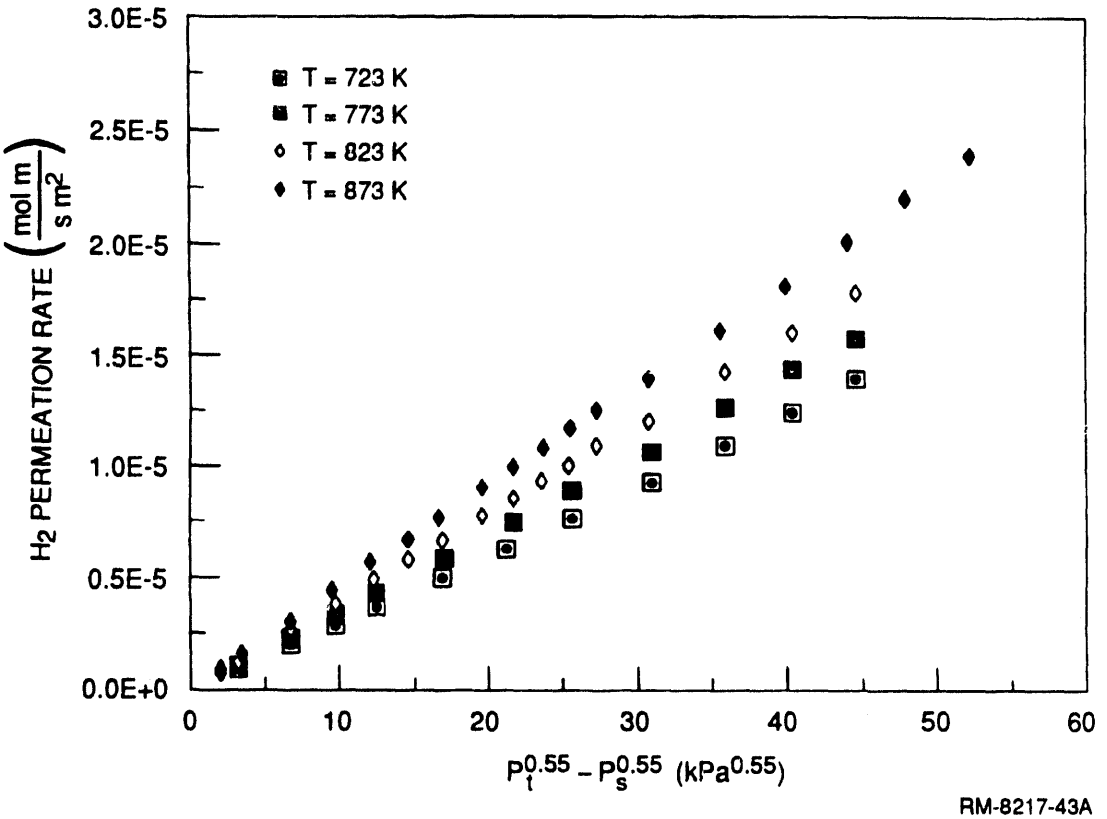

Figure 15. H_2 permeation data for Membrane 2.

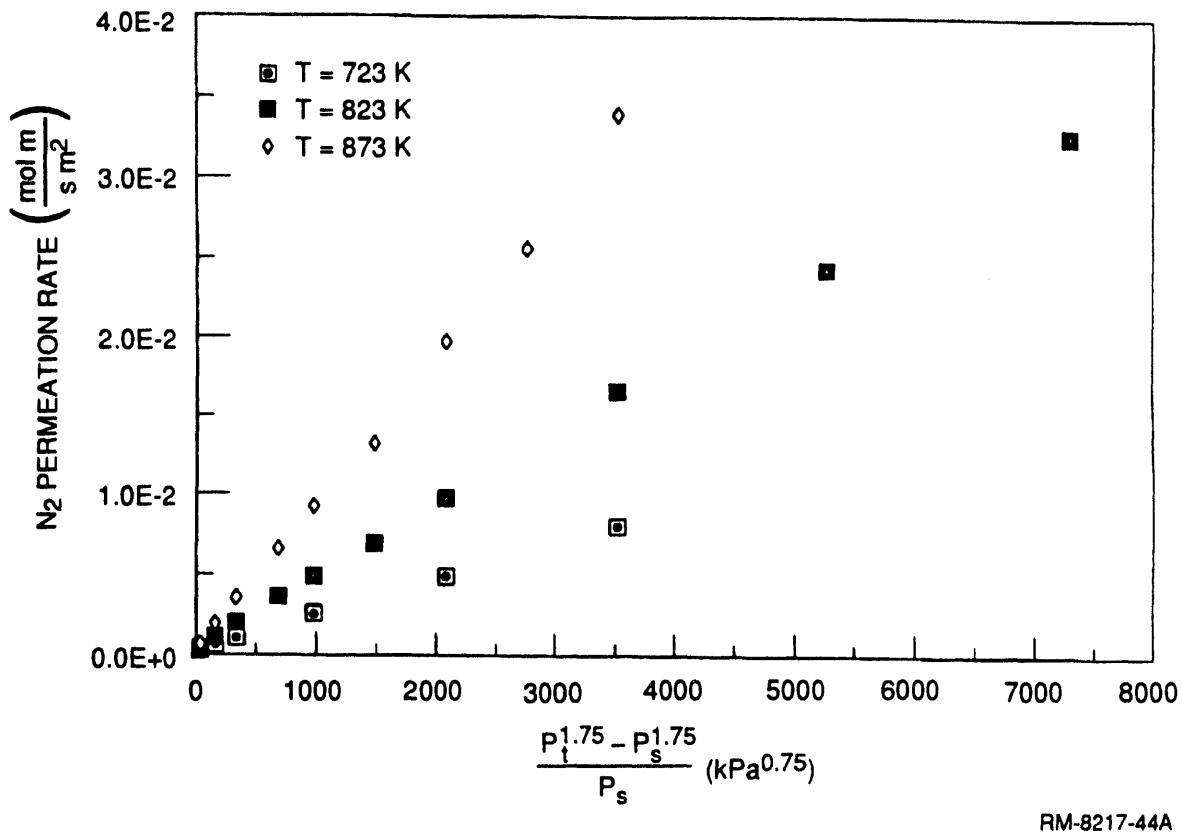

Figure 16. N_2 permeation data for Membrane 3.

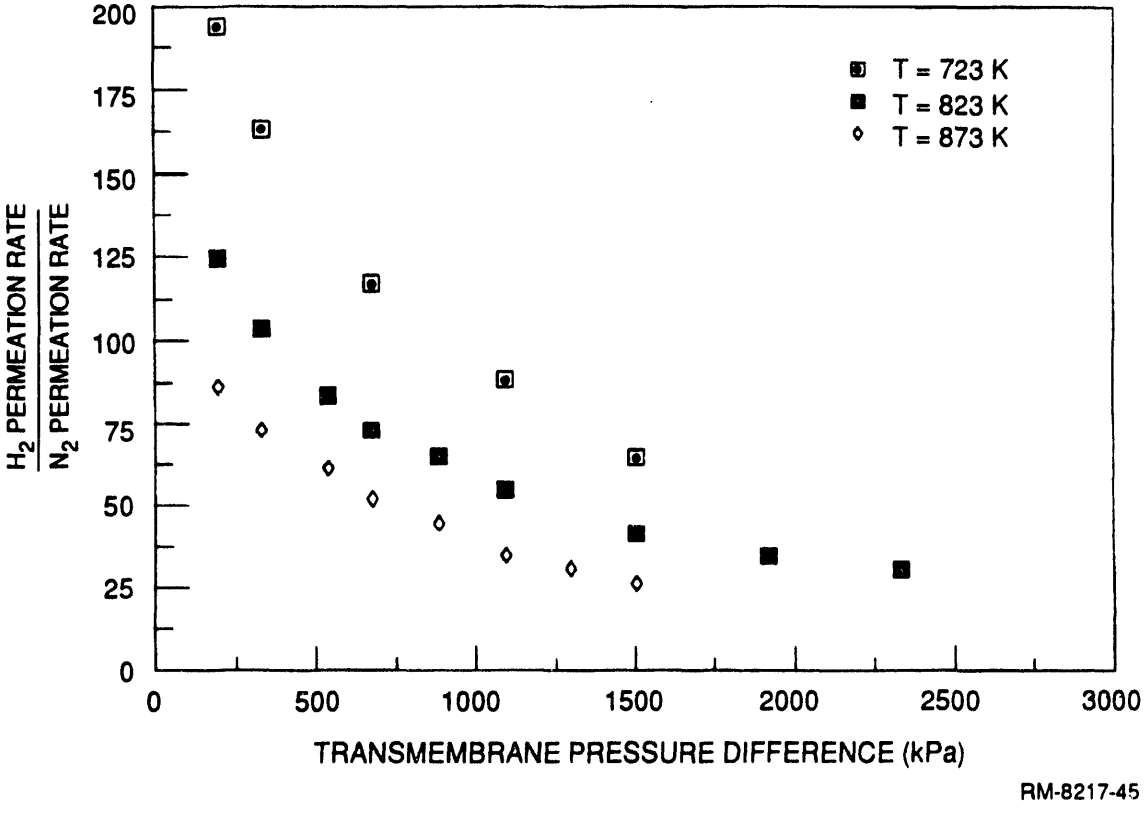

Figure 17. H_2 selectivity of Membrane 3 as a function of transmembrane pressure difference.

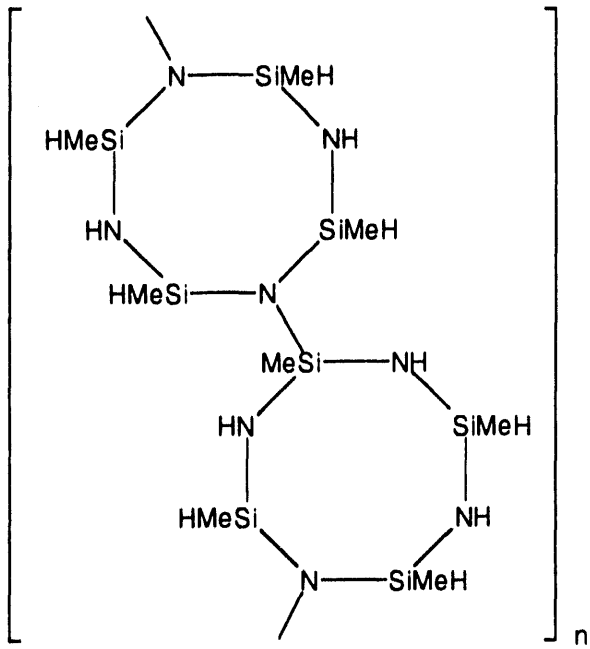

(a) Polycyclohydridomethyl silazane (PCMS)

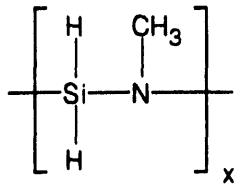

(b) Poly-N-methyl silazane (PNMS)

RM-8217-31A

Figure 18. Polysilazane polymers used for coating alumina substrates.

Both polymers are three-dimensional. Our starting materials had a molecular weight of about 50,000.

Norton Alumina Monolith

The Norton product (Ceraflo) was a 20-mm-O.D. monolith with 19 tubular channels, each of which had an I.D. of 2.2 mm. The wall was asymmetric, a thin 0.2-μm filter layer on top of the macroporous monolith. The permeance of the native Norton monolith to nitrogen at 1 atm pressure (1 psi pressure differential) was 2.1 x 10^{-3} cm^3/cm^2 s cm Hg. It was important to obtain a value here so that later permeance results with polysilazane coatings could be compared to the permeance of the native monolith.

Several methods of solution casting were attempted for applying a polysilazane membrane to the Norton monolith. The variables included the type of solvent (tetrahydrofuran, toluene), the concentration of polysilazane in the solvent, the duration of contact between the monolith and the casting solution, the number of solution-cast layers, and the curing method for the polysilazane. Early results with a 30 wt% solution of PNMS in tetrahydrofuran (THF) showed that a layer of amorphous ceramic could be applied to the monolith wall in a thickness of 2 to 8 μm (Figure 19).

Permeation testing of the Norton monolith proved problematic in that a good seal was very difficult to obtain, even at room temperature. Ultimately, a seal was obtained with Teflon tape wrapped around Teflon ferrules with ordinary Swagelok fittings. Periodically, we were successful making a polysilazane coating that held pressure to 40 psig. However, the frequency of crack formation during curing of the polysilazane led us to conclude that it was simply too ambitious try to coat a multitube device (i.e., the monolith) before we had established techniques on a small patch of ceramic substrate. After some success was achieved with small pieces of an alternative ceramic substrate (Refractron disks, see below), we returned to the Norton monolith and attempted to apply an inorganic glaze (Aremco 617; see section on leachable glaze, below). However, reproducibility on the monolith was poor. Although we planned to return to the monolith work after solving reproducibility problems on the small ceramic substrates, these problems were never fully resolved, and the monolith work was not pursued further.

DuPont PRD 86

The DuPont cordierite tubular membrane had a 2-mm O.D. and a 1-mm I.D. In general, these tubes are wrapped when wet during manufacture, which results in a modular form resembling a spun-wrapped fiber filter. In this form, the packing density of the filtration area is 50% of theoretical (theoretical is 4 divided by the tube diameter, or 2000 m^2/m^3). For our development work, however, DuPont supplied pieces of tubular membrane that were approximately

CP-870532-2

Figure 19. Cross section of Norton's asymmetric filter near the surface of an internal tube after deposition of polysilazane-derived skin.

The thickness of amorphous skin is 2-5 µm.

straight and about 12 in. long. The wall of PRD-86 was homogeneous and contained pores nominally 0.2 μm in diameter.

We attempted to coat small pieces of PRD-86 tubular membrane by painting polysilazane on the outer wall of the membrane. Two polymer solutions were tried: 55 wt% and 80 wt% polysilazane in toluene. The 80 wt% solution could not be readily spread over the membrane. The 55 wt% solution gave a coating with the consistency of household paint, and this coating seemed to apply well. After curing, imperfections evident under electron microscopy were coated again. However, cracks were still evident after curing.

Before these techniques could be developed further, DuPont requested that we withdraw the PRD-86 from the program, essentially because the commercialization efforts for PRD-86 internal to DuPont were being terminated. Therefore, no further work was performed on PRD-86.

Refractron Microfilter

These inorganic microfilters were disks with a diameter of 1-3/8 in. and a thickness of 1/8 in. The disks had a thin alumina skin approximately 250 μm thick on a mixed metal oxide substrate (alumina, silica, small amounts of Na, K, and Fe; Figure 20). The substrate was stable to 1600°F and the skin stable to 2150°F. The small alumina particles that comprise the skin were nominally 0.06 μm in diameter, and the micropores in the skin were about 0.2 μm in size.

The Refractron disks were coated with polysilazanes (primarily PCMS) by manually dipping the disk into a 30 wt% solution of polymer in toluene. Typically these coated disks were cured by heating at a rate of 100°C per hour to 150°C, holding for 30 minutes, increasing the temperature at a rate of 600°C per hour to 800°C, holding 800°C for 1 hour, and then turning the cure oven off. Ammonia or nitrogen was used as the cure atmosphere. Ammonia cures resulted in clearer films. If cracks were evident, either visually or by inference from the permeation results, multiple coats were applied.

Of the four good films made (Table 10), REF-3 was the most interesting one because of its high hydrogen permeance and because it had the highest hydrogen/nitrogen selectivity of any of the polysilazane-on-Refractron membranes. REF-2, -3, -5, and -10 have 1, 2, 3, and 4 coats of polysilazane, respectively. The hydrogen permeance decreases in this sequence of membranes, as one might expect for a thicker coating. However, the hydrogen/nitrogen selectivity does not increase, as might be expected from the inverse relationship between selectivity and permeance usually observed with conventional membranes.

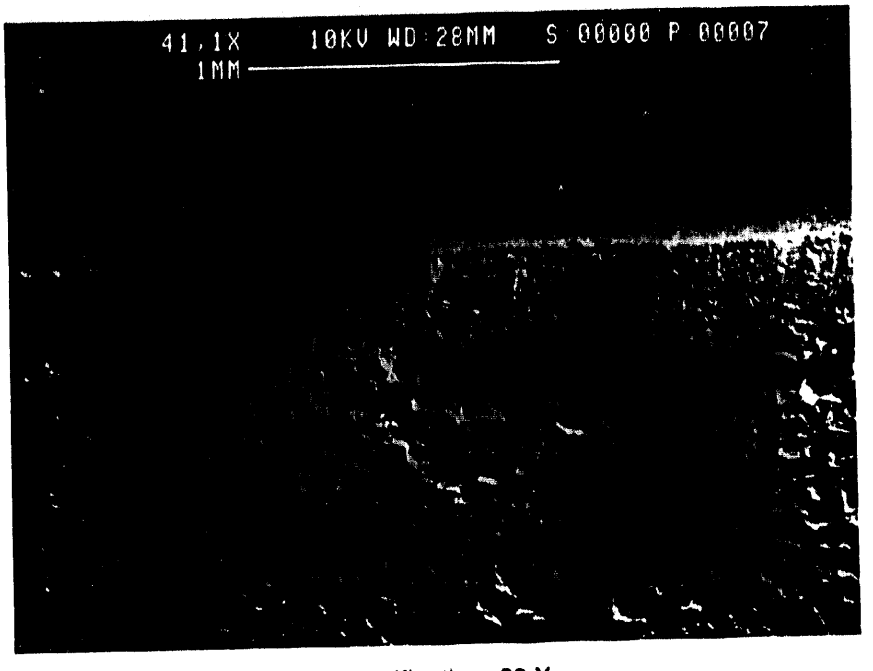

Magnification, 38 X

RP-8217-23

Figure 20. Cross section of native Refractron disk.

In making REF-10, a technique was devised to keep the PCMS from imbibing into the pores of the Refractron macrobody. Instead of dip coating, the Refractron disk was placed on top of a fritted glass disk that itself was placed in a petri dish containing the polysilazane solution. The amount of solution was enough to cover to the top of the fritted glass disk. The Refractron disk was placed inverted on top of the fritted glass disk, and polysilazane wetted the pores of the top layer of the Refractron disk without being imbibed into the pores of the backing. This method, however, did not seem to improve the performance of the coated disks.

Continued problems with cracking of the polymer films during curing and continued problems with irreproducibility caused the polysilazane-on-Refractron work to eventually come to an end, especially as some success was obtained with an alternative approach (glaze on a Refractron disk; see below).

Vycor Glass

The Vycor glass was used as a substrate on the theory that any defects in the applied skin (e.g., polysilazane layer) would be less catastrophic to the performance of the membrane if the support layer itself had a Knudsen selectivity. When we coated a Vycor tube with PCMS, however, the permeation properties were essentially those of the native Vycor tube (Table 10). It was difficult to justify further work on this topic.

LEACHABLE ALUMINA GLAZE ON ALUMINA MICROFILTERS

This approach to making a "molecular sieving" membrane was based on making a completely dense film on top of the Norton monolith or the Refractron alumina microfilter and then leaching the nonalumina components to form atomic holes in the alumina structure. This approach is similar to that used for making hollow gas-selective silica fibers (Hammel et al., 1989; Hammel, 1989; Way and Roberts, 1992).

The preparation of an inorganic glaze coating consisted of dipping the substrate in the glaze (Product #617, Aremco Products, Inc., Ossining, NY), 24 hour air drying, and then curing at high temperature. Some of the membranes were then leached in concentrated HCl. The leaching time was generally 24 hours, since a leach test showed that approximately half of the available leaching material (mainly K^+ ions) could be leached in 24 hours (Figure 21). The wide range of results with these preparation techniques is given in Table 11. A typical coated Refractron disk had a bubbly layer of alumina glaze on top of the alumina skin of the Refractron disk (Figure 22).

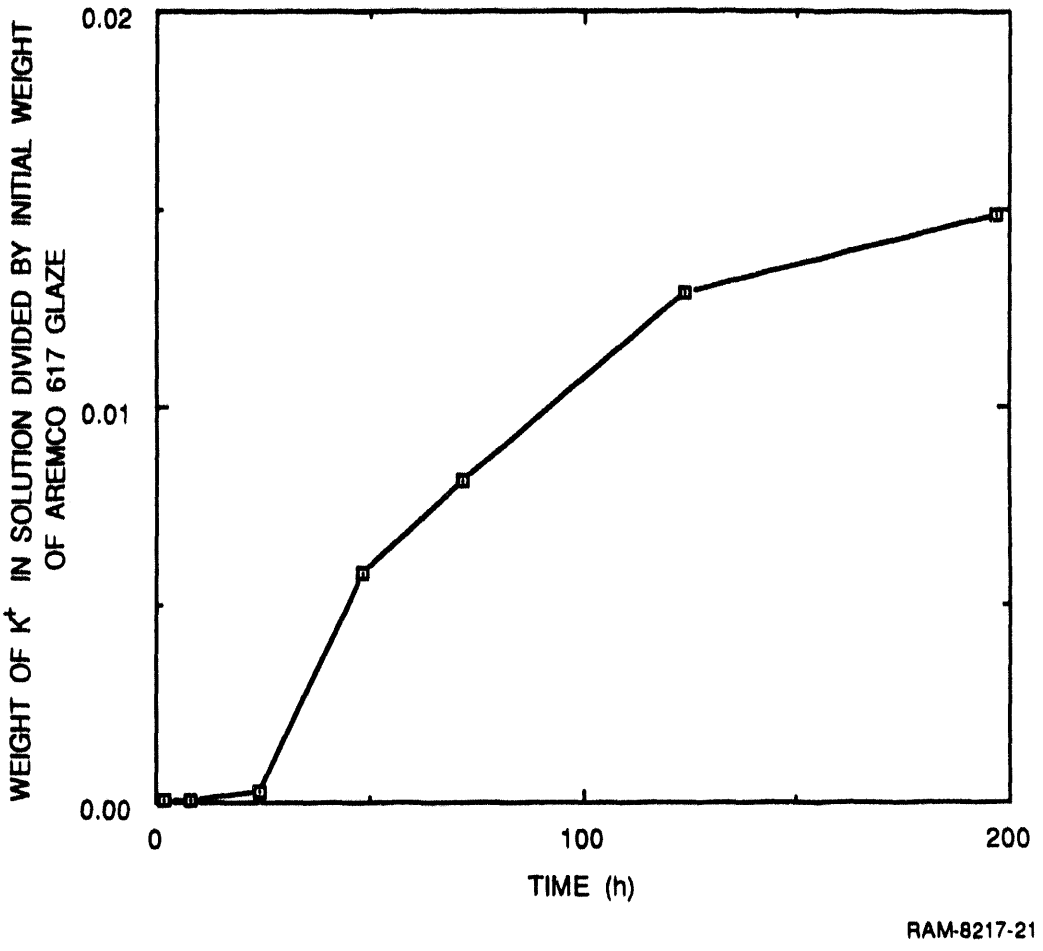

Figure 21. Leaching of potassium ion from Aremco 617 glaze.

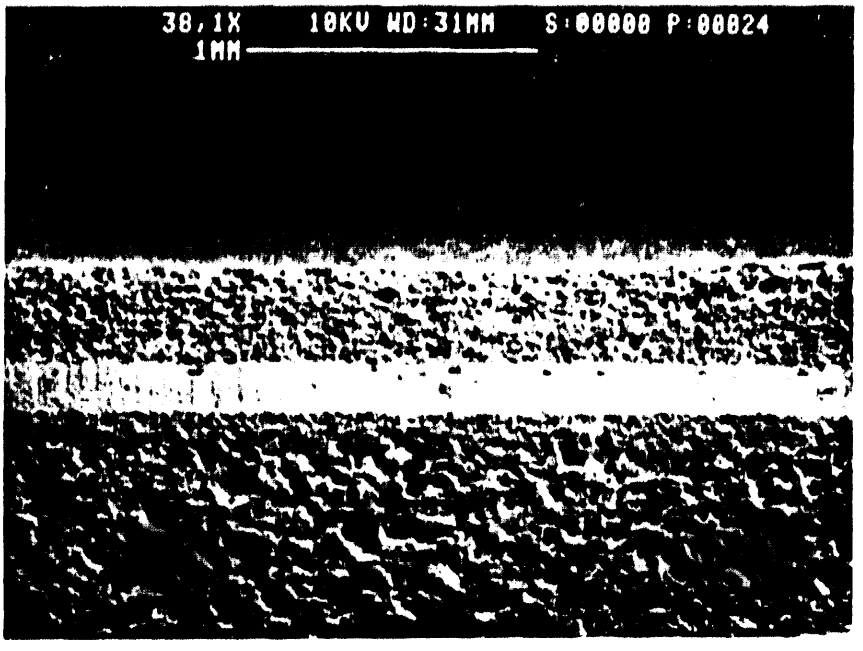

(a) Magnification, 38 X

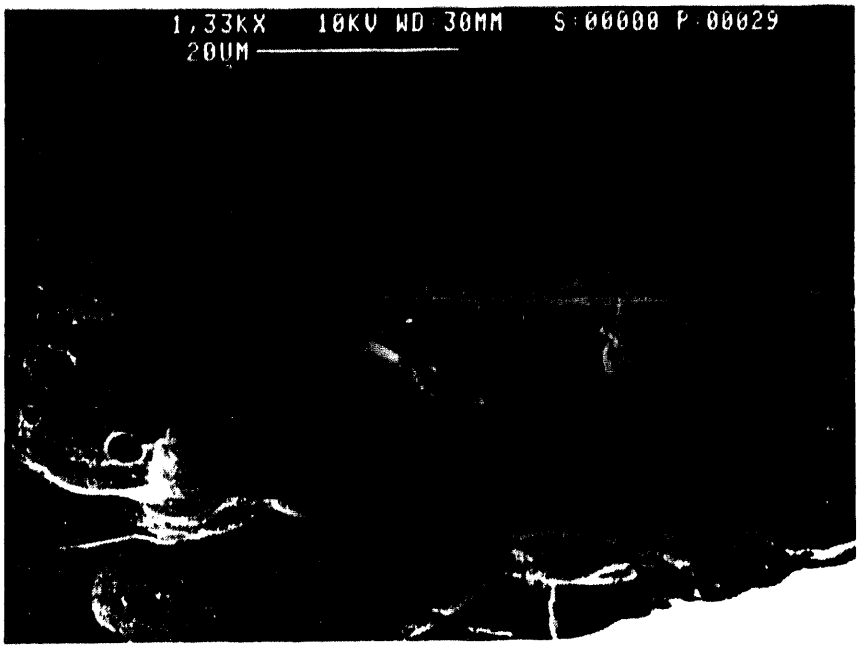

(b) Magnification, 1333 X

RP-8217-24

Figure 22. Inorganic glaze on Refractron disk.

Table 11
MEMBRANES MADE WITH AREMCO 617 ON REFRACTRON ALUMINA MICROFILTERS

Sample Identifier	Cure Conditions	H_2 Permeance (cm^3(STP)/cm^2 s cm Hg)	H_2/N_2 Permeance Ratio
9343-77A	30 min at 800°C	$(1.37 \pm 0.138) \times 10^{-3}$	3.22
9343-81A	15 min at 800°C	$(3.73 \pm 0.72) \times 10^{-3}$	2.03
9343-83A	15 min at 800°C	$(2.56 \pm 0.06) \times 10^{-2}$	3.74
9343-83B	15 min at 800°C	$(4.22 \pm 1.07) \times 10^{-3}$	2.34
9343-83B-1	15 min at 800°C	$(7.03 \pm 1.78) \times 10^{-5}$	2.34
9343-83B-2	15 min at 850°C (reheat of 83B-1)	$(6.10 \pm 1.42) \times 10^{-5}$	1.87
9343-83B-3	15 min at 850°C (reheat of 83B-2)	$(3.05 \pm 0\ 59) \times 10^{-3}$	2.35
9343-83C	15 min at 850°C	$(1.60 \pm 0.19) \times 10^{-5}$	5.41
9343-85A	15 min at 850°C; twice	$\sim 10^{-5}$	1.0
9343-85B	15 min at 850°C; twice	$\sim 10^{-4}$	1.0
9343-85A-2	15 min at 850°C; after leaching in 10 wt% HCl, 1 hr, 25°C	Impermeable film delaminated	---
9343-95A	15 min at 850°C; after leaching in 10 wt% HCl, 1 hr, 25°C	Impermeable 2.14×10^{-5} 5.47×10^{-4}	 2.02 2.40
9343-95B	15 min at 850°C; after leaching in 10 wt% HCl, 1 hr, 25°C	Impermeable 3.32×10^{-5}	 2.17
9849-5B	15 min at 850°C	1.55×10^{-5}	2.98
9849-5C	15 min at 850°C	1.39×10^{-3}	3.31
9849-11A	15 min at 850°C; after leaching in 10 wt% HCl, 1 hr, 25°C	1.73×10^{-5} 4.51×10^{-4}	2.84 1.67
9849-5A	15 min at 850°C; leaching in HCl	1.94×10^{-6}	5.26

Defect-free coatings on the Norton monolith could not be achieved. However, early results with alumina glaze on the Refractron disks were rather encouraging and surprising. When the alumina glaze was applied by dip coating and then cured by ramping the temperature for 40 minutes from room temperature to 850°C and then holding at 850°C for 15 minutes, the resulting membrane had a hydrogen/nitrogen selectivity of 5.41 (Sample 9343-83C).

Reproducibility was a recurring problem. Two membranes were prepared with hydrogen/nitrogen selectivities greater than the Knudsen diffusion value of 3.74. These membranes were Samples 9343-83C and 9849-5A. One of these membranes was leached in HCl, and the other was not. It was surprising that a selectivity exceeding that predicted by Knudsen diffusion could be found without HCl leaching of the glaze. In addition, it was surprising that the permeance of the membrane not leached (Sample 9343-83C) exceeded by a factor of 10 that of the membrane which was leached. These results typified the work with putting alumina glaze on Refractron disks, and it was eventually decided that the approach itself was unlikely to lead to reproducible and useful membranes. A likely contributing factor to the irreproducibility was the instability of Aremco glaze itself, as indicated by the change in pH and viscosity of the stock solutions of glaze over several months' time (Table 12).

Table 12
PROPERTIES OF VARIOUS BATCHES OF AREMCO 617*

Measurement Date	Batch A		Batch B	
	pH	Viscosity (centipoise)	pH	Viscosity (centipoise)
2/28/91	9.98	1,960	10.17	2,070
3/31/91	9.98	2,152	9.99	1,760
4/30/91	10.00	2,150	9.97	1,670
5/31/91	9.59	2,240	9.76	1,680

*Batch A: Stated expiration date of February 1991.
Batch B: Stated expiration date of July 1991.

MISCELLANEOUS MEMBRANE FORMULATIONS

A variety of other techniques for making inorganic membrane layers on Refractron disks were attempted. These techniques included dip coating a Refractron disk into a 33 wt% solution of aluminum phosphate precursor in methanol (the empirical formula of the precursor polymer was $AlPClH_{25}C_8O_8$; the cure conditions were 120°C for 2 hours, then 800°C for 2 hours). Another

approach consisted of adding a few weight percent polyethylene glycol (PEG) to the alumina glaze before coating. During the cure step, the PEG would be burned out of the coating, leaving a nanoporous layer. In other approaches, polysilazanes were added to Vycor tubes and to stainless steel supports. The more significant of these various approaches (namely, the PEG mixtures and the aluminum phosphates) gave rather inconsistent results (Tables 13 and 14).

Table 13
MEMBRANES MADE WITH PEG IN AREMCO 617 ON REFRACTRON MICROFILTERS

Sample Identifier	Carbon Content of PEG/Aremco Mixture	H_2 Permeance (cm^3(STP)/cm^2 s cm Hg)	H_2/N_2 Permeance Ratio
9849-23B	1.8 wt%	6.58×10^{-5}	2.73
9849-25B	5.8 wt%	2.53×10^{-6}	3.11
9849-25D	5.8 wt%	4.32×10^{-5}	2.90
9849-25C	5.8 wt%	5.03×10^{-6}	3.01

Table 14
PERMEATION BEHAVIOR OF $AlPO_4$-COATED MEDIA*

Sample I.D.	Substrate	Coating/ Treatment	H_2 Permeance [cm^3 (STP)/cm^2 s cm Hg)	H_2/N_2 Selectivity
AlP_3 #4	Refractron	2 Coats AlP_3	No integrity	---
AlP_3 #5	Refractron	2 Coats AlP_3	No integrity	---
Ref #21	Refractron	3 Coats AlP	No integrity	---
9432-Vyc-66A	Vycor	Uncoated 900°C, heat treated	1.26×10^{-4}	2.96
Vyc #20	Vycor	Uncoated 900°C, heat treated	1.25×10^{-4}	2.99
Vyc #13	Vycor	2 Coats AlP_3	1.09×10^{-4}	2.91
Vyc #14	Vycor	4 Coats AlP_3	1.30×10^{-4}	3.09
Vyc #16	Vycor	1 Coat AlP	1.36×10^{-4}	2.94
Vyc #21	Vycor	3 Coats AlP_3 (2-hour soak)	7.07×10^{-5}	2.65

*All measurements made at 44.7 psia upstream pressure, 14.7 psia downstream pressure.

MEMBRANE REACTOR EXPERIMENTS

Experiments were performed at OSU on a membrane reactor using the alumina supported Ni catalyst for NH_3 decomposition. The reactor consisted of a shell and tube configuration (Figure 13); the reactor operation is analogous to that shown in Figure 23. To demonstrate the increased NH_3 decomposition that can be achieved by using a membrane reactor, we also conducted NH_3 decomposition in a conventional reactor. The two reactors are different in that the membrane reactor used a permeable tube and the conventional reactor tube was impermeable. Experimental conditions are given in Table 15. The results of these experiments are shown in Figure 24 along with the theoretical equilibrium conversion for a conventional reactor. The membrane reactor had a significantly higher fraction of decomposed NH_3 than either the conventional reactor or the theoretical equilibrium conversion. While NH_3 decomposition in the membrane reactor was low for temperatures below 500°C (it was zero for the conventional reactor), the decomposition was high (95%) at 600°C. These results show that a membrane reactor can be much more effective than a conventional reactor and, under conditions similar to that in an IGCC, can achieve almost complete removal of NH_3.

Table 15

EXPERIMENTAL CONDITIONS FOR MEMBRANE REACTOR EXPERIMENTS

	Membrane Reactor	Conventional Reactor
Feed composition (mol%)		
NH_3	0.34	0.34
N_2	47.6	47.6
H_2	20.1	20.1
He	32.0	32.0
Feed flow rate (sccm)	422	422
Feed pressure (psig)	220	220
Feed temperature (°C)	450-600	450-600
Shell-side pressure (psig)	1.25	—
Shell-side inlet flow rate (sccm)	0	—
Reactor tube diameter, inside (cm)	0.7	0.6
Reactor length (cm)	5.5	8.2
Catalyst weight (g)	1.23	1.23
Membrane material	Pd on alumina ultrafilter	—
Membrane thickness (μm)	11.4	—

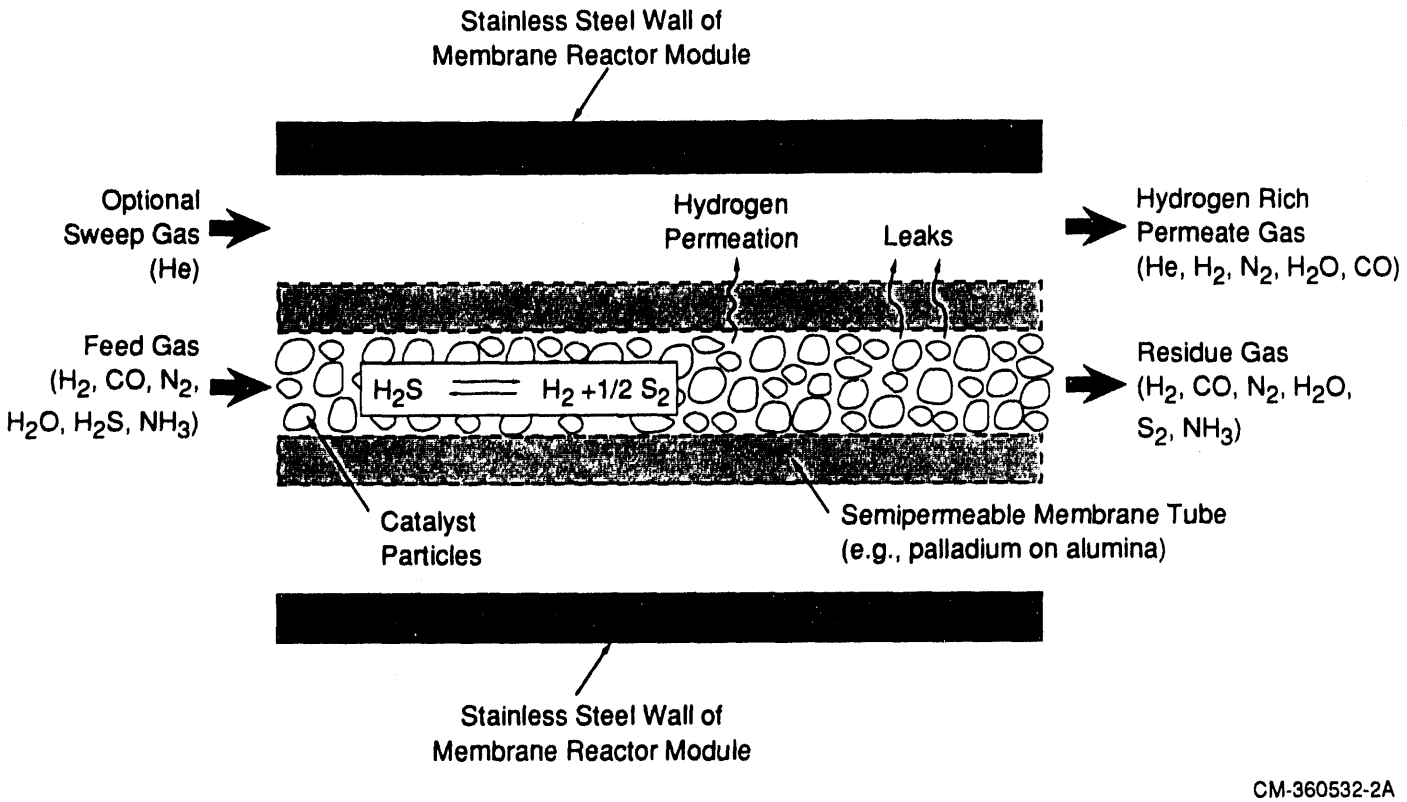

Figure 23. Flow streams in membrane reactor system.

Hydrogen preferentially permeates membrane tube wall as H_2S (or NH_3) is decomposed by catalyst.

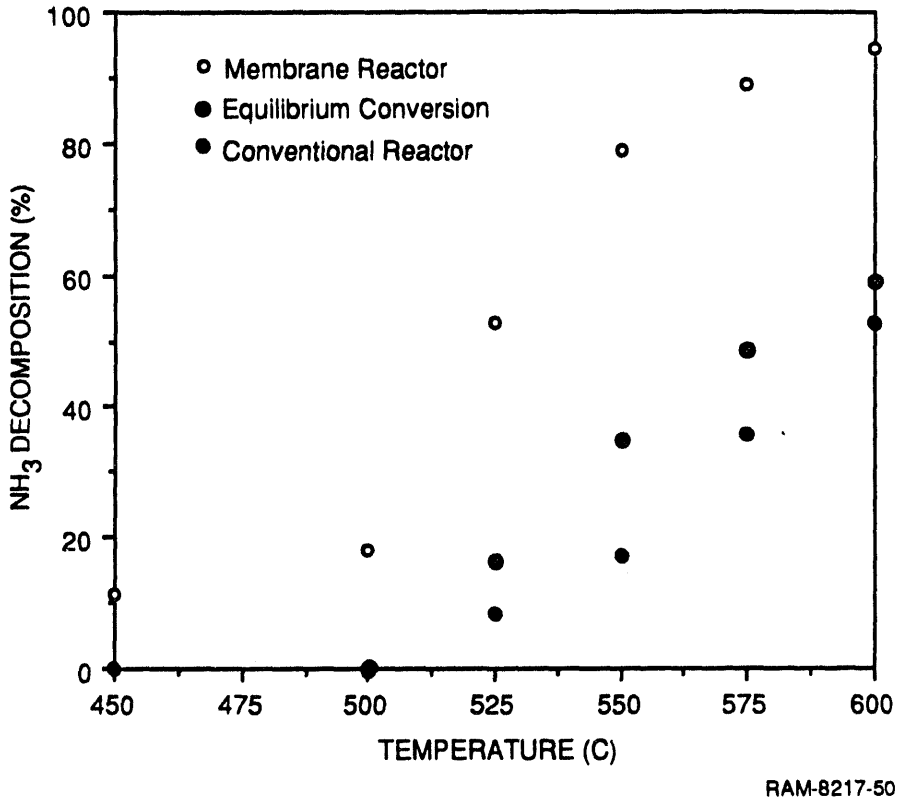

Figure 24. Membrane reactor experiment results.

The membrane reactor had a greater NH_3 decomposition than the conventional reactor under all conditions.

MEMBRANE REACTOR MODELING

The basic principles of a computational model have been expressed adequately by previous investigators for a membrane reactor with the following configuration (Figure 23):

(a) Feed gas on inside of membrane tube

(b) Catalyst inside membrane tube

(c) Plug flow inside and outside membrane tube.

We apply these principles to the decomposition of H_2S and of NH_3 in the following paragraphs.

If the reaction taking place in the membrane reactor is written

$$aA \Leftrightarrow bB + cC \tag{13}$$

and if species I is the (optional) inert sweep gas, then differential conservation equations governing the performance of the reactor are as follows:

$$\frac{dF_A}{dL} = \left[-ar - \frac{2\,N_A}{R_i}\right]\pi R_i^2 \tag{14}$$

$$\frac{dF_B}{dL} = \left[br - \frac{2\,N_B}{R_i}\right]\pi R_i^2 \tag{15}$$

$$\frac{dF_C}{dL} = \left[cr - \frac{2\,N_C}{R_i}\right]\pi R_i^2 \tag{16}$$

$$\frac{dF_I}{dL} = \left[- \frac{2\,N_I}{R_i}\right]\pi R_i^2 = -2\pi R_i N_I \tag{17}$$

$$\frac{dQ_A}{dL} = 2\pi R_i N_A \tag{18}$$

$$\frac{dQ_B}{dL} = 2\pi R_i N_B \tag{19}$$

$$\frac{dQ_C}{dL} = 2\pi R_i N_C \tag{20}$$

$$\frac{dQ_I}{dL} = 2\pi R_i N_I \tag{21}$$

The permeation flux of each species (N_A, N_B, N_C, N_I) may be governed by different permeation rules. For example, if the barrier is microporous, we can expect the permeation of each species to depend on the partial pressure driving force (N_i proportional to the difference in partial pressure across the membrane for each species). In our case, hydrogen permeates through the metallic barrier with a square root dependence on the hydrogen partial pressure (Barrer, 1951) and the other species permeate (only through defects) at a rate proportional to the partial pressure driving force. Hence, if species B is H_2, we have

$$N_A = \overline{P}_A P_T (X_A - \gamma Y_A) \tag{22}$$

$$N_{H_2} = \overline{P}_{H_2} P_T^{1/2} \left[X_{H_2}^{1/2} - (\gamma Y_{H_2})^{1/2}\right] \tag{23}$$

$$N_C = \overline{P}_C P_T (X_C - \gamma Y_C) \tag{24}$$

$$N_I = \overline{P}_I P_T (X_I - \gamma Y_I) \tag{25}$$

where the coefficients $\overline{P}_A$, $\overline{P}_{H_2}$, $\overline{P}_C$, and $\overline{P}_I$ are the experimentally determined permeance coefficients for each species, P_T is the total system pressure on the feed side of the membrane, X_i is the mole fraction of species i on the feed side of the membrane, Y_i is the mole fraction of species i on the permeate side of the membrane, and γ is the ratio of total pressure on the permeate side to that on the feed side. The mole fractions of each species are related to the molar flow rates as follows:

$$X_i = \frac{F_i}{\sum F_j} \tag{26}$$

$$Y_i = \frac{Q_i}{\sum Q_j} \tag{27}$$

Pressure drop relationships

$$\frac{dP_T}{dL} = f_1(Re) \tag{28}$$

$$\frac{d(\gamma P_T)}{dL} = f_2(Re) \tag{29}$$

complete the applicable differential equations [the functions "f_1" and "f_2" in Equations (28) and (29) represent appropriate frictional resistances to flow on both sides of the membrane].

For H_2S decomposition, Reaction (13) becomes

$$H_2S \Leftrightarrow H_2 + \frac{1}{2}S_2 \tag{30}$$

and the reaction rate, r, is given by

$$r = k_1 \left(\frac{P_T}{RT}\right)\left[X_{H_2S} - \left(\frac{P_T}{RT}\right)^{(1/2)} \frac{X_{H_2} X_{S_2}^{1/2}}{K_{eq}\cdot(1\ atm)^{1/2}}\right] \tag{31}$$

For NH_3 decomposition, Reaction (13) becomes

$$NH_3 \Leftrightarrow \frac{1}{2}N_2 + \frac{3}{2}H_2 \tag{32}$$

and the reaction rate, r, is given by

$$r = k_o\left[\left(\frac{f_{NH_3}^2}{f_{H_2}^3}\right)^{\beta} - \frac{f_{N_2}}{K_{eq}^2}\left(\frac{f_{H_2}^3}{f_{NH_3}^2}\right)^{(1-\beta)}\right] \tag{33}$$

The applicable differential equations can be solved subject to appropriate boundary conditions. At the reactor inlet (L = 0), the flow rates of reactants and inerts are known on both sides of the membrane, so that the following equations apply at L = 0:

$$F_a = F_{a,o} \tag{34}$$

$$F_b = F_{b,o} \tag{35}$$

$$F_c = F_{c,o} \tag{36}$$

$$F_i = F_{i,o} \tag{37}$$

$$Q_a = Q_b = Q_c = 0 \tag{38}$$

$$Q_i = Q_{i,o} \tag{39}$$

Here, the quantities $F_{a,o}$, $F_{b,o}$, $F_{c,o}$, and $Q_{i,o}$ are the known values of the reactant, product, and inert flow rates in the feed stream and permeate steam, respectively. (We are assuming that there are no reactants or products introduced into the permeate stream; only inerts at the rate $Q_{i,o}$).

We conducted the computations to solve these differential equations for either H_2S or NH_3 decomposition on a MacIntosh II personal computer using the Gears numerical method incorporated into the IMSL software library. In the next section we describe results of calculations representing various IGCC scenarios. Collins et al. (1992) have used this computer model to explain the interplay of the relevant dimensionless groups characterizing membrane reactor performance in the decomposition of NH_3.

TECHNICAL AND ECONOMIC EVALUATION OF MEMBRANE REACTORS IN AN IGCC ENVIRONMENT

The objective of this task was to make a preliminary economic assessment of membrane reactors for control of H_2S and NH_3 in IGCC systems. We chose as our base case a specific air blown gasifier with sulfur removal downstream of the gasifier accomplished by a zinc ferrite system (Figure 25). The flow diagram is taken from a design study performed primarily by Southern Company Services and M. W. Kellogg on behalf of Morgantown Energy Technology Center (DOE/MC/26019-3004; December 1990).

To appreciate the advantages of a membrane reactor, it is useful first of all to have a simplified flow diagram of the IGCC system (Figure 26). A membrane reactor capable of decomposing H_2S plus a sulfur filter would take the place of the zinc ferrite beds and eliminate the need for the sulfuric acid plant and its attendant oxygen plant (Figure 27). Intuitively, there seems to be a strong likelihood that the capital cost of the one-unit operation (membrane reactor) would be much less than that of the three unit operations (zinc ferrite, sulfuric acid plant, oxygen plant; the membrane reactor makes by-product hydrogen, but the economic value of this by-product is too trivial to bother calculating). A membrane reactor for decomposing ammonia would be placed after the H_2S reactor so as to minimize sulfur poisoning of the ammonia decomposition catalyst. There is no current technology for ammonia decomposition with which to compare the membrane reactor. Even though there is a relatively simple comparison available for the H_2S membrane reactor, the basic issue of "affordability" of either membrane reactor ultimately must be decided by the impact of each technology on the cost of power generated by the IGCC system. In the following paragraphs, we assess this cost impact using, as much as possible, our reaction rate and permeation rate data.

In the IGCC base case, the system produces 420 MW of electricity by consuming 141 tons/h of coal with a heating value of 13,000 Btu/lb. The flow rates, temperatures, pressures, and compositions of the gases entering and exiting the zinc ferrite control device are given in Table 16. The capital and operating costs for the various components of the system are listed in Tables 17 and 18. The zinc ferrite system with the sulfuric acid plant requires a capital investment of $68.6 million. The zinc ferrite system removes 99.3% of the sulfur from the coal gas.

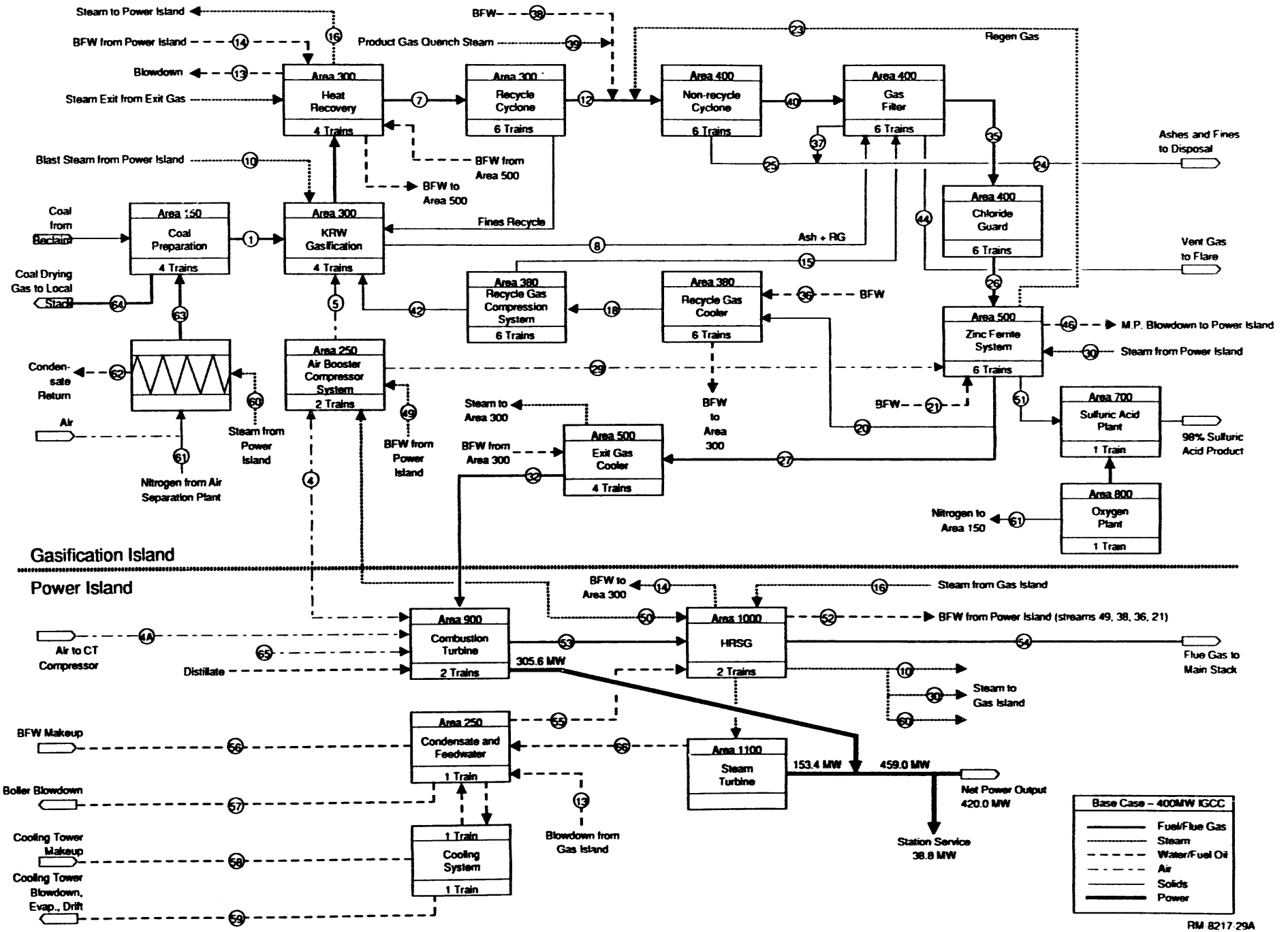

Figure 25. Block flow diagram of IGCC base case. (Adapted from DOE/MC/26019-3004)

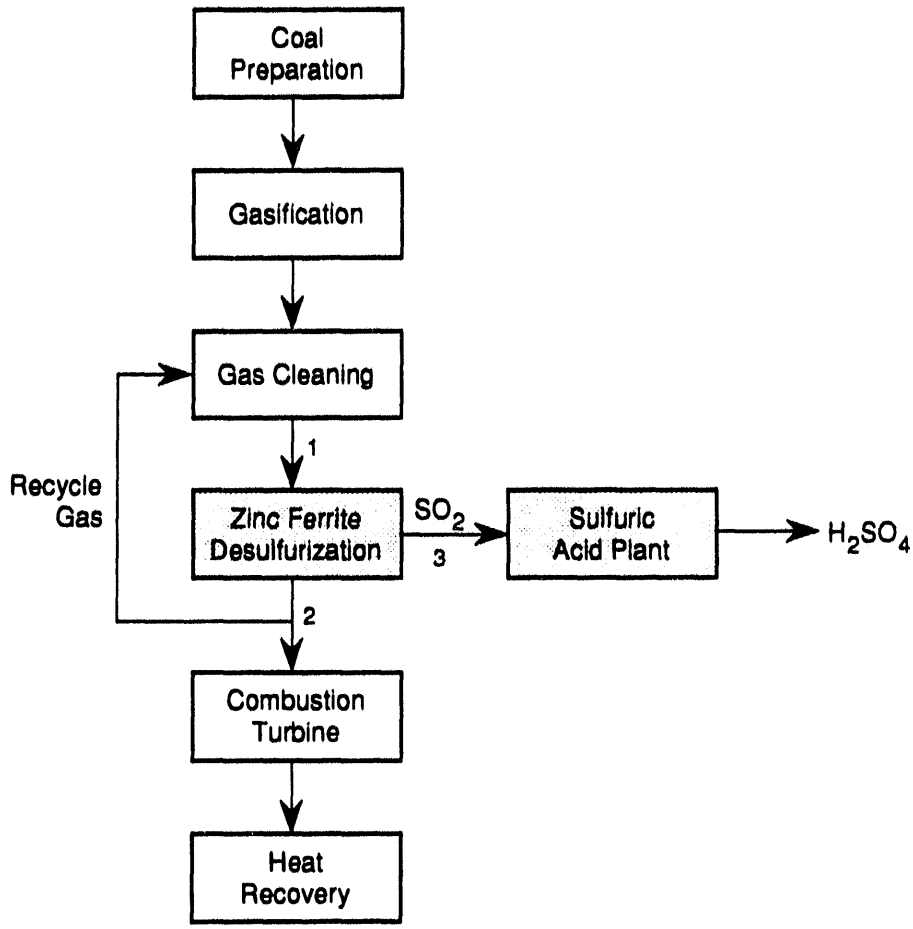

Figure 26. Simplified flow diagram of conventional IGCC technology.

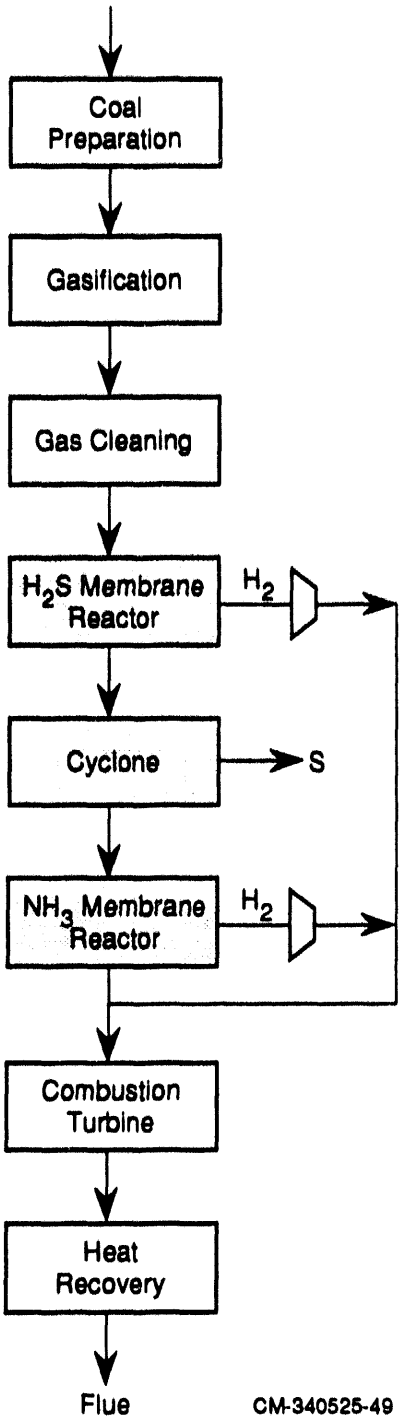

Figure 27. Control of H_2S and NH_3 with hydrogen-selective membrane reactors.

Table 16
INLET STREAM CONDITIONS FOR ZINC FERRITE SYSTEM
IN IGCC BASE CASE

(Stream Number Refers to Figure 26)

Composition (mol%)	Inlet Stream (#1)
CO	7.5
H_2	20.7
CO_2	13.6
CH_4	0.7
N_2	36.3
Ar	0.4
NH_3	750 ppm
H_2S	3110 ppm
SO_2	
H_2O	20.4
Flow Rate	78,300 lb mol/hr; $1.79 \cdot 10^6$ lb/hr
Temperature	1000°F
Pressure	345 psia

Table 17
BREAKDOWN OF PROCESS PLANT COSTS BY PLANT SECTION

(Plant Size, 420.2 MW; Mid-1990 Dollars)

Area No.	Plant Section Description	$ (Thousands)	$/KW
100	Coal receiving/handling	16,245	38.7
150	Limestone receiving/handling	0	0.0
250	Booster compression	9,272	22.1
300	Gasification	63,074	150.1
380	Recycle gas compression	18,044	42.9
400	Gas conditioning	38,645	92.0
500	External desulfurization	32,897	78.3
600	Sulfation	0	0.0
700	Sulfuric acid plant	25,739	61.3
900	Gas turbine system	70,965	168.9
1000	HRSG system	32,092	76.4
1100	Steam turbine system	41,604	99.0
1200	Ash & fines handling/disposal	4,491	10.7
	Total process plant cost	353,068	840.2
	General plant facilities	33,365	79.4
	Engineering fees	26,103	62.1

Source: DOE/MC/26019-3004; December 1990.

Table 18
FIRST YEAR O&M COST SUMMARY*

	Case 5
Net MW (90°F)	420.2
Fuel, $ x 1000	33,576
Variable O&M, $ x 1000	
Limestone	0
Nahcolite	296
Zinc ferrite	9,653
Miscellaneous	1,449
Solids disposal	564
Total, $ x 1000	11,961
Fixed O&M, $ x 1000	
Operating labor	4,571
Supervision	1,165
Maintenance	9,839
Insurance/taxes	3,145
Other	583
Total, $ x 1000	19,302
By-product Credit, $ x 1000	3,471
Total First Year O&M Costs, $ x 1000	61,368
Fuel, mills/kWh	14.03
Variable w/o by-product credit, mills/kWh	5.00
Variable w/by-product credit, mills/kWh	3.55
Fixed, $/kW-yr	45.9
Total First Year O&M Costs mills/kWh	25.65

*Based on mid-1990 dollars and 65% capacity factor. Capacity factor of 65% specified by DOE for comparison to other studies.

To assess the cost of the membrane reactor systems, we chose to require that the H_2S reactor remove the same fraction of H_2S as the zinc ferrite system (99.3%) and that the NH_3 reactor remove 90% of the ammonia (exact requirements for ammonia removal are not currently specified by any regulatory agency, but 90% removal is expected for the future because of the Clean Air Act amendments of 1990). We explain first the system parameters used in the membrane reactor calculations.

Membrane Reactor System Parameters

The important parameters include membrane permeance and decomposition rates for H_2S and NH_3. The H_2 permeance used in these evaluations is based on experimental data from OSU. (Early permeance data were used, since that was all that was available at the time the economic evaluations were performed.) Because we expect the permeance in a commercial membrane module to be less than that in laboratory membranes, we used a permeance value about half that reported by OSU. Although palladium is essentially impermeable to gases other than H_2, there is bound to be a finite leak rate due to fine cracks in the palladium layer or to defects in the seal between the membrane tube and the module. We have assumed that a commercial module would have a leak rate 10 times greater than that measured by OSU for their laboratory membrane. We believe that membranes can be made thinner than those produced by OSU, and therefore we have used a palladium membrane thickness of 5 μm. After adjustment[3] to 1000°F, the membrane parameters used in calculations for H_2S and NH_3 decomposition are as follows:

- Permeance of H_2 (1000°F) = $9.55 \times 10^{-5} \frac{cm^3(STP)\text{-}cm}{cm^2\text{-}s\text{-}cm\ Hg^{0.5}}$
- Leak rate of other species (1000°F) = $8.75 \times 10^{-10} \frac{cm^3(STP)\text{-}cm}{cm^2\text{-}s\text{-}cm\ Hg}$
- Palladium membrane thickness = 5 μm.

The H_2S reaction rate is given by Equation (B-2) and K_{eq} is given by Equation (A-3) (see Appendices A and B). The NH_3 reaction rate is given by Equations (6) and (7) and K_{eq} which is defined by Equation (11), is given by

$$K_{eq} = 1.0132 \times 10^5 \{10^{2250/T - 1.5105 \log(T) - .8534 - 25.90 \times 10^{-5} T + 14.90 \times 10^{-8} T^2)}\} \quad (40)$$

[3] Permeation was adjusted for temperature by using an activation energy of 2564 cal/mol. This activation energy was determined using the data of Uemiya et al. (1988).

where T is the temperature in kelvins. With the model developed by OSU and the parameters mentioned above, we are able to compare the performance between a membrane reactor and a conventional reactor.

H_2S Decomposition

Figure 28 shows the maximum H_2S decomposition attainable with both membrane and conventional reactors[4] over a range of temperatures. The figure shows that at 1000°F, the operating temperature of the IGCC, neither the conventional nor the membrane reactor show any conversion. Even at 1800°F (where K_{eq} is most favorable), the conventional reactor achieves an H_2S conversion of only 40%. The membrane reactor, although substantially better than the conventional reactor, can achieve at best a 92% decomposition, far less than the 99+% removal desired. The reason for the low percentage of H_2S decomposition is that a large fraction of the feed stream leaks through the membrane as we try to achieve high conversions. Any H_2S that leaks through the membrane can not decompose and, if enough leaks through, the result is a low percentage of H_2S decomposition.

The low conversion calculated for the membrane reactor indicates that the reaction rate is low relative to the leak rate. Therefore, to achieve higher H_2S conversion we must increase the reaction rate or lower the leak rate; since the leak rate is difficult to control, we chose to work toward increasing the reaction rate. The reaction rate is low because of three factors: low equilibrium coefficient (see Figure A-1), high H_2 concentration in feed, and low H_2S concentration in feed [see Equation (A-4)]. While we cannot affect the first factor, it is possible to change the concentrations of both H_2 and H_2S in the feed. Bearing this in mind, we have proposed two modified process configurations to increase the fractional decomposition of H_2S in the membrane reactor.

The first configuration provides for preconcentration of the H_2S prior to introduction to the membrane reactor (Figure 29). The second configuration provides for H_2 removal from the feed stream prior to introduction to the membrane reactor (Figure 30). To achieve these two separation

[4] The maximum decomposition with a conventional reactor occurs when enough H_2S decomposes such that the remaining H_2S is in equilibrium with the other gas species. With a membrane reactor, decomposition can continue as long as the reaction product, H_2, is removed by the membrane. Thus the maximum decomposition with a membrane reactor occurs when the entire feed stream has permeated the membrane. (Because some undecomposed H_2S permeates the membrane through leaks, the permeate stream can contain a significant fraction of H_2S.)

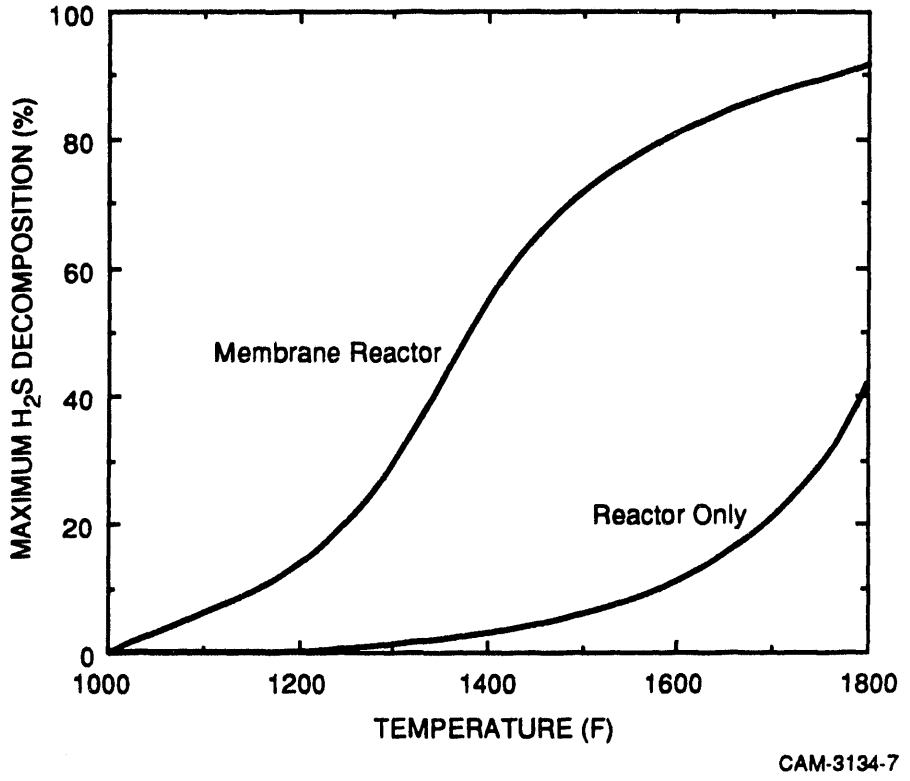

Figure 28. Effect of reactor temperature on decomposition of H_2S.
Temperatures above 1500 °F are necessary for reasonable fractional decomposition of H_2S even with a membrane reactor.

steps, we have not proposed any particular technologies—many are available, including membrane, absorption, and adsorption based processes.

The results of process simulations for these two modified configurations are shown in Figures 31 and 32 for a single temperature, 1000°F. The simulations show that while substantially greater conversions are achieved over the original membrane reactor configuration, neither of the modified configurations can achieve the desired H_2S conversion (>99%). Even if the feed is pre-concentrated until it is pure H_2S, the greatest conversion is only 33%; if all H_2 is removed from the feed before entering the reactor, the greatest conversion is 63%.

While a perfect membrane (no leaks and no permeation of gases other than H_2) would theoretically result in 100% conversion of H_2S (this would, however, require an infinitely long reactor), these simulations show that even a small amount of H_2S leakage (or permeation) through the membrane will severely limit the fraction of H_2S that can be decomposed by the membrane reactor.

NH_3 Decomposition

Unlike the case for the H_2S decomposition reactor, K_{eq} for NH_3 decomposition is quite high (see Figure 33), and at 1000°F a conversion of 89% is achieved. However, this is still below our desired conversion, 90%. If a conventional reactor is used, NH_3 is formed rather than decomposed. As was the case with H_2S, to achieve the desired NH_3 decomposition we must modify the flowsheet—either preconcentrate the NH_3 or remove NH_3 from the feed stream (Figures 29 and 30).

For the case of NH_3 preconcentration, Figure 34 shows the NH_3 decomposition attained with three different reactors: a membrane reactor, a conventional reactor the same size as the membrane reactor, and a conventional reactor large enough that the reaction products leaving the reactor are in equilibrium. In this figure, feed concentrations vary from 0.075% NH_3 (no preconcentration) to 99% NH_3 (almost completely concentrated NH_3). With a membrane reactor, the feed needs only slight preconcentration (by 14%, to 0.086% NH_3) to achieve 90% decomposition. With the equilibrium conventional reactor, the feed must be preconcentrated 68-fold (to 5.1% NH_3) to achieve 90% decomposition. A conventional reactor the same size as the membrane reactor achieves only 27% conversion at best.

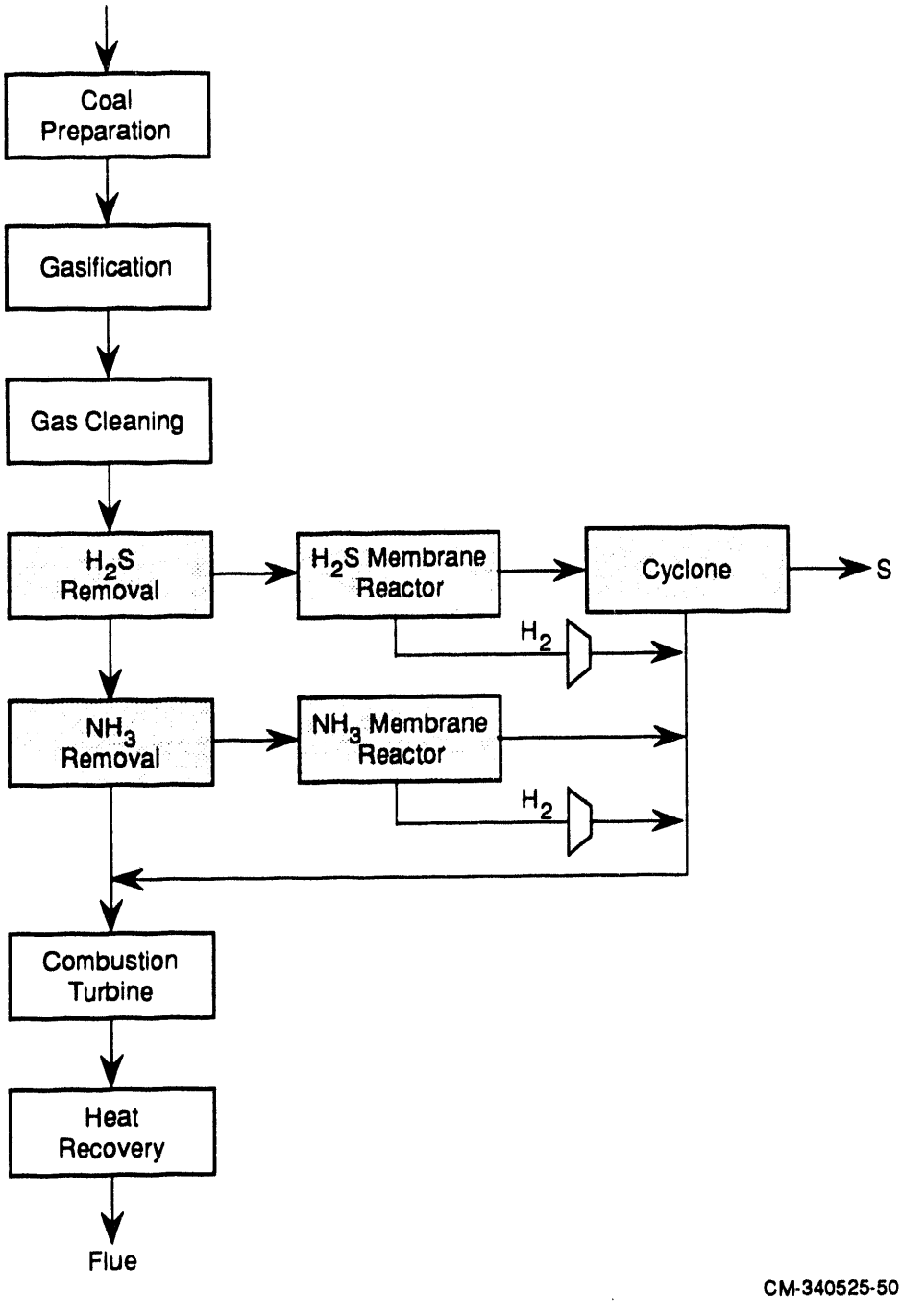

Figure 29. Removal of H_2S and NH_3 before decomposition in a membrane reactor.

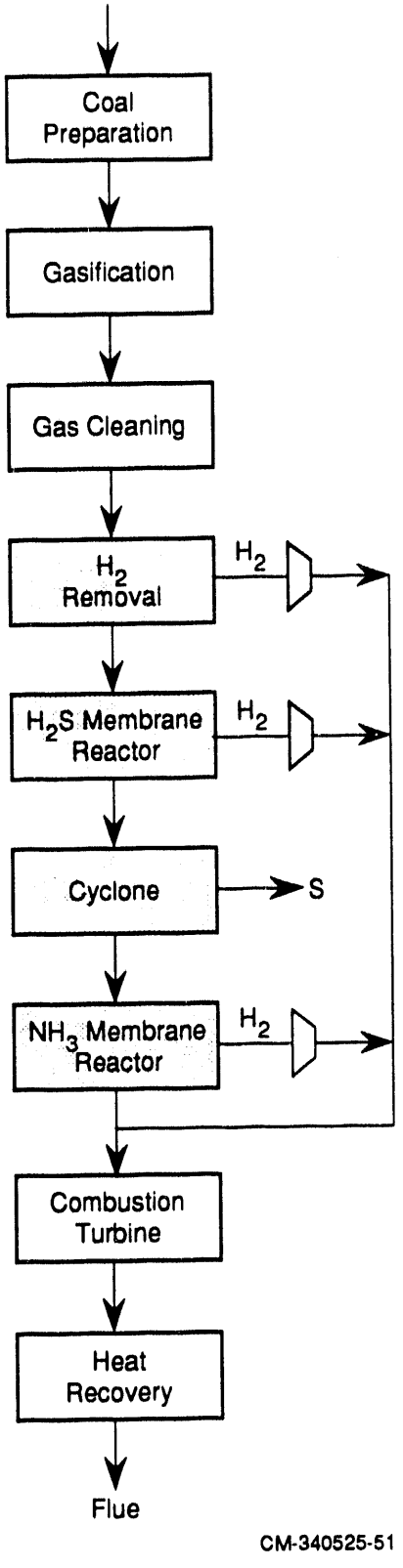

Figure 30. Removal of H_2 before decomposition of H_2S and NH_3 in membrane reactors.

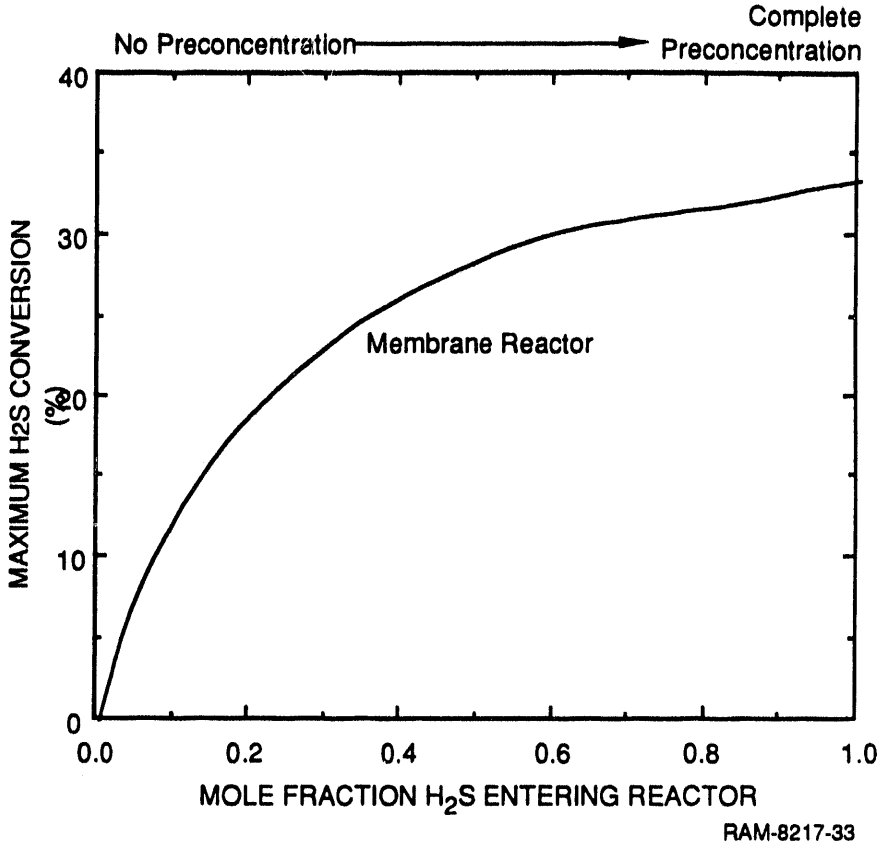

Figure 31. Effect of H_2S preconcentration on decomposition of H_2S.

Even with complete preconcentration, the percentage of H_2S decomposed is only 33%.

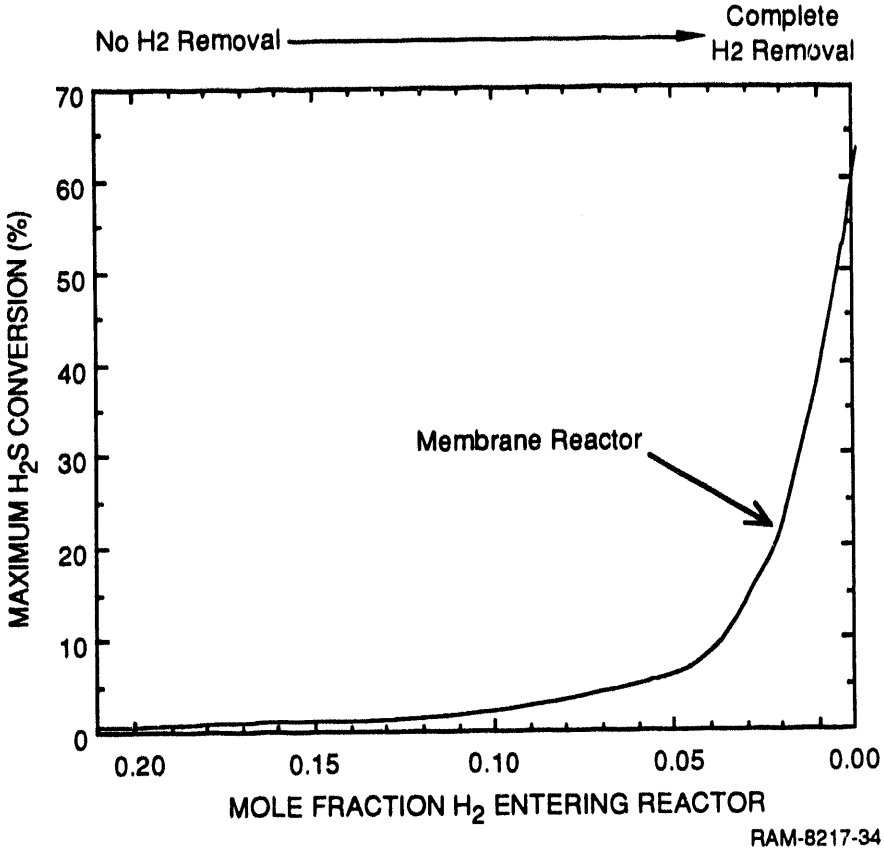

Figure 32. Effect of feed H_2 preconcentration on decomposition of H_2S.

Even with complete removal of H_2 from the feed, the percentage of H_2S decomposed is only 63%.

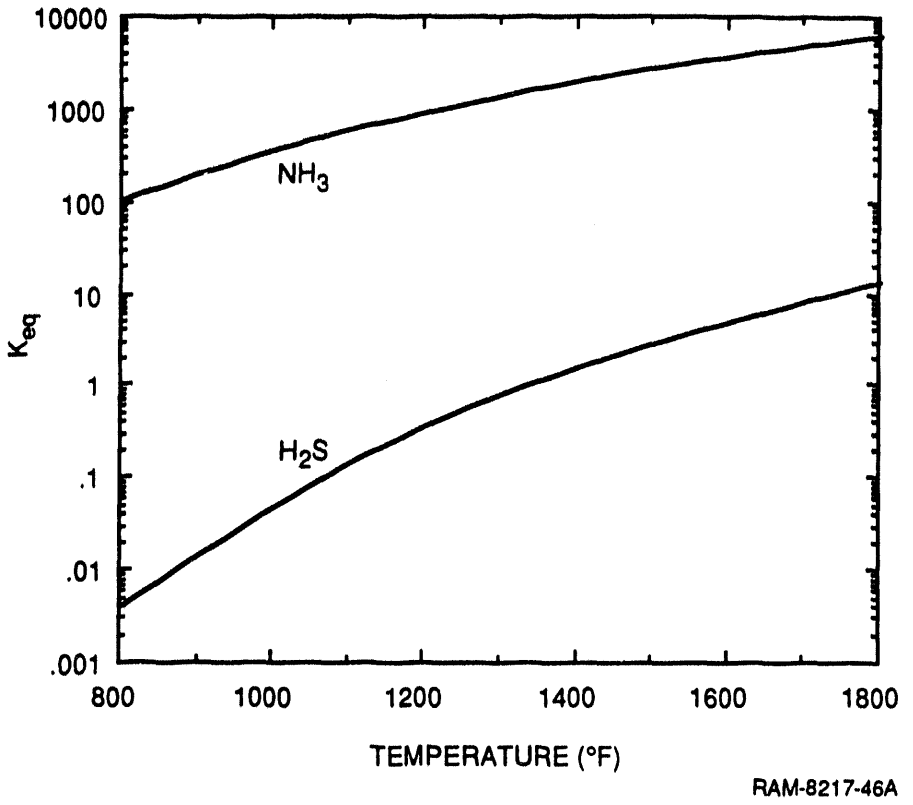

Figure 33. Equilibrium coefficients for NH_3 and H_2S decomposition.

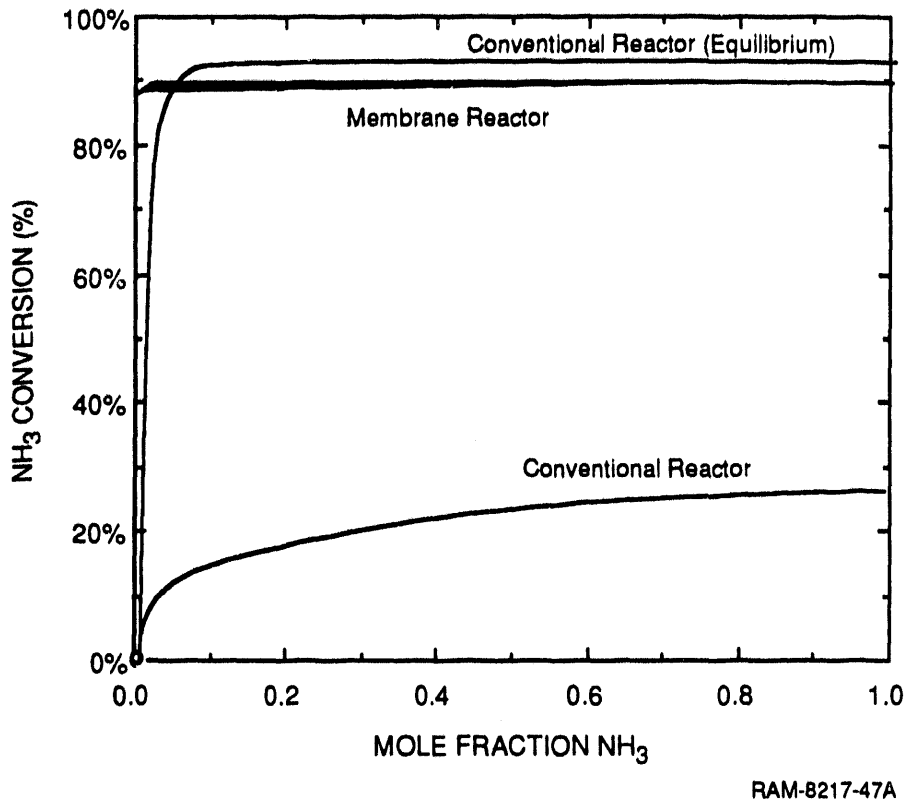

Figure 34. Ammonia decomposition with NH_3 preconcentration.

For the case of H_2 removal from the feed, Figure 35 shows the NH_3 decomposition attained with a membrane reactor and with an equilibrium conventional reactor; feed concentrations vary from 21% H_2 (no preconcentration) to 0.0001% H_2 (almost complete H_2 removal). With a membrane reactor, the H_2 content in the feed needs to be reduced from 21% to 18% to achieve 90% NH_3 decomposition. With a conventional reactor, the feed H_2 content must be less than 2% to decompose 90% of the NH_3.

With either of the two configurations, a membrane reactor is capable of achieving the desired NH_3 decomposition with only minor pretreatment, while a conventional reactor would require substantial pretreatment. These results confirm only the technical feasibility of the NH_3 decomposition process; their economic impact on the overall gasification process must be determined by an economic analysis. We performed an economic analysis of the membrane reactor by the same procedure as was used in the design study[5] upon which our IGCC process was based. Table 19 includes the key parameters used in our analysis.

We performed evaluations on membrane reactors using both NH_3 preconcentration and H_2 removal configurations for conditions in which 90% decomposition could be achieved. We did not include the costs of the pretreatment in this evaluation. As an example, the result for NH_3 decomposition where the membrane reactor feed has been preconcentrated to 1% NH_3 (from 0.075% NH_3) is broken down in Table 20. For this example, the cost for NH_3 decomposition (exclusive of pretreatment) is 2.3 mills/kWh or \$18/lbmol NH_3 decomposed. Compared to the overall electricity price estimated for the IGCC process (60 mills/kWh), the cost for NH_3 decomposition is small but not insignificant.

Figure 36 shows the NH_3 decomposition cost for a membrane reactor with preconcentration of NH_3 in the feed. The cost drops rapidly to 0.5 mills/kWh as the feed concentration increases to 5% NH_3. At higher feed NH_3 concentrations the cost continues to drop, but gradually. Figure 37 shows the NH_3 decomposition cost for a membrane reactor with H_2 removed from the feed. For the cost to be below 1 mill/kWh, the feed must contain less than 1% H_2. These results show that a membrane reactor can decompose 90% of the NH_3 produced in an IGCC process, and can do so at little cost if an inexpensive process to either preconcentrate the NH_3 in the feed or remove H_2 from the feed is available.

[5] This study was performed primarily by Southern Company Services and M. W. Kellogg on behalf of Morgantown Energy Technology Center (DOE/MC/26019-3004; December 1990).

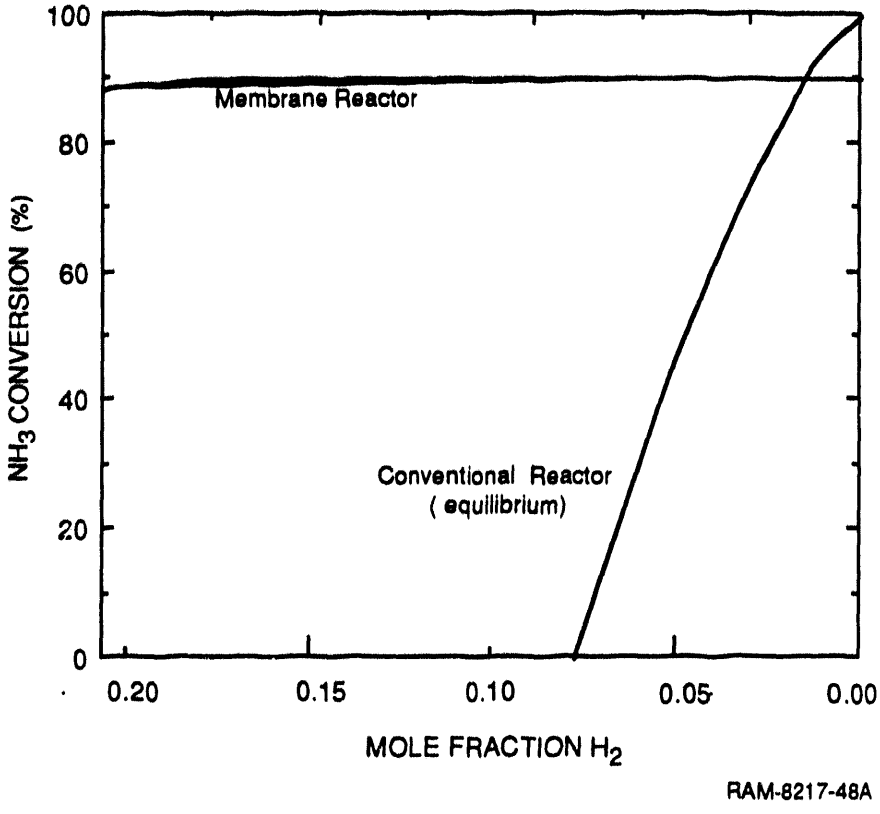

Figure 35. Ammonia decomposition with H_2 removal.

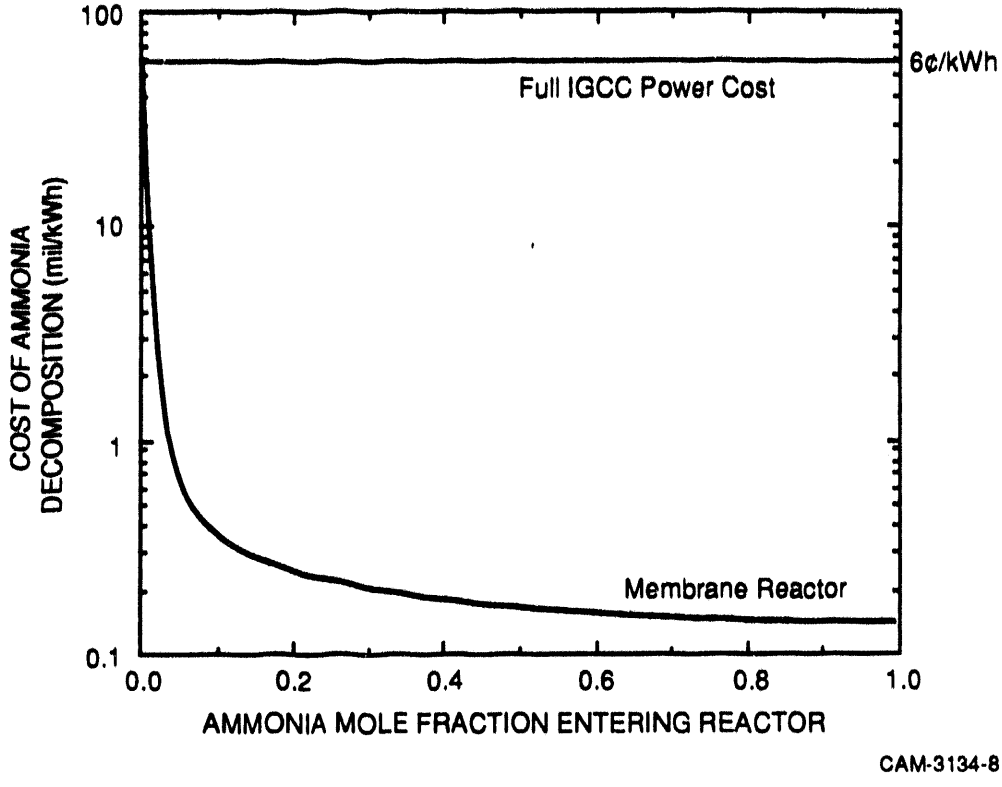

Figure 36. Effect of ammonia preconcentration on total system cost.

If the NH_3 can be preconcentrated to 5% or 10%, decomposition costs can be reasonable.

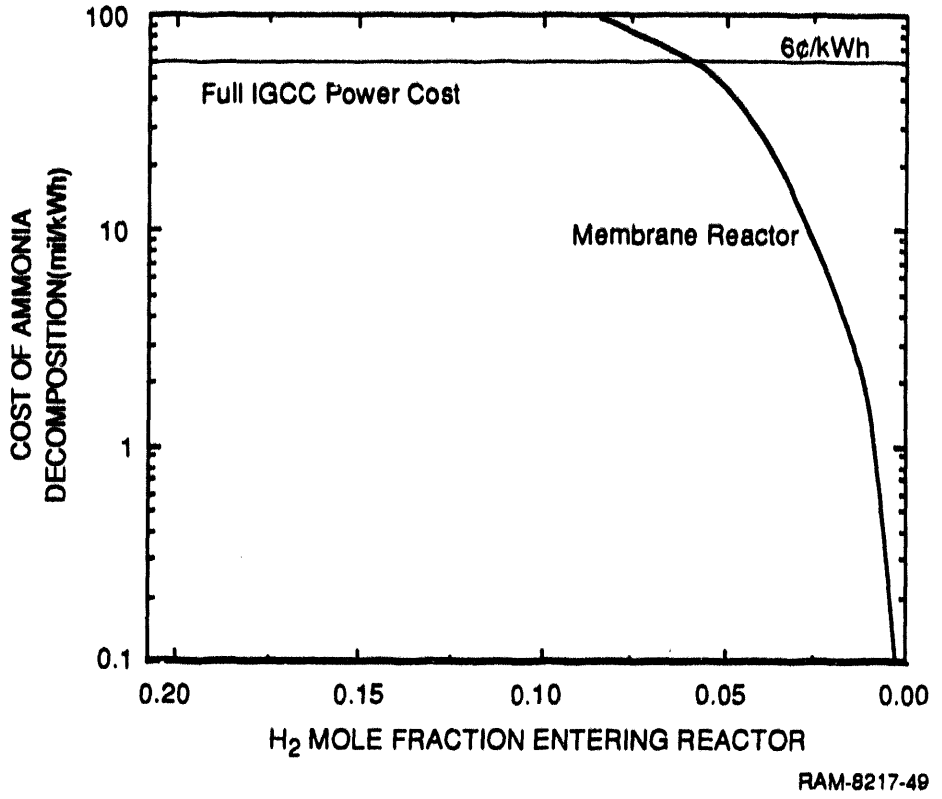

Figure 37. Effect of feed H_2 removal on NH_3 decomposition cost

Reactor cost becomes reasonable if the H_2 concentration in the feed can be reduced to less than 1%.

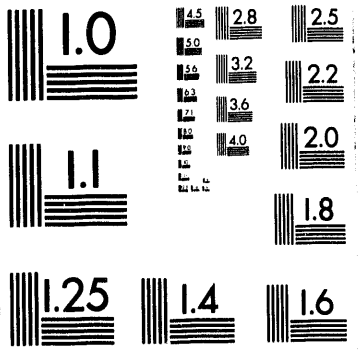
1.0
1.1
1.25
1.4
1.6
1.8
2.0
2.2
2.5
2.8
3.2
3.6
4.0
4.5
5.0
5.6
6.3
7.1

2 of 2

Table 19

KEY ECONOMIC PARAMETERS USED IN THE ECONOMIC ANALYSIS

Plant capacity	420 MW
Plant operation factor	5694 hours per year
Individual membrane tube size	4 mm I.D. x 80 cm long
Membrane cost	$4.50/tube
Fraction of reactor tubes offline for maintenance	17%
Catalyst cost	$350/cu ft
Reactor assembly cost	Equal to membrane housing cost
Reactor installation cost	Twice the membrane housing cost
Thermodynamic compressor efficiency	67.5%
Electricity cost	$0.05/kWh

Table 20

ECONOMIC RESULTS FOR MEMBRANE REACTOR DECOMPOSITION

(Feed preconcentrated to 1% NH_3)

Feed flow rate	5,900 lbmol/hr
Number of membrane tubes	438,000
Percent of feed permeated	2.6 wt%
Compressor power	8,900 bhp
Compressor cost	$2,700,000
Annual electricity cost	$2,100,00
Total membrane cost	$2,400,000
Catalyst required	187 cu ft
Catalyst cost	$65,000
Membrane housing diameter (3 required)	2.6 m
Housing cost (each)	$157,000
Reactor assembly cost	$445,000
Installed reactor cost	$4,200,000
Total system cost	$4,800,000
Levelized charges	
Capital	1.1 mills/kWh
Electricity	0.9 mill/kWh
Operating and Maintenance	0.3 mill/kWh
TOTAL	2.3 mills/kWh ($17.9 /lbmol NH_3 decomposed)

CONCLUSIONS

The objective of this project was to develop high temperature, high pressure catalytic ceramic membrane reactors and to demonstrate the feasibility of using these membrane reactors to control gaseous contaminants (hydrogen sulfide and ammonia) in IGCC systems. Our strategy was to first develop catalysts and membranes suitable for the IGCC application, and then combine these two components as a complete membrane reactor system. We also developed a computer model of the membrane reactor and used it, along with experimental data, to perform an economic analysis of the IGCC application.

The two catalysts we prepared were very effective in increasing the decomposition rate of both NH_3 and H_2S. Our membrane development work demonstrated that palladium membranes produced by electroless plating onto alumina ultrafilters produces an effective membrane for selective H_2 permeation. The NH_3 catalyst was used with the palladium membrane in a membrane reactor. We achieved 95% NH_3 decomposition under some conditions, and under all conditions a membrane reactor resulted in significantly greater NH_3 decomposition than did a conventional reactor.

Economic evaluations indicate that decomposition of H_2S in the IGCC process with a membrane reactor is very difficult (and even more so with a conventional reactor) because of the low value of the H_2S decomposition equilibrium constant and the high ratio of H_2 to H_2S in the feed stream. For NH_3 our evaluations were promising; the maximum conversion that could be achieved was 89%. To achieve the desired level of NH_3 decomposition (90%), the NH_3 should be concentrated in the feed prior to entering the membrane reactor. If the feed NH_3 concentration can be increased to 5%, the cost of producing electricity would increase by about 1% as a result of the costs for the ammonia decomposition reactor. These calculations were performed using early experimental results. Later experiments showed improved membrane properties; if these data were used in the economic analysis, higher conversions and lower costs would have resulted.

This project has demonstrated the feasibility of using a membrane reactor to remove trace contaminants from an IGCC process. Experiments showed that NH_3 efficiencies of 95% can be achieved. Our economic evaluation predicts costs of less than 1% of the total electricity cost; improved membranes would give even higher conversions and lower costs. We believe the catalysts are sufficiently developed and that the primary need for future work is improvements in the H_2 selective membrane. Methods for fabricating inexpensive and robust membranes are needed.

REFERENCES

MEMBRANES

Anderson, M., M. Gieselmann, and Q. Xu, "Titania and Alumina Ceramic Membranes," *J. Memb. Sci.*, **39**, 243-258 (1988).

Bhave, R. R., D. F. Flowers, J. L. Pszczolkowski, and P.K.T. Liu, "Assessment of Commercial Ceramic Membranes for High Temperature Gas Separations," presented at 6th Symposium on Separation Science and Technology for Energy Applications, Knoxville, TN, October 22-26, 1989.

Egan, B. Z., "Using Inorganic Membranes to Separate Gases: R & D Status Review," ORNL/TM-11345, November 1989.

Hwang, S.T., and K. Kammermeyer, *Membranes in Separations* (Robert E. Krieger, Malabar, FL, 1984).

Keizer, K., R.J.R. Uhlhorn, R. J. Van Vuren, and A. J. Burggraaf, "Gas Separation Mechanisms in Microporous Modified γ-Al_2O_3 Membranes," *J. Memb. Sci.*, **39**, 285-300 (1988).

Koresh, J. E., and A. Sofer, "The Carbon Molecular Sieve Membranes," *Sep. Sci. Technol.*, **22**, 973-982 (1987).

Moore, R. H., C. H. Allen, G. F. Schiefelbein, and R. J. Maness, "A Process for Cleaning and Removal of Sulfur Compounds from Low BTU Gases," Interim Report, October 1972-August 1974, GPO Catalog No. I:63, 10:100/Int. 1 (1974).

Pez, G. P., and R. T. Carlin, "Method for Gas Separation," U.S. Patent 4617029, October 14, 1986; Assignee: Air Products and Chemicals, Inc.

Suzuki, H., U.S. Patent 4699892 (1987).

Way, J. D., and D. L. Roberts, "Hollow Fiber Inorganic Membranes for High Temperature Gas Separations," presented at 6th Symposium on Separation Science and Technology for Energy Applications, Knoxville, TN, October 22-26, 1989.

CATALYSIS - HYDROGEN SULFIDE

Chivers, T., J. B. Hyne, and C. Lau, "The Thermal Decomposition of Hydrogen Sulfide over Transition Metal Sulfides," *Int. J. Hydrogen Energy*, **5**, 499-506 (1980).

Chivers, T., and C. Lau, "The Thermal Decomposition of Hydrogen Sulfide over Vanadium and Molybdenum Sulfides and Mixed Sulfide Catalysts in Quartz and Thermal Diffusion Column Reactors," *Int. J. Hydrogen Energy*, **12**, 235-243 (1987a).

Chivers, T., and C. Lau, "The Use of Thermal Diffusion Column Reactors for the Production of Hydrogen and Sulfur from the Thermal Decomposition of Hydrogen Sulfide over Transition Metal Sulfides," *Int. J. Hydrogen Energy*, **12**, 561-569 (1987b).

Fukuda, K., M. Dokiya, T. Kameyama, and Y. Kotera, "Catalytic Decomposition of Hydrogen Sulfide," *Ind. Eng. Chem. Fund.*, **17**, 243-248 (1978).

Katsumoto, M., K. Fueki, and T. Mukaibo, "An Investigation of the Gas-Solid Interface Reaction," *Bull. Chem. Soc. Japan*, **46**, 3641-3644 (1973).

Raymont, M.E.D., "Make Hydrogen from Hydrogen Sulfide," *Hydrocarbon Processing*, **54**, 139-142 (1975).

Sugioka, M., and K. Aomura, "A Possible Mechanism for Catalytic Decomposition of Hydrogen Sulfide over Molybdenum Disulfide," *Int. J. Hydrogen Energy*, **9**, 891-894 (1984).

CATALYSIS - AMMONIA

Ertl, G., and M. Huber, "Mechanism and Kinetics of Ammonia Decomposition on Iron," *J. Catal.*, **61**, 537-539 (1980).

Friedlander, A. G., P. R. Courty, and R. E. Montarnal, "Ammonia Decomposition in the Presence of Water Vapor, I. Nickel, Ruthenium and Palladium Catalysts," *J. Catal.*, **48**, 312-321 (1977a).

Friedlander, A. G., P. R. Courty, and R. E. Montarnal, "Ammonia Decomposition in the Presence of Water Vapor, II. Kinetics of the Reaction of Nickel Catalysts," *J. Catal.*, **48**, 322-332 (1977b).

Gates, B., J. Katzer, and G. Schuit, *Chemistry of Catalytic Processes* (McGraw-Hill, New York, 1979).

Klimisch, R., and K. Taylor, "Catalytic Reduction of Nitric Oxide on Ruthenium," *Ind. Eng. Chem., Prod. Res. Dev.*, **14**, 26-29 (1975).

Krishnan, G. N., B. J. Wood, and A. Sanjurjo, "Study of Ammonia Removal in Coal Gasification Processes, Topical Report: Literature Review," DOE Contract DE-AC21-86MC23087, May 1987.

Krishnan, G. N., B. J. Wood, G. T. Tong, and J. G. McCarty, Final Report, DOE Contract DE-AC21-86MC23087, September 1988.

McCabe, R. W., "Kinetics of Ammonia Decomposition on Nickel," *J. Catal.*, **79**, 445-450 (1980).

Nielsen, A., "Review of Ammonia Catalysis," in: *Catalysis Reviews*, Vol. 4, H. Heinemann (Ed.) (Marcel Dekker, Inc., New York, 1971), pp. 1-25.

Rostrup-Nielson, J. R., "Activity of Nickel Catalysts for Steam Reforming of Hydrocarbons," *J. Catal.*, **31**, 173-199 (1973).

Satterfield, C. N., *Heterogeneous Catalysis in Practice* (McGraw-Hill, New York 1980).

Taylor, K., R. Sinkevitch, and R. Klimisch, "The Dual State Behavior of Supported Noble Metal Catalysts," *J. Catal.*, **35**, 34-43 (1974).

Tsai, W., J. Vajo, and W. H. Weinberg, "Mechanistic Details of the Heterogeneous Decomposition of Ammonia on Platinum," *J. Phys. Chem.*, **89**, 4926-32 (1985).

MEMBRANE REACTORS

Abe, F., "Porous Membrane for Use in Reaction Process," European Patent Application 228885, dated July 15, 1987; filed December 22, 1986; Applicant: NGK Insulators, Ltd.

Armor, J. M., "Catalysis with Permselective Inorganic Membranes," *Appl. Catal.*, **49**, 1-25 (1989).

Gryaznov, V. M., and A. N. Karavanov, *Khim-Farm. Zh.*, **13**, 74 (1979).

Gryaznov, V. M., and M. G. Slinko, *Discuss Faraday Soc.*, 73 (1982).

Gryaznov, V. M., "Hydrogen Permeable Palladium Membrane Catalysts," *Platinum Met. Rev.*, **30**, 68-72 (1986).

Itoh, N., Y. Shindo, K. Haraya, K. Obata, and T. Hakuta, "A Membrane Reactor for Promoting a Reversible Reaction," Paper No. 11-P04, International Congress on Membranes and Membrane Processes, Tokyo, Japan, June 8-12, 1987.

Itoh, N., Y. Shindo, K. Haraya, K. Obata, T. Hakuta, and H. Yoshitome, "Simulation of a Reaction Accompanied by Separation," *Ind. Chem. Eng.*, **25**, 138-142 (1985).

Kameyama, T., M. Dokiya, K. Fukuda, and Y. Kotera, "Differential Permeation of Hydrogen Sulfide through a Microporous Vycor-Type Glass Membrane in the Separation System of Hydrogen and Hydrogen Sulfide," *Sep. Sci. Tech.*, **14**, 953-957 (1979).

Kameyama, T., M. Dokiya, M. Fujishige, H. Yokokawa, and K. Fukuda, "Possibility of Effective Production of Hydrogen from Hydrogen Sulfide by Means of a Porous Vycor Glass Membrane," *Ind. Eng. Chem. Fundam.*, **20**, 97-99 (1981a).

Kameyama, T., K. Fukuda, M. Fujishige, H. Yokokawa, and M. Dokiya, "Production of Hydrogen from Hydrogen Sulfide by Means of Selective Diffusion Membranes," *Hydrogen Energy Prog.*, **2**, 569-579 (1981b).

Mischenko, A. P., V. M. Gryaznov, V. S. Smirnov, E. D. Senina, I. L. Parbuzina, N. R. Roshan, V. P. Polyakova, and E. M. Savitsky, U.S. Patent 4179470 (1979).

Mohan, K., and R. Govind, "Analysis of a Cocurrent Membrane Reactor," *AIChE J.*, **32**, 2083-2086 (1986)

Shinji, O., M. Misono, and Y. Yoneda, "The Dehydrogenation of Cyclohexane by the Use of a Porous Glass Reactor," *Bull. Chem. Soc. Japan*, **55**, 2760-2764 (1982).

Sun, Y. M., and S. J. Khang, "Catalytic Membrane for Simultaneous Chemical Reaction and Separation Applied to a Dehydrogenation Reaction," *Ind. Eng. Chem. Res.*, **27**, 1136-1142 (1988).

GENERAL

Barrer, R. M., "*Diffusion in and through Solids*" (Cambridge University Press, New York, 1951).

Blum, Y., R. M. Laine, K. B. Schwartz, D. J. Rowcliffe, R. C. Benning, and D. C. Cotts, "A New Catalytic Method for Producing Preceramic Polysilazanes," in *Better Ceramics through Chemistry II*, C. J. Brinker, E. D. Clark, and D. R. Ulrich, Eds., *Mater. Res. Soc. Symp. Proc.*, **73**, 389 (1986).

Blum, Y. D., K. B. Schwartz, and R. M. Laine, "Preceramic Polymer Pyrolysis I. Pyrolytic Properties of Polysilazanes," *J. Mat. Sci.*, **24**, 1707-1718 (1989).

Collins, J. P., J. D. Way, and N. Kraisuwansarn, "A Mathematical Model of a Catalytic Membrane Reactor for the Decomposition of NH_3," North American Membrane Society, Lexington, KY, May 1992.

Hammel, J. J., "Porous Inorganic Siliceous-Containing Gas Enriching Material and Process of Manufacture and Use," U.S. Patent 4,853,001, Assignee: PPG Industries, Inc., Pittsburgh, PA (August 1, 1989).

Hammel, J. J., W. J. Robertson, W. P. Marshall, H. W. Barch, B. Das, M. A. Smoot, and P. Beaver, "Process of Gas Enrichment with Porous Siliceous-Containing Material," U.S. Patent 4,842,620, Assignee: PPG Industries, Inc., Pittsburgh, PA (June 27, 1989).

Okubo, T., K. Haruta, K. Kusakabe, S. Morooka, H. Anzai, and S. Akiyama, "Equilibrium Shift of Dehydrogenation at Short Space-Time with Hollow Fiber Ceramic Membrane," *Ind. Eng. Chem. Res.*, **30**, 614-616 (1991).

Rhoda, R. N., "Electroless Palladium Plating," *Trans. Inst. Metal Finishing*, **36**, 82-85 (1959).

Roberts, D. L., I. C. Abraham, Y. Blum, and J. D. Way, "Gas Separation with Glass Membranes," Final Report, DOE Contract DE-AC21-88MC25204, May 1992.

Uemiya, S., Y. Kuda, K. Sugino, N. Sato, T. Matuda, E. Kikuchi, "A Palladium/Porous Class Composite Membrane for Hydrogen Separation," *Chem. Lett.*, pp. 1687-90 (1988).

Wise, E. M., *Palladium—Recovery, Properties, and Uses* (Academic Press, New York, 1968).

Appendix A

THERMODYNAMICS OF THE DECOMPOSITION OF HYDROGEN SULFIDE

APPENDIX A

THERMODYNAMICS OF THE DECOMPOSITION OF HYDROGEN SULFIDE

Kaloidas and Papayannakos (*Int. J. Hydrogen Energy*, **12**, 403-409, 1987) have provided the most complete description of the thermodynamics of H_2S decomposition. We record in this Appendix a few of the key points that we used in our modeling work.

These authors describe the formation of all eight sulfur species (S_1, S_2, ..., S_8) after the decomposition of H_2S as follows:

$$H_2S \Leftrightarrow H_2 + \frac{1}{2} S_2 \tag{A-1}$$

$$S_i \Leftrightarrow \frac{i}{2} S_2 \ (i=1,\ 2,\ .....,\ 8) \tag{A-2}$$

We have taken a simplified approach by assuming that only diatomic sulfur species are produced [represented by Reaction (A-2), above]. We made this simplification to make the modeling problem tractable. It would also be difficult to gather reasonable kinetic data for the formation of the nondiatomic sulfur species. It is unclear exactly what impact this simplification has on the economic assessment of membrane reactors. However, in the pressure range studied by Kaloidas and Papayannakos (1-4 atm), the S_2 species constituted 99.8% of the sulfur when the temperature was between 1300°F and 1560°F. Hence, there are practical conditions under which the species S_2 is the only important species.

The equilibrium coefficient, K_{eq}, for Reaction (A-1) can be written as a function of temperature as follows:

$$\begin{aligned} RT\ln K_{eq} = {} & \Delta\hat{H}_{f,H_2S} - \frac{1}{2}\Delta\hat{H}_{f,S_2} + 298K\left[\Delta\hat{S}_{f,H_2} + \frac{1}{2}\Delta\hat{S}_{f,S_2} - \Delta\hat{S}_{f,H_2S}\right] \\ & + [T\ln T - 298\ln 298]\left(a_{H_2} + \frac{1}{2}a_{S_2} - a_{H_2S}\right) + \left(\frac{T^2 - 298^2}{2}\right)\left(b_{H_2} + \frac{1}{2}b_{S_2} - b_{H_2S}\right) \\ & + \left(\frac{T^3 - 298^3}{6}\right)\left(c_{H_2} + \frac{1}{2}c_{S_2} - c_{H_2S}\right) \end{aligned} \tag{A-3}$$

Here, the coefficients a_i, b_i, and c_i come from expressing the heat capacity of each species as a function of temperature ($C_{p,i} = a_i + b_iT + c_iT^2$). The symbol $\Delta\hat{H}_{f,i}$ is the heat of formation of species i at 298 K and 1 atm, and $\Delta\hat{S}_{f,i}$ is the entropy of formation of species i at 298 K and 1 atm. Table A-1 lists values for a_i, b_i, c_i, $\Delta\hat{H}_{f,i}$, and $\Delta\hat{S}_{f,i}$ taken from Kaloidas and Papayannakos.

Table A-1
THERMODYNAMIC PARAMETERS FOR DECOMPOSITION OF H_2S

Species	$\Delta\hat{H}_f$ (cal/mol)	$\Delta\hat{S}_f$ (cal/mol K)	a (cal/mol K)	b (cal/mol K^2)	c (cal/mol K^3)
H_2	0	31.21	6.52	7.8×10^{-4}	1.2×10^{-6}
H_2S	-4,900	49.16	7.02	3.68×10^{-3}	0
S_2	31,200	54.4	8.54	2.8×10^{-4}	-7.9×10^{-6}

Source: Kaloidas and Papayannakos (1987).

Figure A-1 is a plot of Equation (3) in the temperature range of interest to IGCC processes. At 1000°F, our base case process temperature, the value of K_{eq} is 5.47×10^{-2}.

The equilibrium coefficient K_{eq} is related to the partial pressures of the gaseous species H_2, H_2S, and S_2 in the usual manner:

$$K_{eq} = \left(\frac{P_{H_2}}{1\text{ atm}}\right)\left(\frac{P_{S_2}}{1\text{ atm}}\right)^{1/2}\left(\frac{P_{H_2S}}{1\text{ atm}}\right)^{-1} \qquad \text{(A-4)}$$

Here we have taken the fugacity of each species as being equal to the partial pressure and explicitly included the reference state pressure (1 atm) so that the equilibrium coefficient is dimensionless.* Kalaidos and Papayannakos state that the fugacity coefficient ratios are between 0.998 and 1.00 for this system when the pressure is between 1 and 4 atm and the temperature is between 932°F and 2012°F. In general, the fugacity coefficent ratios are not precisely known.

* That the equilibrium coefficient is dimensionless is often ignored by statements to the effect that the reference pressure is "unit" pressure. See Eq. (3.1) in Denbigh (*The Principles of Chemical Equilibrium*, 3rd ed., Cambridge University Press, Cambridge, England, 1971, p. 111) to see why our Equation (A-4) is the proper way to include the reference pressure.

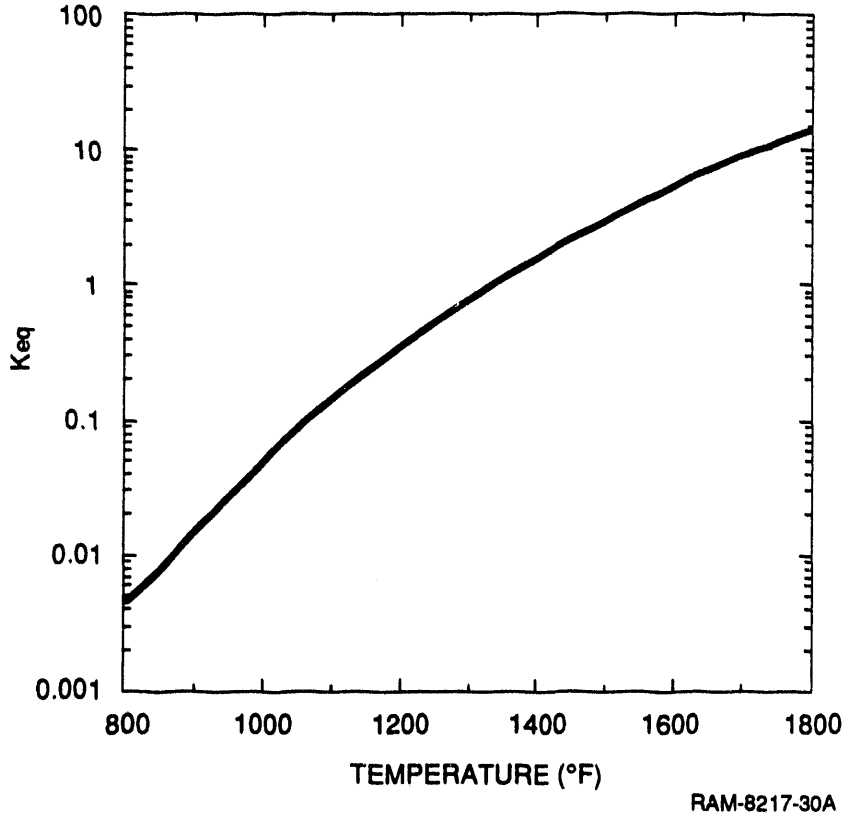

Figure A-1. Equilibrium coefficient for decomposition of H_2S ($H_2S \rightleftharpoons H_2 + 1/2\ S_2$).

Appendix B

REACTION RATE FOR DECOMPOSITION OF HYDROGEN SULFIDE

APPENDIX B

REACTION RATE FOR DECOMPOSITION OF HYDROGEN SULFIDE

We estimated the reaction rate coefficient for H_2S decomposition by using data obtained with the MoS_2 catalyst developed at SRI under this contract; this data were reported in Monthly Report No. 6 (Figure 2a). In using these data, we assumed that the reaction was first-order and that there was no significant reverse reaction during the experiments. The data used to determined the reaction rate at each of two temperatures are given in Table B-1. These reaction rates were used to calculate the reaction rate coefficient as a function of temperature:

$$k_1 = 305\ s^{-1} * \exp(-7790\ K/T) \qquad \text{(B-1)}$$

The reaction rate is given by:

$$r = \varepsilon\, k_1 \left(\frac{P_T}{RT}\right)\left[X_{H_2S} - \left(\frac{P_T}{RT}\right)^{1/2} \frac{X_{H_2} X_{S_2}^{1/2}}{K_{eq}\,(1atm)^{-1/2}}\right] \qquad \text{(B-2)}$$

where

- k_1 = Reaction rate coefficient (s^{-1})
- r = Reaction rate $\left(\frac{mol}{cm^3\text{-}s}\right)$
- ε = Catalyst bed porosity
- P_T = Total pressure (atm)
- X = Mole fraction
- R = Gas constant
- T = Temperature (K)
- K_{eq} = Equilibrium coefficient

Table B-1
DATA USED TO DETERMINE H_2S REACTION RATE COEFFICIENT

Temperature (°C)	Reaction Time (s)	Fraction of H_2S Decomposed (%)	Reaction Rate Coefficient (s^{-1})
500	4	5.1	1.28×10^{-2}
600	4	16.2	4.06×10^{-2}